



THE OHIO STATE UNIVERSITY

# Bicycle Regenerative Braking System Final Written Report

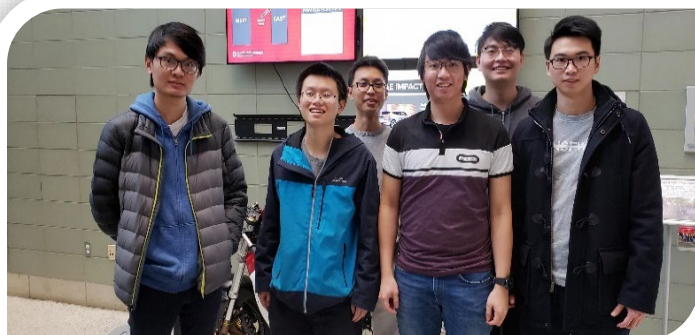
**Submitted to:**

Dr. Anthony Luscher

**Created by:**

EcoBoost

Jun Wei Yap, John Ouyang, Jianhong Xie, Kai Chuen Tan, Jiadi Tian, Qihang Zeng



Mechanical Engineering 3671

The Ohio State University

Columbus, OH

7<sup>th</sup> December 2018

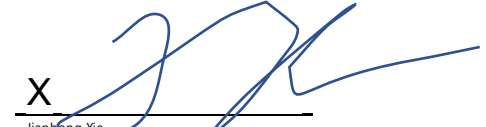
X  
  
Kai Chuen Tan

X  
  
Jun Wei Yap

X  
  
John Ouyang

X  
  
Jiadi Tian

X  
  
Qihang Zeng

X  
  
Jianhong Xie

## Executive Summary

Regenerative braking system is an energy recovery system that helps to slow down a vehicle by converting its kinetic energy into any other forms of energy including chemical energy, rotational kinetic energy and electric energy that would be stored in an energy device. The energy recovery system concept has been widely used in today's modern world; for instance, Formula-1 cars utilized flywheel or high voltage batteries to store and to recover a moving F-1 cars' kinematic energy under braking (ref). EcoBoost Team aimed to apply the magic of the regenerative braking concept on a bicycle to store part of the braking capacity in a 9 kg flywheel for later use in propelling riders' bicycle when starting and to improve the bicycle performance. The great engineering behind the regenerative braking system will help the rider to save riders' pedal energy by boosting the starting the starting acceleration of the bicycle during a ride. EcoBoost Team designed the regenerative braking system with several important machine elements which were sprockets, chain, bearings, cone clutch, planetary gear, compression springs (absorber), extension spring, and flywheel.

The process of EcoBoost's regenerative braking system has two stages which are energy storing stage and energy release stage. During the energy storing stage, the flywheel sprocket was driven by the rear wheel sprocket with the flywheel; energy storing phase began after the brake cable was pulled, and the kinetic energy was transfer from the rear wheel to the flywheel through actuated cone clutch and planetary gear that helped to increase rotational speed of the flywheel. The maximum energy that could be stored in flywheel in 3.8617 kJ. During the energy release stage, the rider was required to press a control button to kick-start the bicycle at a certain speed from rest to allow the transferring of rotational kinetic energy from the flywheel to the rear wheel

through planetary gear, cone clutch, flywheel sprocket, chain, and rear wheel sprocket. The output kinetic energy from the flywheel to the rear after undergoing energy release and clutch friction process was calculated to be 0.82656 kJ, which corresponds to the overall brake energy regeneration efficiency of 12.17 %, thus boosting the bicycle to start from 0 to 16.9934 km/h without exerting pedal force from the cyclist after the last braking cycle (assumed that the initial bicycle speed before the regenerative breaking process is 40 km/h). The Regenerative Project Write-up will further discuss about the overall design layout and description, energy sizing, storage, and system level engineering, detailed design of the energy storage element, detailed design of energy storage drivetrain and system, conclusion, and lesson learned from EcoBoost Team.

## Contents

1. Overall Design Layout and Description.....	10
2. Energy Sizing, Storage, and System Level Engineering .....	29
3. Detailed Design of Energy Storage Element .....	39
4. Detailed Design of Energy Storage and Release Drivetrain and System .....	41
5. Conclusions .....	94
6. Lessons Learned.....	96
7. Appendix .....	98
8. References .....	144

## List of Figures

<b>Figure 1:</b> Regenerative Braking Design and Handbrake Control Design.....	11
<b>Figure 2:</b> Mass Properties of Regenerative Braking Design.....	12
<b>Figure 3:</b> The Position of the Regenerative Braking System on the Bicycle.....	13
<b>Figure 4:</b> The Position of the Rear Wheel Sprocket on the Bicycle .....	13
<b>Figure 5:</b> 1st Half of the Exploded-view of the Regenerative Braking System.....	14
<b>Figure 6:</b> 2nd Half of the Exploded-view of the Regenerative Braking System .....	15
<b>Figure 7:</b> Modified Right Handbrake Control System Design .....	16
<b>Figure 8:</b> Exploded-View Modified Right Handbrake Control System Design .....	17
<b>Figure 9:</b> The mass of the handbrake control mechanism design .....	18
<b>Figure 10:</b> Initial-Starting Phase of the Energy Storing Stage (Left) and the Initial Handbrake and Ratchet Wheel's Teeth Positions (Right).....	19
<b>Figure 11:</b> Beginning of the Energy Storing Phase of the Energy Storing Stage .....	20
<b>Figure 12:</b> Ending of the Energy Storing Phase of the Energy Storing Stage (Left), and the Ending of the Energy Storing Phase Handbrake and Ratchet Wheel's Teeth Positions (Right)..	20
<b>Figure 13:</b> Friction Braking Phase of the Energy Storing Stage (Left), and the Friction Braking Phase Handbrake, and Ratchet Wheel's Teeth Positions (Right).....	22
<b>Figure 14:</b> The Flowchart of the Energy Storing Portion .....	23
<b>Figure 15:</b> Ratchet Wheel Mechanism Process during the Energy Release Portion of the Regenerative Braking Design. ....	25
<b>Figure 16:</b> The Flowchart of the Energy Releasing Portion .....	27
<b>Figure 18:</b> Velocity Ratio, $\eta$ vs. Overall Regeneration Efficiency when $I_e = 12.4444 \text{ kg m}^2$ and $I_f = 0.1005 \text{ kg m}^2$ .....	33
<b>Figure 17:</b> CAD Flywheel Design and Material Properties.....	40
<b>Figure 19:</b> Specification of the larger sprocket for the regeneration system .....	42
<b>Figure 20:</b> Specification of the larger sprocket for the regeneration system .....	43
<b>Figure 21:</b> Two-inertia system consisting $I_1$ and $I_2$ .....	45
<b>Figure 22:</b> CAD model of the cone clutch designed.....	48
<b>Figure 23:</b> Three important position for the three bar linkage.....	49
<b>Figure 24:</b> Free body diagram of the actuation mechanism at different positions.....	50
<b>Figure 25:</b> Specifications of spring 2 .....	51

<b>Figure 26:</b> CAD model of spring 2 .....	52
<b>Figure 27:</b> Free body diagram of pin .....	54
<b>Figure 28:</b> Plot of $ F_c - F_{s1} $ with respect to the connecting link position $\alpha$ .....	56
<b>Figure 29:</b> Specifications of spring 1 .....	57
<b>Figure 30:</b> CAD model of extension spring 1 .....	60
<b>Figure 31:</b> Analysis of the hand brake .....	61
<b>Figure 32:</b> B4-1 - Compression Springs picture and specification table .....	63
<b>Figure 33:</b> Ratcheting Mechanism when at position $\theta_0$ .....	64
<b>Figure 34:</b> Free body diagram for ratchet and pawl at position $\theta_0$ .....	65
<b>Figure 35:</b> Ratcheting Mechanism when at position $\theta_{1.5}$ .....	67
<b>Figure 36:</b> Free body diagram for ratchet and pawl at position $\theta_{1.5}$ .....	68
<b>Figure 37:</b> Ratcheting Mechanism when handbrake is push down. ....	70
<b>Figure 38:</b> Free body diagram for ratchet and pawl for when the handbrake is push down.....	71
<b>Figure 39:</b> Ratcheting Mechanism when button is pushed.....	73
<b>Figure 40:</b> Free body diagram for ratchet and pawl for when the button is pushed.....	74
<b>Figure 41:</b> Free body diagram of shaft 1.....	76
<b>Figure 42:</b> Free body diagram, shear force and bending moment diagrams of shaft 1 .....	77
<b>Figure 43:</b> Free body diagram of shaft 2.....	80
<b>Figure 44:</b> The free body diagram, shear force and bending moment diagram of shaft 2 .....	82
<b>Figure 45:</b> Specifications of bearing 1 ( AST 6003ZZ deep groove bearing, from AST website) .....	86
<b>Figure 46:</b> CAD model of bearing 1 ( AST 6003ZZ deep groove bearing, from AST website)	87
<b>Figure 47:</b> Specification of bearing 2 ( AST 6003ZZ deep groove bearing, from AST website)	88
<b>Figure 48:</b> CAD model of bearing 2 ( AST 6003ZZ deep groove bearing, from AST website)	89
<b>Figure 49:</b> Tensile Stress Testing of the 0.064" Diameter Bike Cable.....	92
<b>Figure 50:</b> Regenerative Braking Design 2D Drawing.....	98
<b>Figure 51:</b> B18.22M-M14 Washer 2D Drawing.....	99
<b>Figure 52:</b> Flywheel Drawing .....	100
<b>Figure 53:</b> Cup drawing .....	101
<b>Figure 54:</b> Driven shaft drawing .....	102
<b>Figure 55:</b> Key drawing .....	103

<b>Figure 56:</b> Flywheel Flange End Threaded Drawing.....	104
<b>Figure 57:</b> Right Flange Drawing .....	105
<b>Figure 58:</b> 75-7 MLD drawing.....	106
<b>Figure 59:</b> Cone drawing .....	107
<b>Figure 60:</b> Friction line drawing .....	108
<b>Figure 61:</b> Folk assenby drawing.....	109
<b>Figure 62:</b> Left Flange V2 Drawing .....	110
<b>Figure 63:</b> Linkage bar drawing.....	111
<b>Figure 64:</b> 2302K115 Rear Wheel Sprocket with 29 Teeth Drawing (After Machined) .....	112
<b>Figure 65:</b> Lower part .....	113
<b>Figure 66:</b> Brake Road Cable Drawing.....	114
<b>Figure 67:</b> PlanetaryGearFxiedBar .....	115
<b>Figure 68:</b> Brake lever sport Drawing .....	116
<b>Figure 69:</b> Handbrake Drawing .....	117
<b>Figure 70:</b> Ratchet drawing.....	118
<b>Figure 71:</b> Pawl drawing.....	119
<b>Figure 72:</b> Handbrake spacer drawing .....	120
<b>Figure 73:</b> Handbrake Control Design 2D Drawing .....	121
<b>Figure 74:</b> Handbrake Brake Cable 2D Drawing.....	122
<b>Figure 75:</b> 2302k115 Sprocket with 29 Teeth Drawing (Before Machined) .....	123
<b>Figure 76:</b> 2302k115 Sprocket with 29 Teeth Drawing (Before Machined) .....	124
<b>Figure 77:</b> 6027K71 Roller Chain 2D-Drawing (Before Machined).....	125
<b>Figure 78 :</b> B3-43 Compression Spring for the Ratchet Wheel Mechanism 2D-Drawing .....	126
<b>Figure 79 :</b> B3-20 Extension Spring for the Three Bar Linkages 2D-Drawing .....	127
<b>Figure 80:</b> 72123 Compression Spring for the Three Bar Linkages 2D-Drawing.....	128
<b>Figure 81:</b> 2302K240 Machined Sprocket with 18 Teeth 2D-Drawing .....	129
<b>Figure 82:</b> 6000ZZ Single Row Deep Groove Bearing Technical Specs .....	130
<b>Figure 83 :</b> 6003ZZ Single Row Deep Groove Bearing Technical Specs .....	131
<b>Figure 84 :</b> 75-7MLD (LGU 75-M) Technical Specs .....	132

## List of Tables

1.	Values of unknowns for ratchet and pawl at position $\theta_0$ .....	67
2.	Values of unknowns for ratchet and pawl at position $\theta_{1.5}$ .....	69
3.	Values of unknowns for ratchet and pawl for when the handbrake is push down.....	72
4.	Values of unknowns for ratchet and pawl for when the button is pushed .....	75
5.	Bearing loads corresponding to shaft 2.....	81
6.	Bearing loads corresponding to shaft 1.....	84
7.	Components Table List.....	135

## List of Equations

<u>1.</u> Total Mass of the bicycle .....	.29
<u>2.</u> Total Moment of Inertia of wheel.....	.29
<u>3.</u> Velocity ratio between flywheel and rear wheel.....	.29
<u>4.</u> Braking capacity.....	.29
<u>5.</u> Conversion between angular velocity and velocity.....	.30
<u>6.</u> Equation 6: Energy storage efficiency .....	.30
<u>7.</u> Alternate form of energy storage efficiency equation.....	.30
<u>8.</u> Flywheel energy equation.....	.31
<u>9.</u> Energy regeneration efficiency.....	.31
<u>10.</u> Efficiency combining equation.....	.31
<u>11.</u> Overall regeneration efficiency equation.....	.31
<u>12.</u> rearrange form of overall regeneration efficiency equation.....	.31
<u>13.</u> Condition to find maximum regenerative efficiency.....	.32
<u>14.</u> Simplification of the overall regenerative efficiency equation .....	.32
<u>15.</u> Equation to find optimum velocity ratio .....	.33
<u>16.</u> Chain velocity ratio calculation (between planetary gear and sprocket) .....	.34
<u>17.</u> Chain velocity ratio calculation (between small sprocket and large sprocket) .....	.34
<u>18.</u> Total velocity ratio of the regenerative braking system during energy storing.....	.35
<u>19.</u> Total velocity ratio of the regenerative braking system during energy regeneration... .	.35
<u>20.</u> Equation to calculate flywheel velocity after energy storage.....	.35
<u>21.</u> Calculation for flywheel velocity.....	.36
<u>22.</u> Equation to calculate wheel velocity after regeneration.....	.37
<u>23.</u> Velocity ratio between flywheel and wheel.....	.37
<u>24.</u> overall efficiency of the energy storage system.....	.37
<u>25.</u> Actual calculation for overall efficiency generative breaking syste.....	.38
<u>26.</u> Sprocket specification calculations.....	.44
<u>27.</u> Inertia calculation.....	.44
<u>28.</u> Angular velocity of both side of the shaft.....	.46
<u>29.</u> Energy due to friction loss for cone clutch.....	.46
<u>30.</u> Cone clutch operating force.....	.47
<u>31.</u> Maximum pressure for cone clutch.....	.48
<u>32.</u> Geometrical approach to find initial angles of the linkages.....	.49
<u>33.</u> Calculate the length of the two movable linkages when they are straight.....	.50
<u>34.</u> Maximum deflection for spring.....	.50
<u>35.</u> Desired spring rate calculation.....	.51
<u>36.</u> Modified Goodman failure criterion approach to calculate fatigue safety factor for spring used in three bar linkage.....	.52
<u>37.</u> Force analysis in y-direction for return spring.....	.55
<u>38.</u> Length of the return spring equation.....	.55

<u>39.</u> Force differences base on connecting link position (alpha).....	55
<u>40.</u> Fatigue strength of return spring verification (Body).....	59
<u>41.</u> Bending Fatigue of return spring verification (End hook) .....	59
<u>42.</u> Force analysis when ratchet and pawl at position $\theta_0$ .....	66
<u>43.</u> Force analysis when ratchet and pawl at position $\theta_{1.5}$ .....	69
<u>44.</u> Force analysis when ratchet and pawl when handbrake is pushed down.....	72
<u>45.</u> Force analysis when ratchet and pawl when button is pushed.....	75
<u>46.</u> Shaft 1 safety factor calculation.....	79
<u>47.</u> Relationship of linear impact and maximum impact force .....	80
<u>48.</u> Forces acted by the bearing on to the shaft 2.....	81
<u>49.</u> Moment analysis of shaft 2.....	82
<u>50.</u> Safety factor of shaft 2.....	83
<u>51.</u> Force acted on shaft 1 by bearings.....	84
<u>52.</u> Equivalent ball bearing load.....	85
<u>53.</u> C10 rating of bearing 1.....	85
<u>54.</u> Service life of bearing 1.....	86
<u>55.</u> Equivalent ball bearing load (bearing 2) .....	87
<u>56.</u> C10 rate of bearing 2.....	88
<u>57.</u> Service life of bearing 2.....	88
<u>58.</u> Equivalent ball bearing load (bearing 3 and 4) .....	90
<u>59.</u> C10 rate for bearing 3 and 4.....	90
<u>60.</u> Desired life for bearing 3 and 4.....	90
<u>61.</u> Tensile stress for wire rope.....	91
<u>62.</u> Factor of safety for wire rope.....	92

## 1. Overall Design Layout and Description

EcoBoost team came up with an eco-friendly and safe kinetic energy recovery system which is also known as the regenerative braking system by utilizing the flywheel for the energy storage of a bicycle. The regenerative braking process involves transferring rotational energy from the rear-wheel to the flywheel through a gear train as shown in **Figure 1**. Then, the energy stored is released to aid in moving a stationary bicycle. Dedicated EcoBoost team brainstormed several design ideas of the regenerative braking system that would help to increase the efficiency and effectiveness of the energy storage system with a flywheel by amplifying the speed from the rear wheel and transferring kinetic energy to the flywheel using a flywheel sprocket with 18 teeth (*McMaster-CARR*, 2018), a rear wheel sprocket with 29 teeth (*McMaster-CARR*, 2018) and a planetary gear with a velocity ratio 7:1 (*MATEX*, 2018). The overall velocity ratio is 11.278. Other than that, the large amount of mass of the flywheel (i.e., 8.997 kg) heavily influence the capability of storing a certain amount of huge energy. The diameter of the flywheel used here is 30.0 cm as shown in the 2D-Drawing of the flywheel (**Figure 52**), and the maximum energy stored possible in the flywheel is 3.8617 kilo-Joules. All calculations regarding the sizing of flywheel, efficiency and maximum energy stored will be explained in detail in the “**Energy Sizing, Storage, and System Level Engineering**” and “**Detailed Designed of Energy Storage Element**” sections.

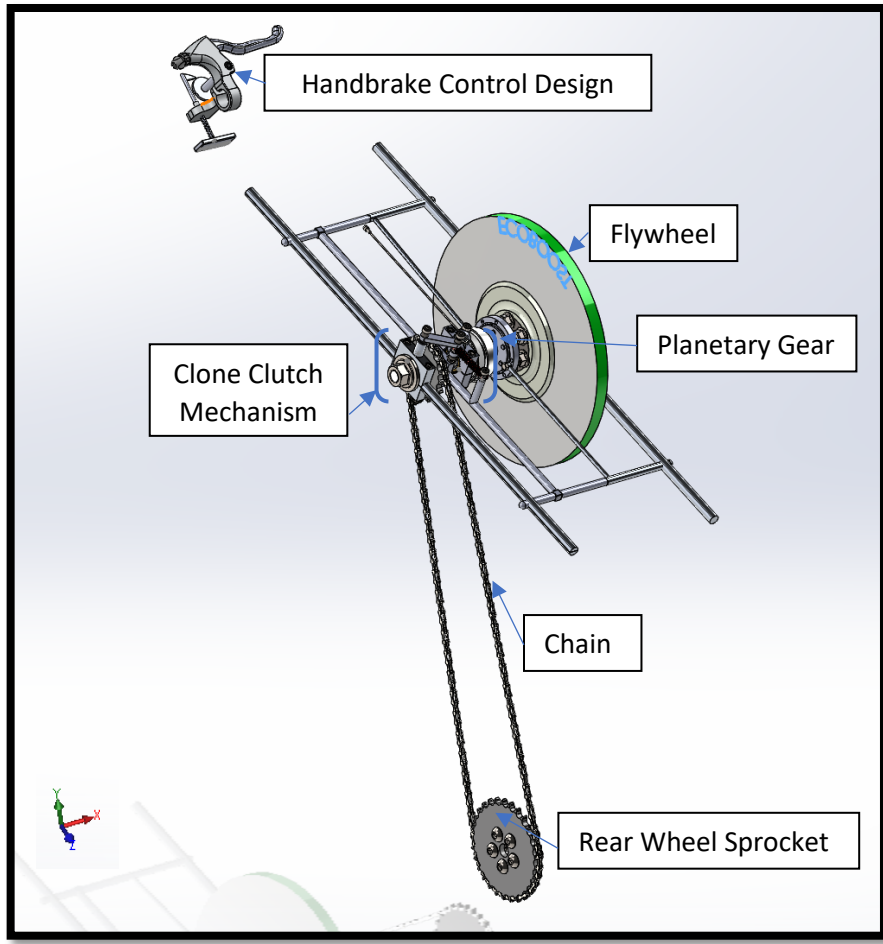


**Figure 1:** Regenerative Braking Design and Handbrake Control Design

**Figure 1** above shows that the combination of the regenerative braking design and the handbrake control design. The overall dimensions of the regenerative braking design including the height excluding the bottom sprocket with 29 teeth, width and length are 30.00 cm, 24.73 cm, and 48.80 cm, respectively as shown the Regenerative Braking Design 2D Drawing (**Figure 50**). The mass of the regenerative braking design is approximately 10.65 kg as shown in **Figure 2** that presents the mass properties of the regenerative braking design assembly from the **SolidWorks 2018**.

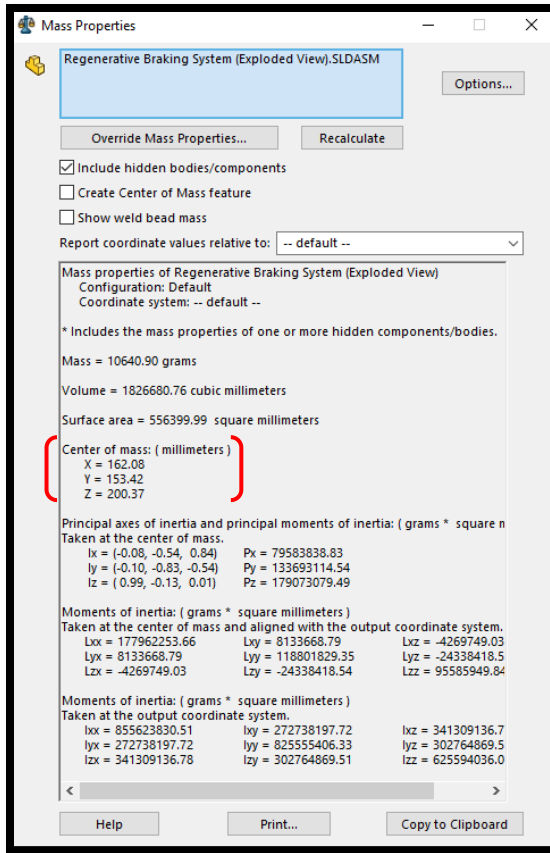


**Figure 2: Mass Properties of Regenerative Braking Design**

The regenerative braking system was designed to build and to mount in-front and slightly below a bicycle saddle; the position of the regenerative braking design is crucial to ensure that the center of mass of the regenerative braking design and the center of mass of the bicycle are relatively near to each other, and the weight distribution of the bicycle is not lob-sided. According to **Figure 2** center of mass values, the difference between the overall width and the center of mass of the regenerative braking design in the x-direction (i.e., width) is 8.53 cm; the difference between the overall height and the center of mass of the regenerative braking design in the y-direction (i.e., height) is 14.7 cm; the difference between the overall length and the center of mass of the regenerative braking design in the z-direction (i.e., length) is 28.8 cm; therefore, the center of the

mass of the regenerative braking design is approximately half of the overall dimension in each axis (i.e., x, y, z-axis). Furthermore, the mass of the regenerative braking design is 10.64 kg (**Figure 2**). **Figure 3** below clearly shows the position of the regenerative braking system on the bicycle. The regenerative braking system chain will be linked from the flywheel to the rear wheel that was attached to the rear wheel as shown in the **Figure 4**.

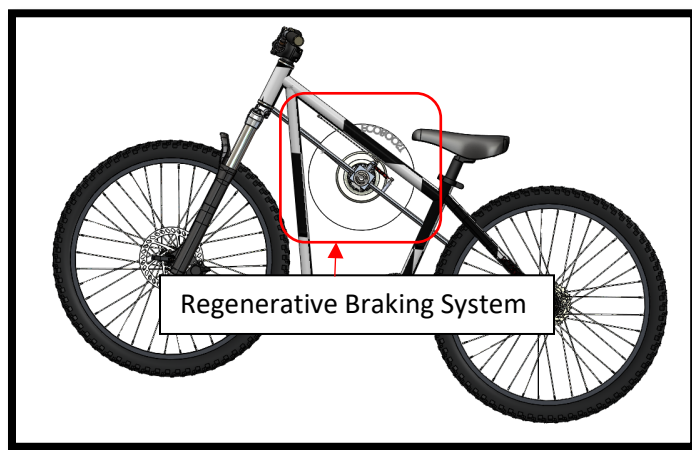


**Figure 3:** The Position of the Regenerative Braking System on the Bicycle

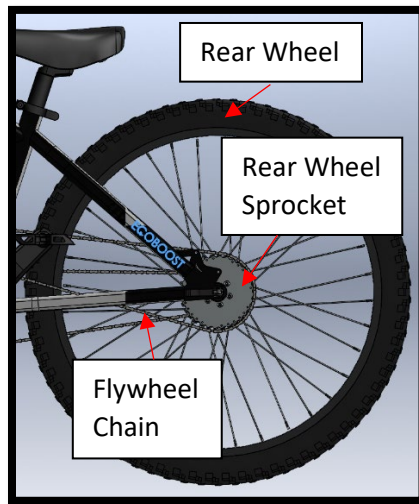


**Figure 4:** The Position of the Rear Wheel Sprocket on the Bicycle

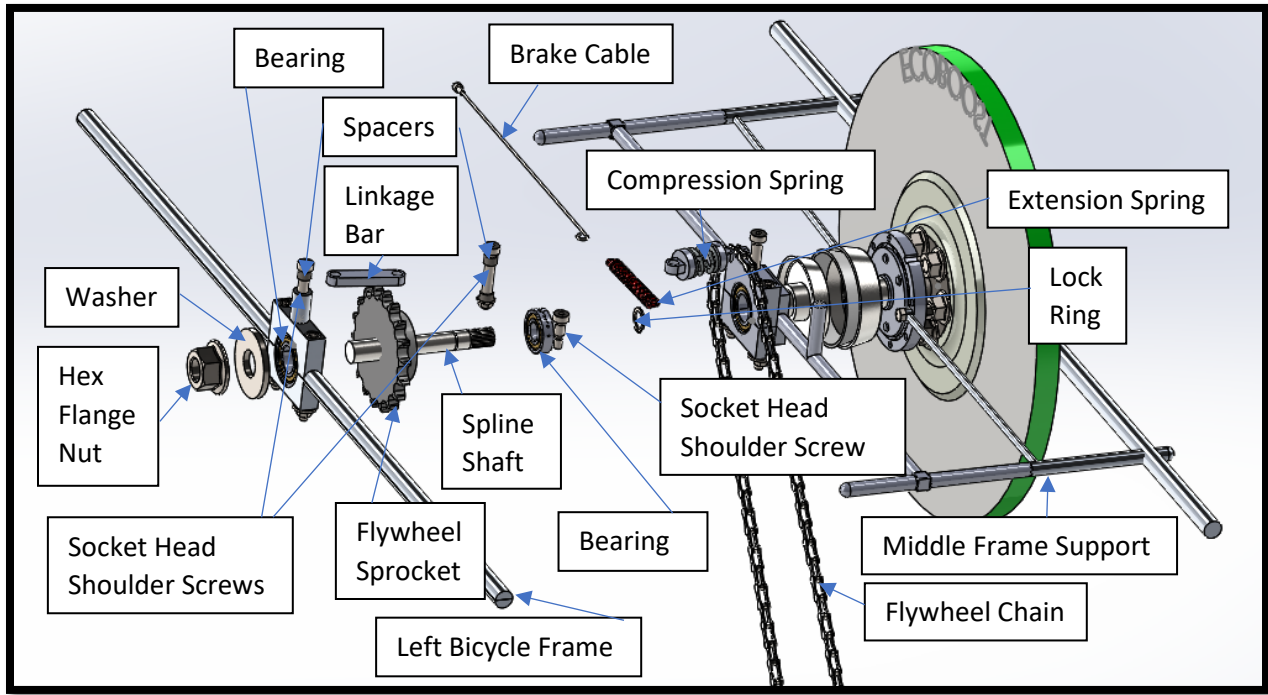


**Figure 5:** 1st Half of the Exploded-view of the Regenerative Braking System

**Figure 5** illustrates several machine elements for the regenerative braking system including the washer, hex flange nut, socket head shoulder screws, bearings, spacer, linkage bar, spline shaft, flywheel sprocket, flywheel chain, compression spring, extension string, brake cable/wire rope, and retaining/lock ring. The left bicycle frame, the middle frame support, and the right bicycle frame were welded together to fix and support the regenerative braking system on the bicycle.

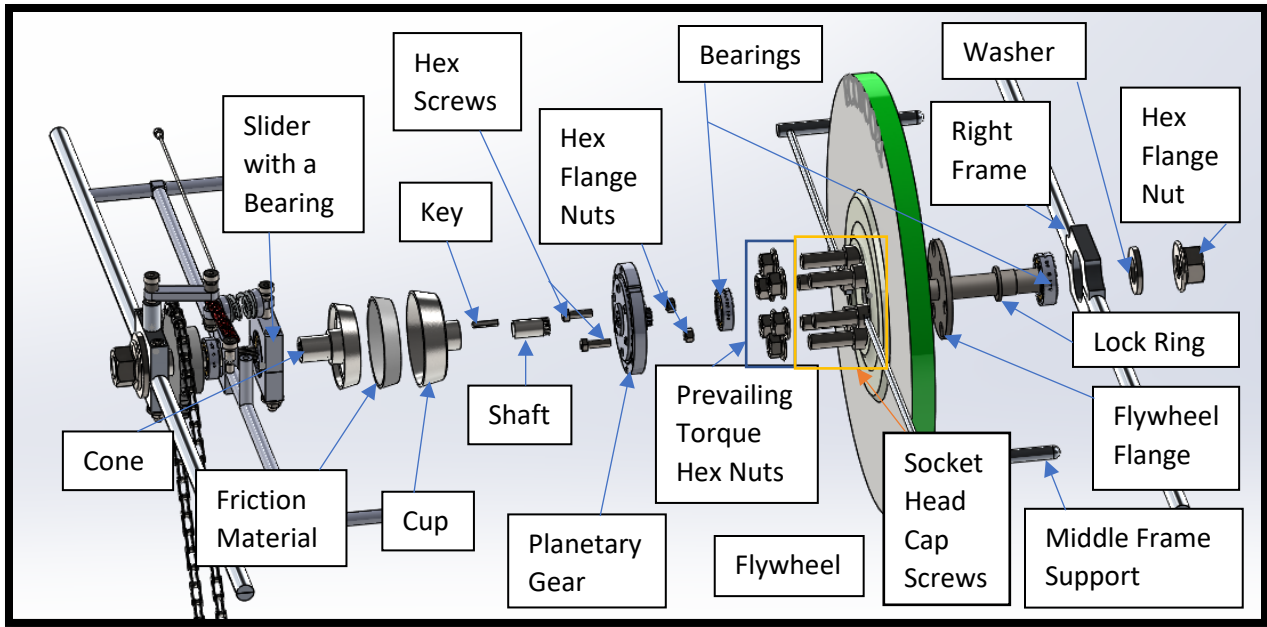


**Figure 6:** 2nd Half of the Exploded-view of the Regenerative Braking System

**Figure 6** presents several machine elements that are similar to **Figure 5** except certain components which are cone, friction material, cup, shaft, key, hex screws, planetary gear, prevailing torque hex nuts, flywheel, socket head screw caps, and flywheel flange. The planetary gear and the labelled left bearing were fixed to the middle frame support, and the middle frame support was connected to the right bicycle frame. A slider with a bearing inside was implemented to the regenerative braking design to actuate the cone clutch in a linear motion along the spline shaft.

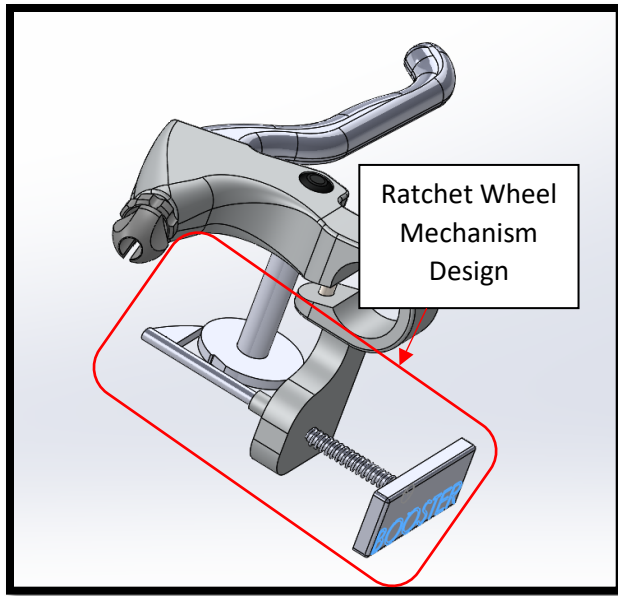


**Figure 7:** Modified Right Handbrake Control System Design

**Figure 7** illustrates the modified right handbrake control system design that was patterned by the EcoBoost Team to control the regeneration energy from the flywheel to the bicycle rear wheel portion.

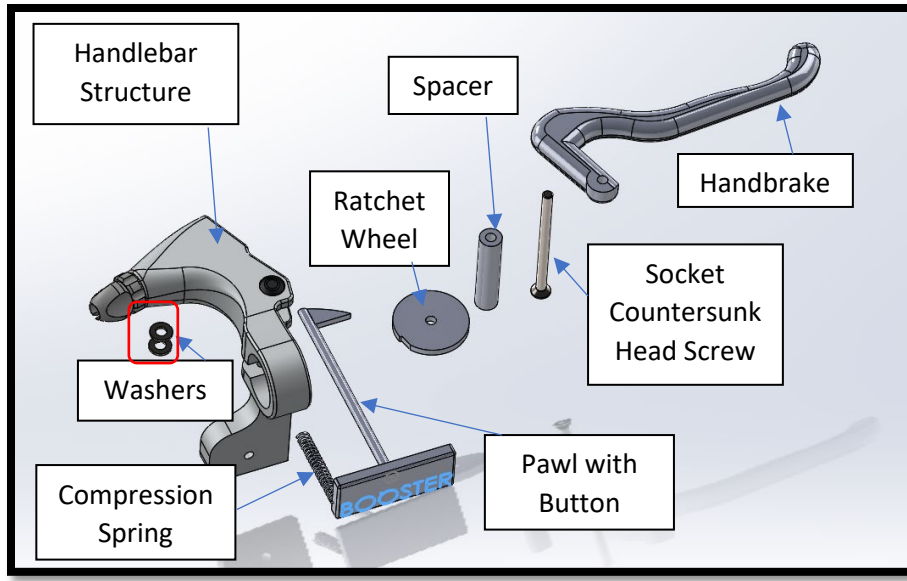


**Figure 8:** Exploded-View Modified Right Handbrake Control System Design

**Figure 8** presents a more detail version of the **Figure 7** by showing the components of the system including washers, compression springs, pawl with a push button which is also known as the “Booster” button, ratchet wheel, spacer, and a socket countersunk head screw. In order to rotate the ratchet wheel, the ratchet wheel was mounted to the socket countersunk head screw. As the rider applied a force on the handbrake, the handbrake would rotate together with the socket countersunk head screw and the ratchet wheel. Based on the 2D-Drawing of the handbrake control design, the overall dimensions of the modified right handbrake control system design including the height, length and width are 57.51 mm, 172.45 mm, and 113.50 mm, respectively (**Figure 73**). The mass of the handbrake control mechanism design is just 57.33 grams as shown in **Figure 9**.

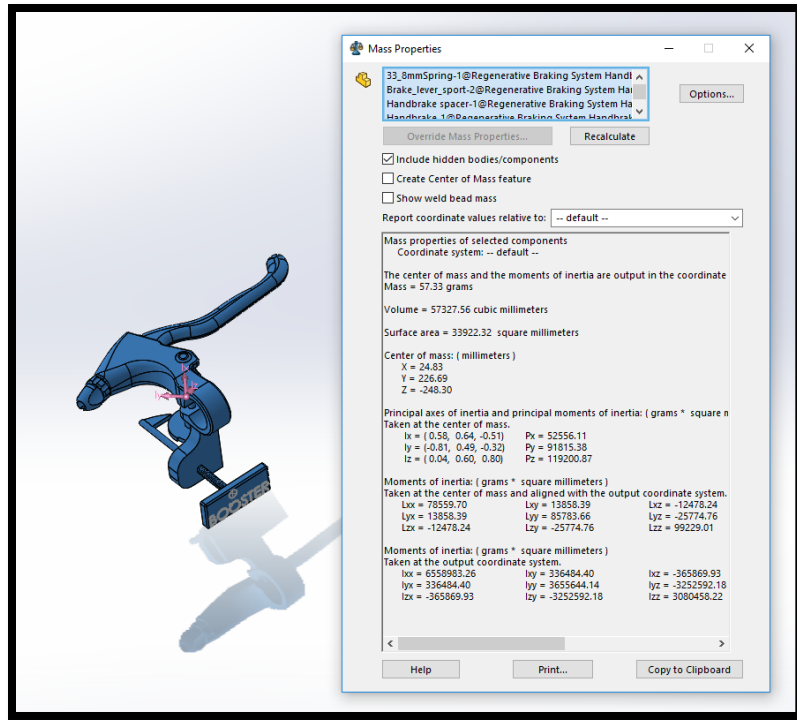


**Figure 9:** The mass of the handbrake control mechanism design

## Energy Storage Portion of the Regenerative Braking System

The energy storage portion of the regenerative braking system was divided into 3 different phases which are the initial-starting phase, energy storing phase, and friction braking phase. To control when the bicycle enter which stage, a three bar linkage is placed above the cone clutch spline, and one of the bars was a compression springs (**Figure 10**). Based on the actuation of linkages, the bicycle would enter into three different phases.

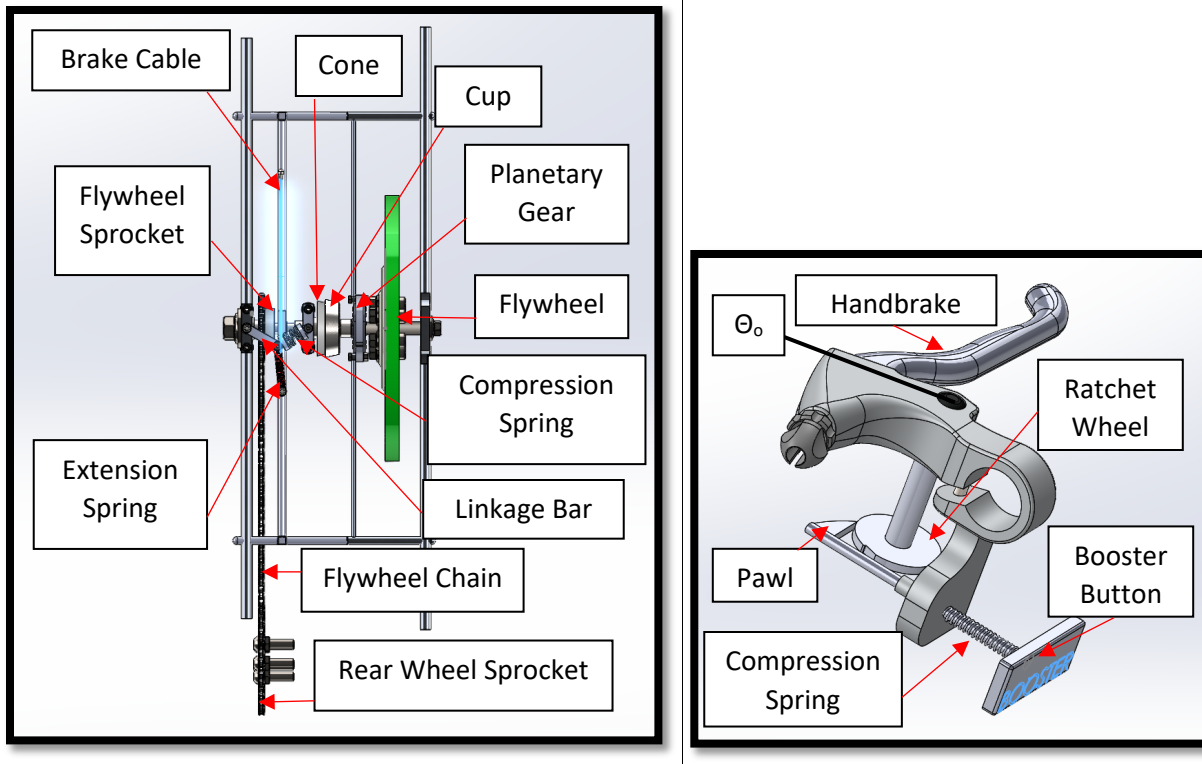


**Figure 10:** Initial-Starting Phase of the Energy Storing Stage (Left) and the Initial Handbrake and Ratchet Wheel's Teeth Positions (Right)

The control of the linkage was done by using a combination of an extension spring and the right braking cable that was located at the cone clutch middle pin **Figure 10 (Left)**. The purpose of the extension spring was to force the linkage back to its original position when the handbrake was not actuated. One end of the cable was connected to the pin located at the intersection between the movable bar and a compression spring; whereas, the other end of the cable was connected to the handbrake. When the handbrake was not pushed down (the starting stage,  $\theta_0$ ) as shown in the **Figure 10 (Right)**, the extension spring would be at its initial length, and the linkage bar and the compression spring would resemble an arrow shape point inward to the extension spring as shown in **Figure 10 (Left)**.

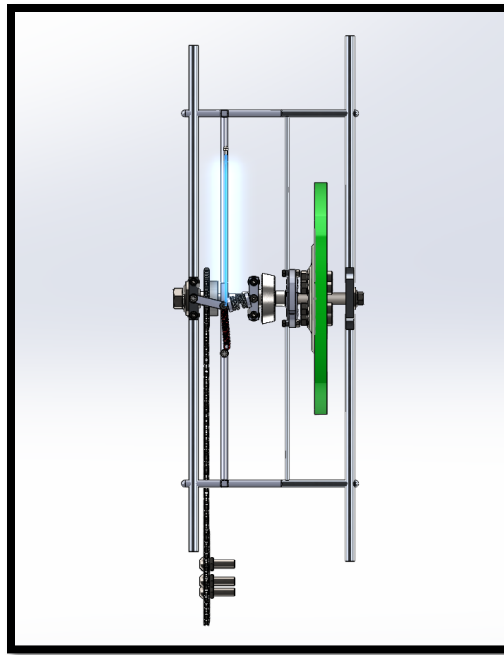


**Figure 11:** Beginning of the Energy Storing Phase of the Energy Storing Stage

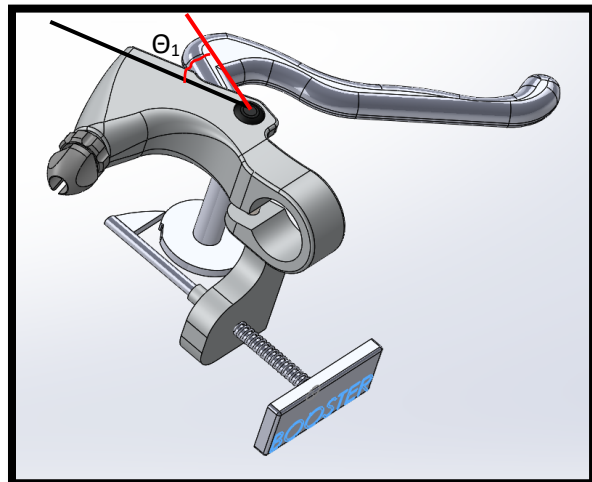
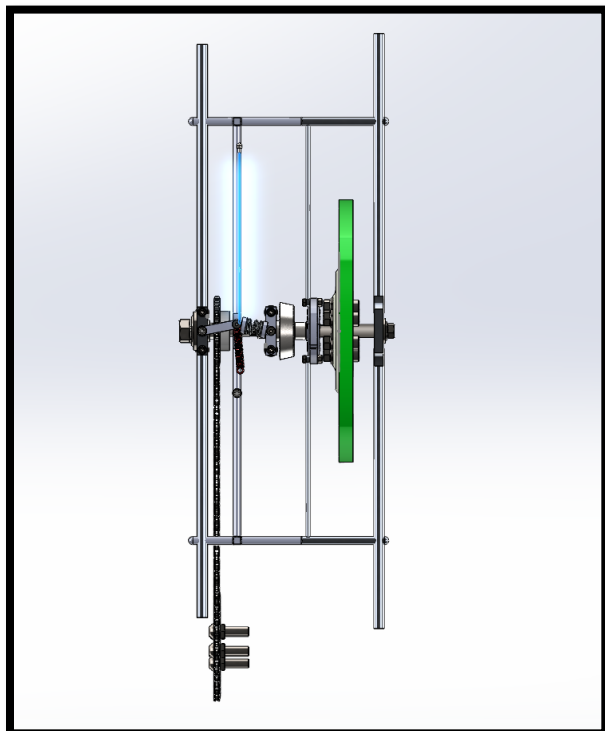


**Figure 12:** Ending of the Energy Storing Phase of the Energy Storing Stage (Left), and the Ending of the Energy Storing Phase Handbrake and Ratchet Wheel's Teeth Positions (Right)

The entire subassembly would remain in the initial position as shown in **Figure 10** until the left braking cable is pulled. When the rider pressed down the handbrake to an angle of few degrees after  $\theta_0$  where the energy storing stage began to the halfway point,  $\theta_1$ , where the energy storage ended (**Figure 12 (Right)**), the moveable bar and the compression spring would be in the position seen in **Figure 11 (Left)** and **Figure 12 (Left)**. The ratchet wheel would rotate to an exact same angle (i.e.,  $\theta_1$ ) as the handbrake, and the teeth of the ratchet wheel was just below the pawl as shown in **Figure 12 (Right)**. In the energy storing phase (regenerative), the cone clutch cone would be pushed towards the cone clutch cup by the linkage bar and the compression spring to connect with the cup as shown in **Figure 11** and **Figure 12 (Right)**. The compression spring in the three bar linkage would aid in increasing the contact time between the cone and cup of the cone clutch in this scenario. After the cone clutch was engaged, the flywheel would be linked to the rear-wheel-flywheel small sprocket. As a result, the kinetic energy was transferred from the rear wheel to the flywheel, and this process would reduce the speed of the bicycle.

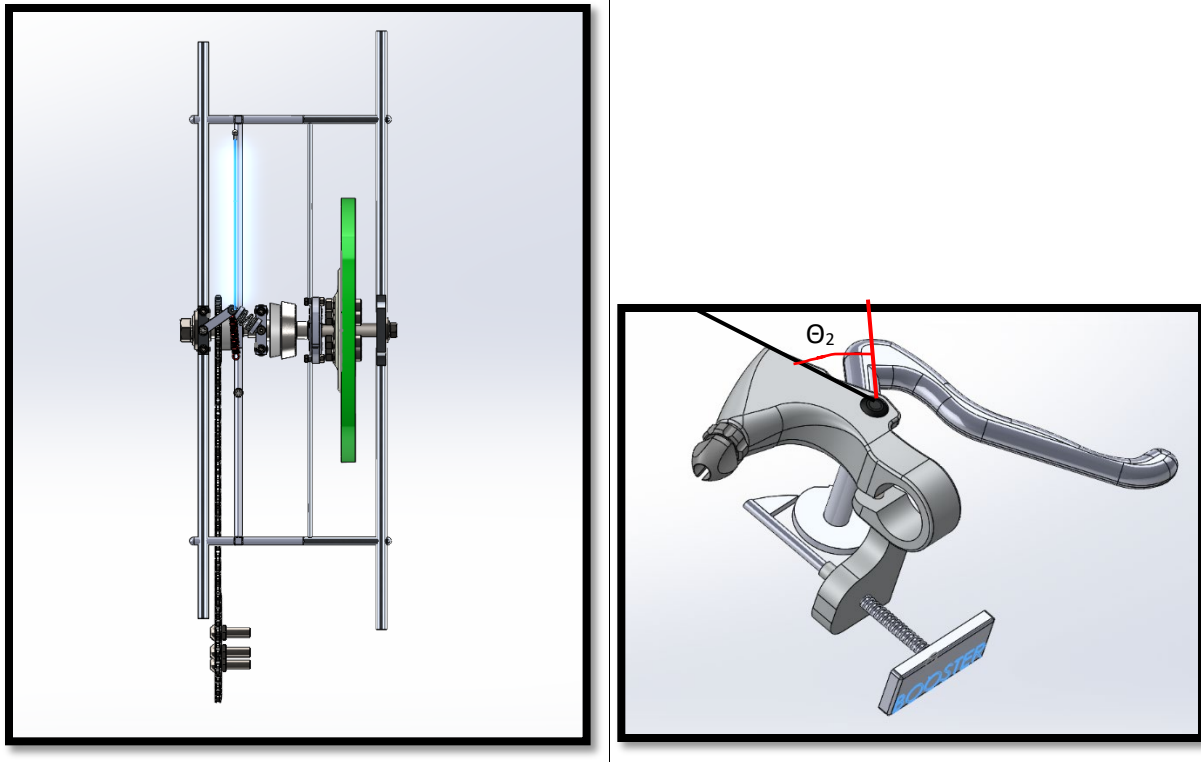


**Figure 13:** Friction Braking Phase of the Energy Storing Stage (Left), and the Friction Braking Phase Handbrake, and Ratchet Wheel's Teeth Positions (Right)

To initiate friction braking, the rider was required to press the handbrake down to the end,  $\theta_2$  (**Figure 13 (Right)**). At the friction braking stage, the linkage and the compression spring would resemble the one shown in **Figure 13 (Right)**. The cone and cup of the cone clutch would be pulled apart by the linkage. This caused the flywheel to disconnect from the flywheel sprocket, and the friction pad would stop the bicycle accordingly without stopping the flywheel in the process. The position of the ratchet wheel teeth would be on the right of the pawl as shown in **Figure 13 (Left)**.

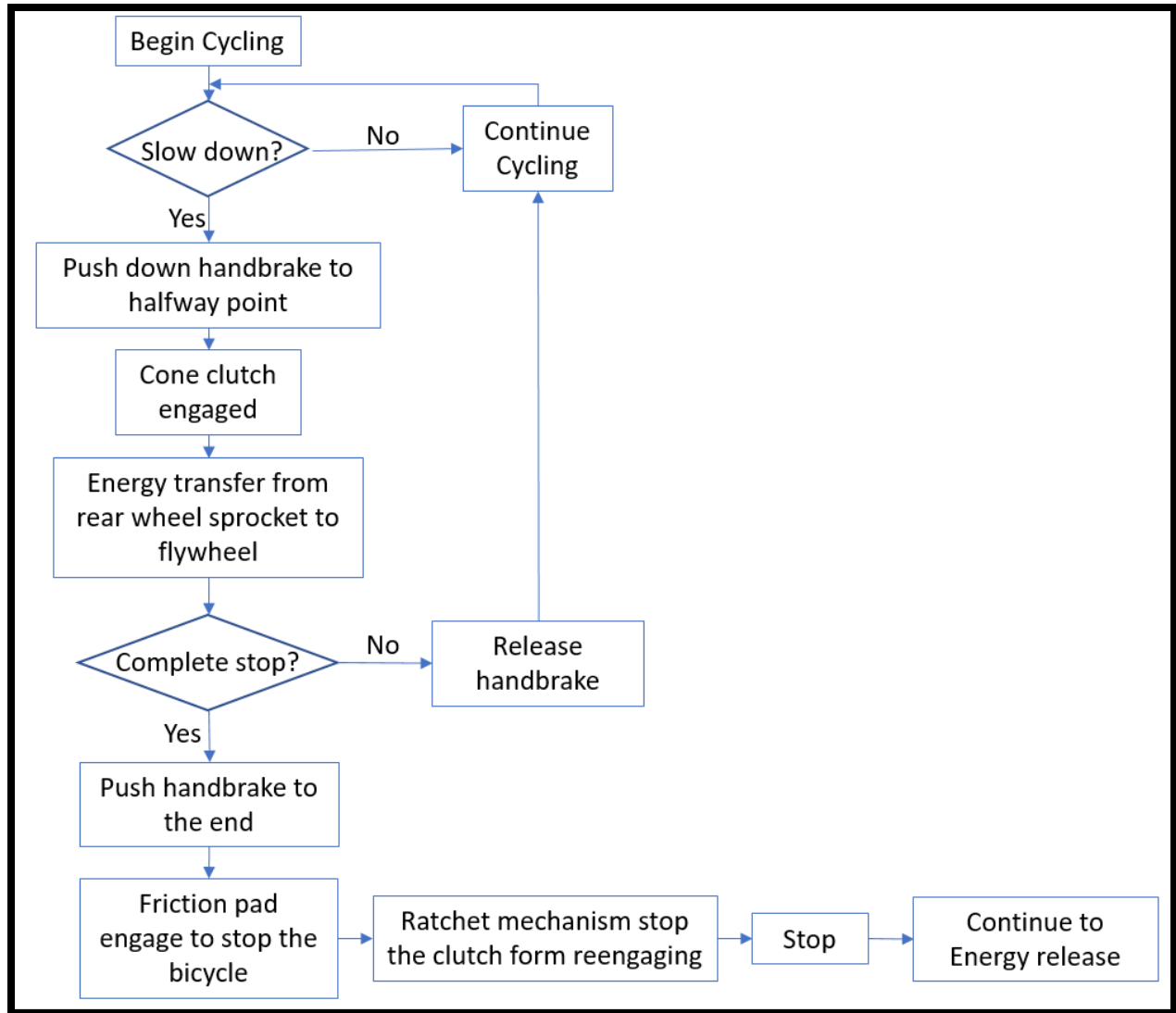


**Figure 14:** The Flowchart of the Energy Storing Portion

**Figure 14** clearly summarizes the sequence of the energy storage and presents how the rider of the bicycle could control the regenerative braking system with the handbrake mechanism easily during the energy storing process. With the handbrake control mechanism, the rider could easily control the engagement and disengagement of the cone clutch to allow the regenerative braking system to enter into two different modes which are the energy storing phase and friction braking phase by exerting a relatively small amount of force on the handbrake. Based on the EcoBoost analysis on the **Figure 14** flowchart, the speed of the rear wheel, sprockets, the cone of

the cone clutch would decrease, but the speed of the cone clutch cup, planetary gear, and the flywheel would increase at the beginning of the energy storing phase; then, the speed of the rear wheel, sprockets, cone, cup, planetary gear, and flywheel would reach to an equilibrium speed during the energy transfer before the end of the energy storing phase. Since the power was conserved throughout the regenerative braking energy storing stage, the torque of the components (i.e., the rear wheel, sprockets, and the cone of the cone clutch) would increase as the speed was decreased; if the speed of the components were increased, the torque of the components (i.e., cone clutch cup, planetary gear, and the flywheel) would decrease at the beginning of the energy storing phase.

## Energy Release Portion of the Regenerative Braking System

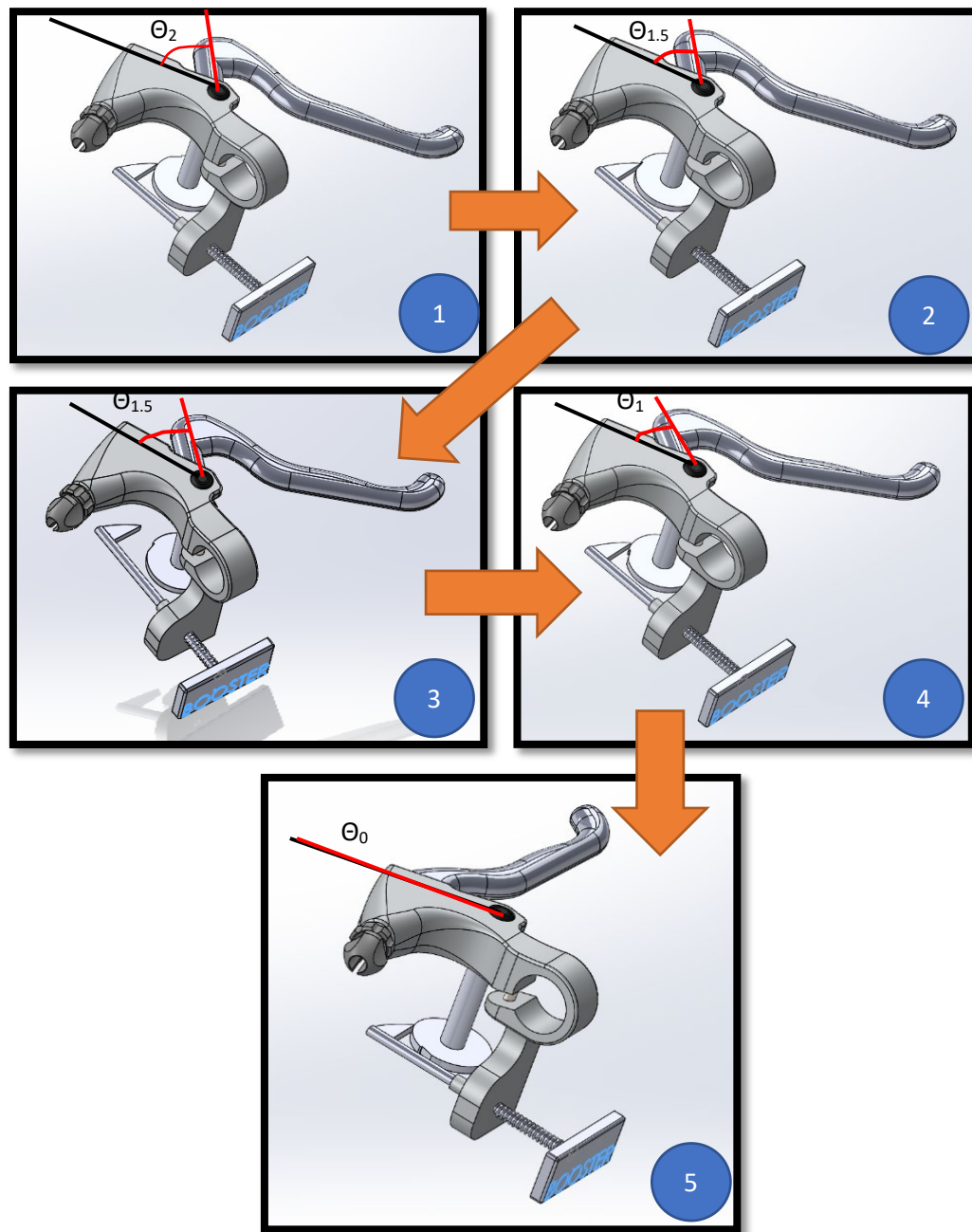


**Figure 15:** Ratchet Wheel Mechanism Process during the Energy Release Portion of the Regenerative Braking Design.

To precisely control the position where each stage triggers, a ratcheting mechanism was installed below the left handbrake to hold the handbrake in place at different stages as shown in

**Figure 15.** This gives bikers an option to have the handbrake released from  $\Theta_2$  and stuck at  $\Theta_{1.5}$  ( $\Theta_{1.5}$  is in between  $\Theta_1$  and  $\Theta_2$ ) as shown **Figure 15 (2)**. This option was to ensure that while the bicycle was at a complete stop, the braking pad was not in contact with the bicycle rear-wheel rim, and the cone and the cup was not in contact. The position  $\Theta_{1.5}$  was a special friction braking phase region to prevent the regenerative braking system entering the regeneration stage automatically without the awareness of the rider due to the actuation of the linkages that were pulled by an extension springs that have the sufficient elastic potential energy to return to their initial length as shown in **Figure 10 (Left)**. At the position  $\Theta_{1.5}$ , the bicycle was in a complete stop after the friction braking phase, the braking pad would not be in contact with the bicycle rear-wheel rim, and the cone clutch was still remained disengaged. To release energy back to the bicycle, the biker could press the “Booster” button as shown in **Figure 15 (3)**, which raises the pawl, allowing the handbrake to rotate back to  $\Theta_1$ . However, to fully utilize the energy stored, bikers should maintain the handbrake at an angle in between  $\Theta_1$  and  $\Theta_0$  as shown in **Figure 15 (4)**, **Figure 11** and **Figure 12**, until the bicycle is moving at the rider’s desired bicycle velocity. After that, the rider can release the handbrake entirely and start cycling like normal. To enter the entire regenerative braking system process again, the rider can repeat the steps as mentioned previously.

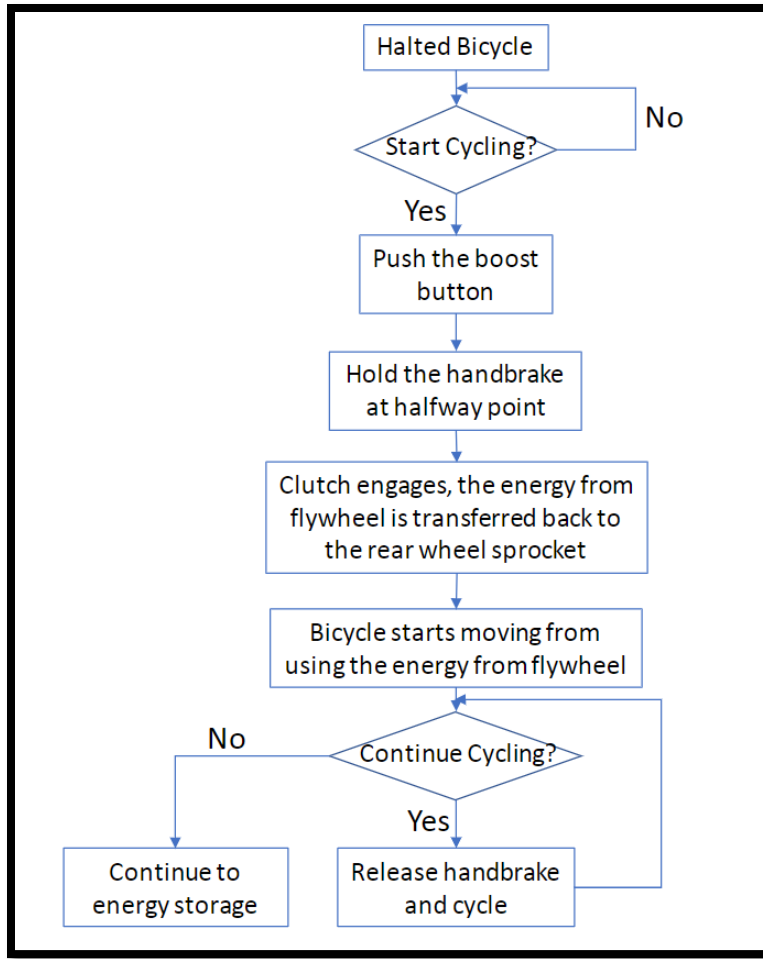


**Figure 16:** The Flowchart of the Energy Releasing Portion

**Figure 16** clearly summarizes the sequence of the energy release back to the bicycle rear wheel and demonstrates the ratchet wheel mechanism that was built below the handbrake had played an important role during the energy releasing stage. Based on the flowchart of the energy releasing portion, the locking between the ratchet wheel and the pawl helped to prevent the energy releasing stage to start automatically when the handbrake was released, and the rider could rest its hands while stopping. Pushing the pawl upwards by pressing the “Booster” button could help to accelerate the bicycle at a certain speed from rest by releasing energy from the rotating flywheel to the bicycle rear wheel; Furthermore, the rider was encouraged to hold the handbrake in between  $\theta_1$  and  $\theta_2$  to allow the rotational kinetic energy from the flywheel transfers to the rear wheel of the

bicycle fully. The rider could choose to re-enter the energy storing stage and energy releasing stage again by controlling the right handbrakes. Based on the EcoBoost analysis on the ***Figure 16*** flowchart, the speed of the rear wheel, sprockets, the cone of the cone clutch would increase, but the speed of the cone clutch cup, planetary gear, and the flywheel would decrease at the beginning of the energy releasing phase; then, the speed of the rear wheel, sprockets, cone, cup, planetary gear, and flywheel would reach to an equilibrium speed during the energy transfer before the end of the energy releasing phase. Since the power was conserved throughout the regenerative braking energy release stage, the torque of the components (i.e., cone clutch cup, planetary gear, and the flywheel) would increase as the speed was decreased; if the speed of the components were increased, the torque of the components (i.e., the rear wheel, sprockets, and the cone of the cone clutch) would decrease at the beginning of the energy releasing phase.

## 2. Energy Sizing, Storage, and System Level Engineering

From the first project report, ***Generative Brake Capacity Report***, of brake energy calculations, we have a total mass of 109.65 kg, a total moment of inertia of wheels =  $0.1870 \text{ kg}\cdot\text{m}^2$  as shown in the calculation below.

$$\text{Total Mass, } m_{\text{total}} = m_{\text{cyclist}} + m_{\text{bicycle}} + m_{\text{regenerative braking system}} + m_{\text{maximum payload}} = 109.65 \text{ kg}$$

*Equation 1: Total Mass of the bicycle*

$$\begin{aligned} \text{Total Moment of Inertia of wheels, } I_w &= I_{\text{rear wheel}} + I_{\text{front wheel}} \\ &= (mr^2)_{\text{rear wheel}} + (mr^2)_{\text{front wheel}} \\ &= 0.1870 \text{ kg}\cdot\text{m}^2 \end{aligned}$$

*Equation 2: Total Moment of Inertia of wheels*

$$\text{Brake Capacity, } E_{\text{Braking Capacity}} = 6.874 \text{ kJ}$$

Where  $I_f$  = the moment of inertia of the flywheel

$$n = \frac{\omega_f}{\omega_w}$$

*Equation 3: Velocity ratio between flywheel and rear wheel*

### Derivation of energy storage equation

For the process of energy storage, the energy conservation can be described with the following expression and can be assumed there is no friction loss from the cone clutch.

$$E_{\text{Braking Capacity}} = \frac{1}{2}m_{\text{total}}v^2 + \frac{1}{2}I_w\omega_w^2 + \frac{1}{2}I_f\omega_f^2$$

*Equation 4: Braking capacity*

Where  $E_f = \frac{1}{2} I_f \omega_f^2$  is the rotational energy of the flywheel after energy storage

We also have the relation

$$v = R\omega_w$$

*Equation 5: Conversion between angular velocity and velocity*

Where R denotes the radius of bike wheels

Then, the energy storage efficiency can be expressed as

$$\eta_1 = \frac{E_f}{E_{Braking\ energy}} = \frac{\frac{1}{2} I_f \omega_f^2}{\frac{1}{2} m_{total} v^2 + \frac{1}{2} I_w \omega_w^2 + \frac{1}{2} I_f \omega_f^2} = \frac{\frac{1}{2} I_f \omega_f^2}{\frac{1}{2} I_e \omega_w^2 + \frac{1}{2} I_f \omega_f^2} = \frac{I_f}{\frac{I_e}{n^2} + I_f}$$

*Equation 6: Energy storage efficiency equation*

Where  $I_e = m_{total}R^2 + I_w$  is the equivalent moment of inertia of the whole bicycle.

The energy storage efficiency becomes

$$\eta_1 = \frac{I_f}{\frac{I_e}{n^2} + I_f} \quad (1)$$

*Equation 7: Alternate form of energy storage efficiency equation*

From equation (1), it obvious that the energy storage efficiency is determined by flywheel inertia  $I_f$ , overall velocity ratio, and the equivalent moment of inertia of the whole bicycle  $I_e$

## Derivation of energy regeneration equation

For the process of regeneration, the velocity of the bicycle is zero while the flywheel has rotational kinetic energy  $E_f$  stored from the previous braking cycle. The equation describing the energy regeneration process due to energy conservation is presented as follows

$$E_f = \frac{1}{2} I_f \omega_f^2 = \frac{1}{2} I_e \omega_w'^2 + \frac{1}{2} I_f \omega_f'^2$$

**Equation 8: Flywheel energy equation**

Where  $E_k = \frac{1}{2} I_e \omega_w'^2$  : is the kinetic energy of the bicycle and the cyclist after energy regeneration

$\frac{1}{2} I_f \omega_f'^2$  : is the remaining rotational energy of the flywheel after energy regeneration.

Then, the energy regeneration efficiency can be expressed as

$$\eta_2 = \frac{E_k}{E_f} = \frac{\frac{1}{2} I_e \omega_w'^2}{\frac{1}{2} I_f \omega_f^2} = \frac{I_f}{I_e + I_f * n^2} \quad (2)$$

**Equation 9: Energy regeneration efficiency**

## Ideal Overall regeneration efficiency

The overall regeneration efficiency when friction loss during clutch engagement can be written as

$$\eta = \eta_1 \eta_2 \quad (3)$$

**Equation 10: Efficiency combining equation**

Substitute equations (1) (2) into (3) to obtain the ideal overall regeneration efficiency equation

$$\eta = \frac{I_f I_e}{(I_e + I_f n^2)(\frac{I_e}{n^2} + I_f)} \quad (4)$$

**Equation 11: overall regeneration efficiency equation**

Where  $I_e = m_{total} R^2 + I_w$  is the equivalent moment of inertia of the whole bicycle

$I_f$  is the moment of inertia of the flywheel

## Optimized selection of total velocity ratio for the regenerative braking system

It is noticed that the overall regenerative efficiency

$$\eta = \frac{I_f I_e}{(I_e + I_f n^2)(\frac{I_e}{n^2} + I_f)} \quad (4)$$

*Equation 11: overall regeneration efficiency equation*

Can reach the maximum value when

$$(I_e + I_f n^2) = (I_f + \frac{I_e}{n^2}) \quad (5)$$

*Equation 12: rearrange form of overall regeneration efficiency equation*

Solve equation (5) to obtain the following condition for maximum regenerative efficiency

$$n^2 = \frac{I_e}{I_f} \quad \text{Or} \quad n = \sqrt{\frac{I_e}{I_f}} \quad (6)$$

*Equation 13: Condition to find maximum regenerative efficiency*

Substitute (6) into (4) and the maximum overall regenerative efficiency becomes

$$\eta = \frac{I_f I_e}{(I_e + I_f \frac{I_e}{I_f})(I_f + I_f)} = \frac{1}{4} = 0.25$$

*Equation 14: Simplification of the overall regenerative efficiency equation*

Therefore, the maximum possible overall regenerative efficiency is 25%, which is independent of the flywheel inertia and the equivalent moment of inertia of the bicycle. The optimized velocity ratio,  $\eta$  should follow the relation

$$\eta = \sqrt{\frac{I_e}{I_f}}$$

From initial brake capacity calculations and flywheel design,  $I_e$  and  $I_f$  are known and they are

$I_e = 12.4444 \text{ kgm}^2$  and  $I_f = 0.1005 \text{ kgm}^2$  separately. Then the optimum overall velocity ratio

$$n_{optimum} = \sqrt{\frac{I_e}{I_f}} = \sqrt{\frac{12.4444}{0.1005}} = 11.12$$

$$n_{optimum} = 11.12$$

*Equation 15: Equation to find optimum velocity ratio*

To verify the derived optimum overall velocity ratio, a graph of velocity ratio,  $\eta$  versus.

Overall regeneration efficiency is plotted as is shown in **Figure 18**.

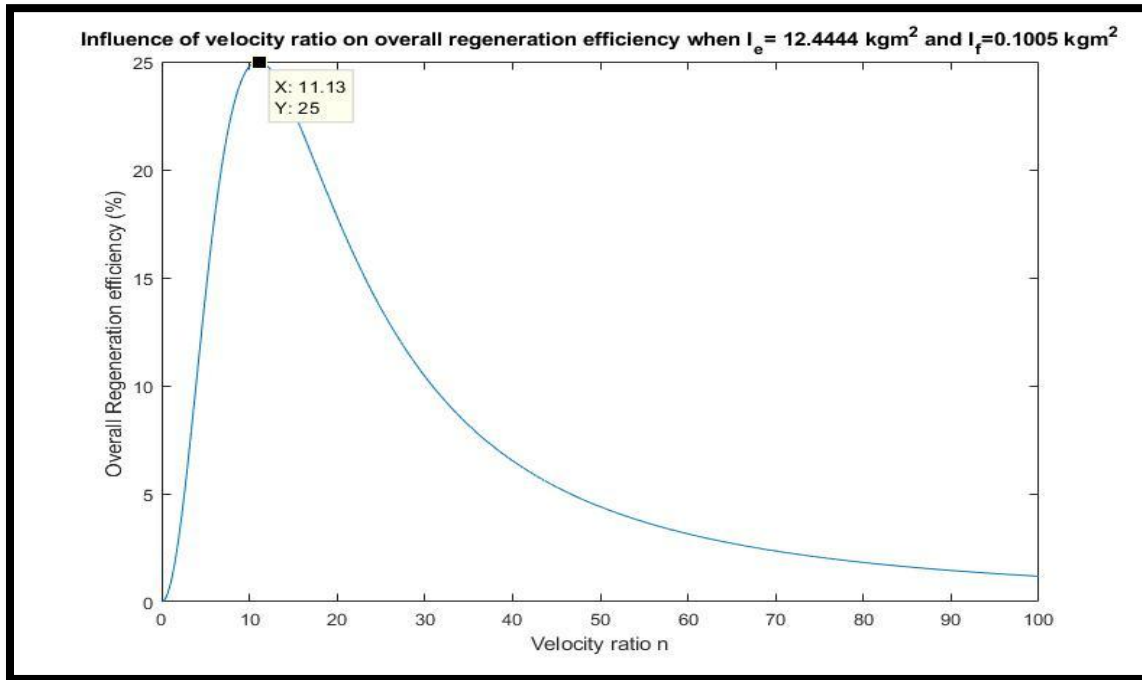


**Figure 17:** Velocity Ratio,  $\eta$  vs. Overall Regeneration Efficiency when  $I_e = 12.4444 \text{ kg m}^2$  and  $I_f = 0.1005 \text{ kg m}^2$

According to **Figure 18**, the maximum efficiency point occurs when the velocity ratio,  $n$  is 11.13, which is closed to the  $n_{optimum}$  (i.e., 11.12) from the previous calculation.

Based on the optimum total velocity ratio  $n_{optimum}$  is 11.12, the team plans to adopt a two-stage power transmission system which includes a planetary gearbox, a roller chain, and sprockets. The planetary gearbox forms the second stage of regenerative brake power transmission, while the sprockets and the chain form the first stage of brake energy transmission. The velocity ratio of the designed regeneration powertrain,  $\eta$  is 11.12 that is the same as the optimum value so that the system has the maximum overall regenerative efficiency of 25%. In this case, for the planetary gearbox, a steel planetary gears (Model: 75-7MLD) with a velocity ratio,  $VR_{Gearbox}$  of 7 was selected from MATEX (*Matex Gears*, 2018). Therefore, the optimum velocity ratio between the 2 sprockets,  $VR_{Chain}$  should be equal to 1.5886 as shown in the calculation below.

$$VR_{chain} = \frac{11.12}{7} = 1.5886$$

*Equation 16: Chain velocity ratio calculation (between planetary gear and sprocket)*

Considering that the number of teeth on the smaller sprocket,  $N_1$  is 18, the number of teeth on the larger sprocket,  $N_2$  is  $N_1$  divided by  $VR_{Chain}$  which is approximately 28.6. Since  $N_2$  should be an integer, the actual number of teeth in the larger sprocket,  $N_2$  is determined to be 28. The actual velocity ratio between the 2 sprockets is

$$VR_{chain} = \frac{N_1}{N_2} = \frac{29}{18} = 1.611$$

*Equation 17: Chain velocity ratio calculation (between small sprocket and large sprocket)*

The overall velocity ratio of the regenerative braking system during energy storage is calculated to be

$$VR_{energy\ storage} = VR_{chain} * VR_{gearbox} = 7 \times 1.611 = 11.2778$$

*Equation 18: Total velocity ratio of the regenerative braking system during energy storing*

The overall velocity ratio of the regenerative braking system during regeneration is:

$$VR_{regeneration} = \frac{1}{VR_{energy\ storage}} = 0.08867$$

*Equation 19: Total velocity ratio of the regenerative braking system during energy regeneration*

Which corresponds to the overall regenerative efficiency of 24.9975% when friction loss due to the cone clutch is neglected. Using all information of the actual velocity ratio above, the energy efficiency of the energy storage process,  $\eta_1$  is 49.53 %, and the energy efficiency of the regeneration efficiency,  $\eta_2$  is 50.47 %.

### **Analysis for energy and velocity of the bicycle and the flywheel at different states**

At the beginning of the energy storage (regenerative braking) process, the velocity of the bicycle is assumed to be 40 km/h and corresponding the braking capacity is 6.874 kJ. The flywheel angular velocity is assumed to be 0 rad/s at the outset. After the process of energy storage, the angular velocity of the flywheel is calculated to be 277.2164 rad/s. The calculation is done using the formula below:

$$\eta_1 = \frac{\frac{1}{2}I_f\omega_f^2}{E_{braking\ capacity}}$$

*Equation 20: Equation to calculate flywheel velocity after energy storage*

The value of  $\eta_1$  is 0.561, the efficiency during the regenerative braking phase. E braking capacity is the total energy of the bicycle before the regenerative braking happens. It includes

the kinetic energy of the bicycle and rotational energy from both of the wheels. The equation on the numerator is the energy stored inside the flywheel. By rearranging this equation and get an expression for  $\omega_f$ (angular velocity of the flywheel), the value for it can be calculated. Then the stored flywheel energy is calculated as:

$$E_s = \frac{1}{2} I_f \omega_f^2 = 3.8617 \text{ kJ}$$

*Equation 21: Calculation for flywheel velocity*

Using “ $v = R\omega_w$ ,” the velocity of the bicycle after generative braking is calculated to be 26.48 km/h, which means that the flywheel energy storage process can reduce the bike speed from 40 km/h to 26.4803 km/h.

### **Final velocity when at rest**

For the purpose of the design process, the velocity of flywheel when at rest will be the same as the velocity when regenerative braking ended. In addition, the assumption of the flywheel not slowing down over time due to friction and drag is in place. Therefore when at rest, the flywheel angular velocity remains 277.2164 rad/s.

### **Flywheel velocity after regeneration & overall energy efficiency of the system**

During the regeneration stage, assume that the initial speed of the bicycle is zero, and the flywheel is the only component that has a stored energy, which is  $E_s = 3.8617 \text{ kJ}$ . Assume that the rider does not step on the pedals, and the bicycle is started by flywheel energy only. To simplify the problem, it is also acceptable to assume there is no energy losses due to friction

between the ground and the tires, and the air drag. The equation below described the regeneration process can then be written as:

$$\eta_2 = \frac{\frac{1}{2}I_e\omega_w'^2}{E_s}$$

*Equation 22: Equation to calculate wheel velocity after regeneration*

Using the above equation, with the assumptions and value calculated from before, all terms will be known except  $\omega_w'$  (wheel velocity). The final value for  $\omega_w'$  is 13.8436 rad/s. The final velocity of the bicycle after regeneration then become  $v_{final} = \omega_w' r_{wheel} = 16.9934 \text{ km/h}$ . Then, the velocity ratio equation shown below is used to relate angular velocity of the wheel to the flywheel.

$$n = \frac{\omega_f'}{\omega_w'}$$

*Equation 23: Velocity ratio between flywheel and wheel*

As a result, the remaining angular velocity in the flywheel,  $\omega_f'$  is calculated to be 1.4248 rad/s.

The overall efficiency of the energy storage system, can be calculated as

$$\eta_{actual} = \frac{E_{total}\eta - E_{loss}}{E_{total}}$$

*Equation 24: overall efficiency of the energy storage system*

where  $E_{total}$  = the total kinetic energy of the bicycle, calculated from previous analysis

$\eta$  = is the ideal overall efficiency of the system, calculated from previous calculations

$E_{loss}$  is the frictional loss during clutch engagement process,  $E_{loss} = 881.9460 J$

from cone clutch analysis in chapter 5

Substitute all numerical values into the equation above to obtain the overall efficiency generative breaking system being 12.1%

$$\eta_{actual} = \frac{E_{total}\eta - E_{loss}}{E_{total}} = \frac{6.8744*10^3 * 0.25 - 881.9460}{6.8744*10^3} = 12.17\%$$

*Equation 25: Actual calculation for overall efficiency generative breaking system*

### 3. Detailed Design of Energy Storage Element

#### Dimensions and Mass moment of inertia for Flywheel design

The moment of inertia of the flywheel  $I$  can be calculated as  $I_f = \frac{1}{2}mR^2$ , which means that the flywheel inertia can be increased by improving the radius and the mass. The team measured the sizes and dimensions of one BO-CB024 bicycle and the results show that the flywheel diameter has to be less than 33 mm in order to be installed on the bike. Therefore the flywheel diameter was determined to be 30mm. The flywheel thickness  $t$  was determined to be  $t = 10\text{mm}$  to leave sufficient lateral space to mount the adjacent gearbox, sprocket, and the cone clutch. Choose AISI 1015 Steel as the flywheel material which has a density of  $7870 \text{ kg/m}^3$ . Apply the material to the flywheel CAD model established on Solidworks, and the flywheel moment of inertia was calculated to be  $0.1005 \text{ kg}\cdot\text{m}^2$  as shown in **Figure 17**.

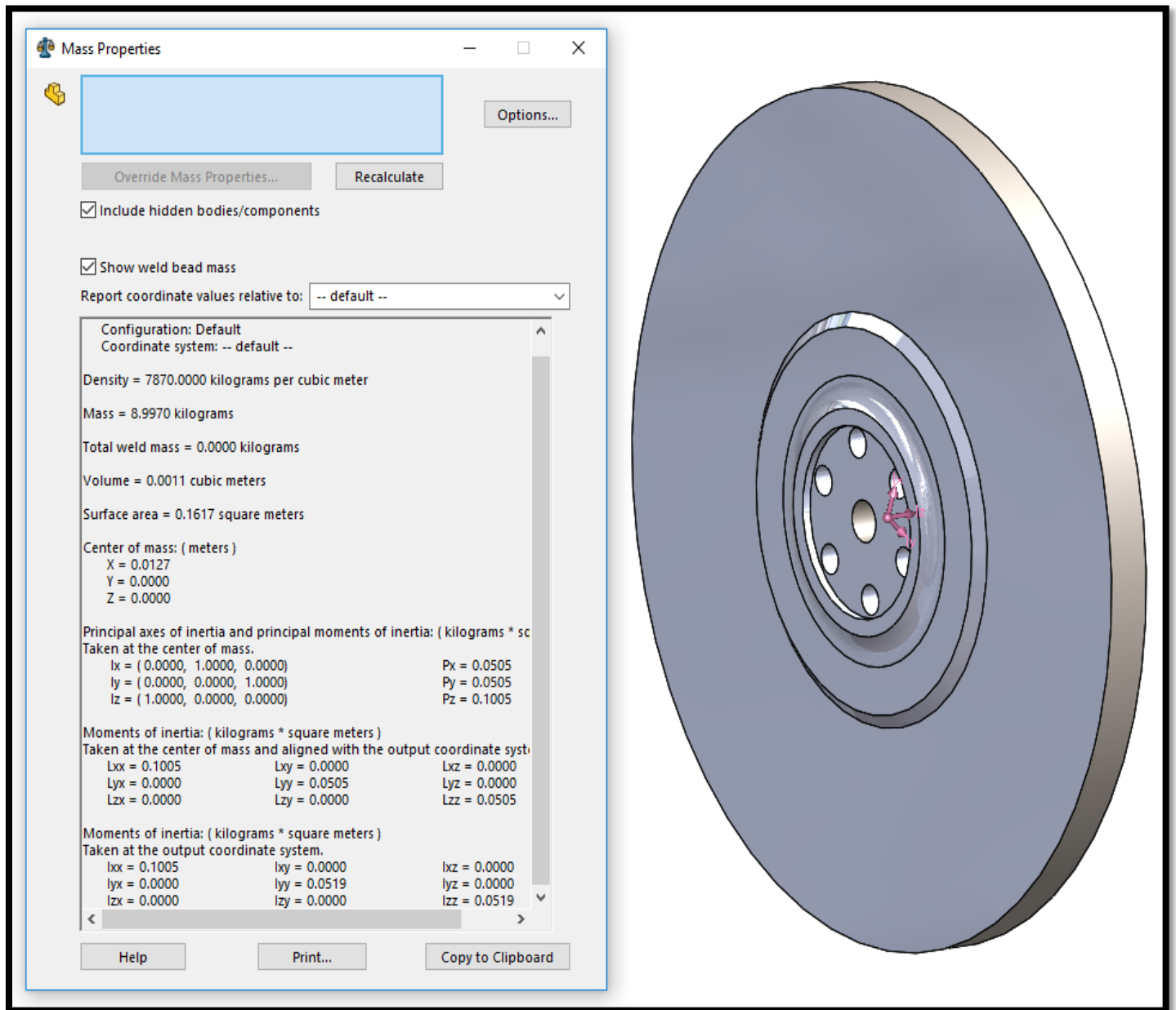


**Figure 18:** CAD Flywheel Design and Material Properties.

## 4. Detailed Design of Energy Storage and Release Drivetrain and System

Although sprockets with more teeth is preferred for delivering a high speed, in many scenarios, a smaller sprocket is more advantageous in the ways of providing a smooth ride, a better life expectancy, and low noise. More importantly, if sprockets are selected improperly, the chain drive would synchronize the cutting of the film, when the cut sheets' lengths have large variation, it can cause vibration within the system. With such considerations, sprocket sizes were selected. According to *Intermediate Report*, regeneration efficiency reaches peak value at velocity ratio of 11.13 (**Figure 18**). Based on which, the team plans to adopt a two-stage power transmission system which includes a planetary gearbox, a roller chain, and sprockets. The planetary gearbox forms the second stage of regenerative brake power transmission, while the sprockets and the chain form the first stage of brake energy transmission. The velocity ratio of the designed regeneration powertrain,  $n$  is 11.12 that is the same as the optimum value so that the system has the maximum overall regenerative efficiency of 25%. In this case, for the planetary gearbox, a steel planetary gears (Model: 75-7MLD) with a velocity ratio,  $VR_{Gearbox}$  of 7 was selected from MATEX ( Matex Gears , 2018). Therefore, the optimum velocity ratio between the 2 sprockets,  $VR_{Chain}$  should be equal to 1.5886 as shown in the calculation below.

$$VR_{Chain} = \frac{11.12}{7} = 1.5886$$

*Equation 16: Chain velocity ratio calculation (between planetary gear and sprocket)*

Considering that the number of teeth on the smaller sprocket,  $N_1$  is 18, the number of teeth on the larger sprocket,  $N_2$  is  $N_1$  divided by which is approximately 28.6. Since  $N_2$  should be an integer,

the actual number of teeth in the larger sprocket,  $N_2$  is determined to be 29. The actual velocity ratio between the 2 sprockets is

$$V R_{Chain} = \frac{N_2}{N_1} = \frac{29}{18} = 1.611$$

*Equation 17: Chain velocity ratio calculation (between small sprocket and large sprocket)*

### Selection of sprocket and roller chain

The specifications of the two sprockets are shown in **Figure 19** and **Figure 20**.

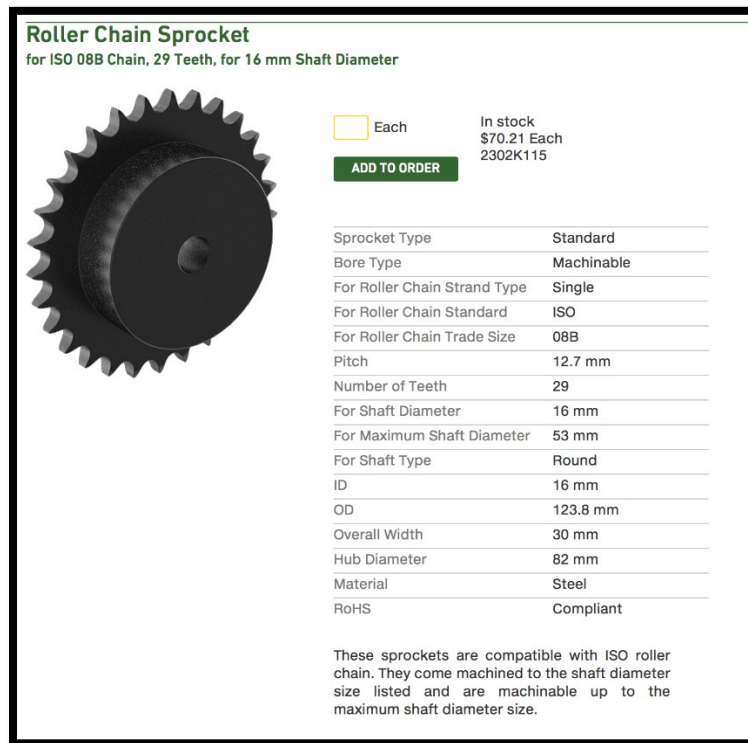


**Figure 19:** Specification of the larger sprocket for the regeneration system

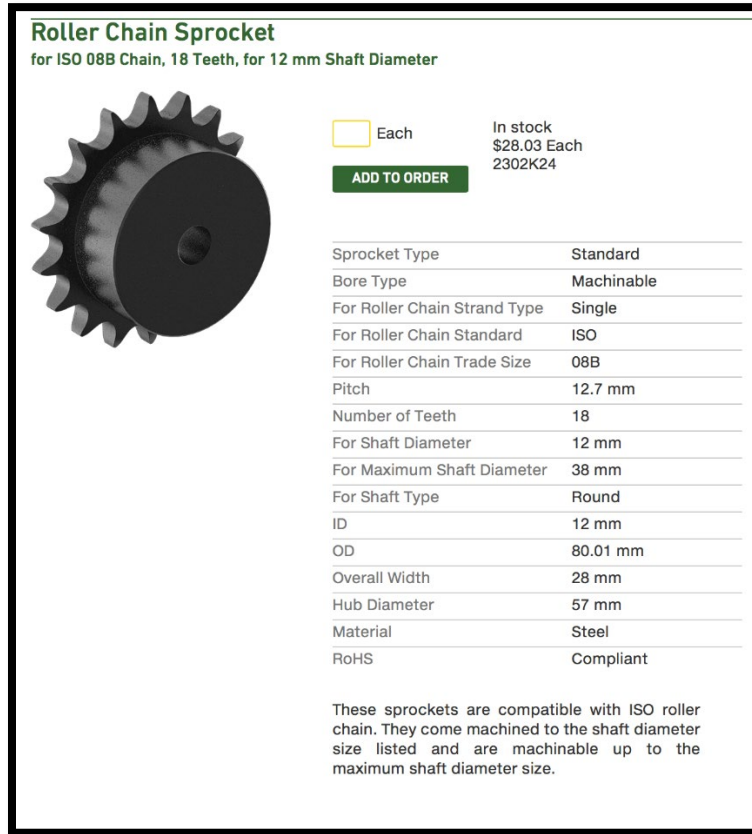


**Figure 20:** Specification of the larger sprocket for the regeneration system

Parameters including sprocket diameter, chain velocity, maximum and minimum exit velocity, and speed variation were calculated:

$$D_{18\ teeth} = \frac{p}{\sin(180^\circ/N)} = \frac{12.7}{\sin(180^\circ/18)} = 73.136\text{mm}$$

$$D_{29\ teeth} = \frac{p}{\sin(180^\circ/N)} = \frac{12.7}{\sin(180^\circ/29)} = 117.46\text{mm}$$

$$V_{18teeth} = \frac{Npn}{12} = 388\text{ft/min}$$

$$V_{29teeth} = \frac{Npn}{12} = 626ft/min$$

$$v_{max18} = \frac{\pi Dn}{12} = 390ft/min$$

$$v_{max29} = \frac{\pi Dn}{12} = 627ft/min$$

$$v_{min18} = \frac{\pi dn}{12} = 384ft/min$$

$$v_{min29} = \frac{\pi dn}{12} = 623ft/min$$

$$\frac{\Delta V}{V_{18teeth}} = \frac{v_{max} - v_{min}}{V} = 0.1546$$

$$\frac{\Delta V}{V_{29teeth}} = \frac{v_{max} - v_{min}}{V} = 0.00639$$

*Equation 26: Sprocket specification calculations*

In this section, a detail analysis of both the cone clutch and ratchet mechanism will be given. The cone clutch's analysis will be discussed before the ratchet mechanism. To find a suitable cone clutch and its complementary components, the following analysis is done.

## Capacity of the cone clutch

To calculate the capacity of the cone clutch, the bicycle and the regenerative braking device should be simplified as a two-inertia system consisting  $I_1$  and  $I_2$  as is shown in **Figure 21 below**.

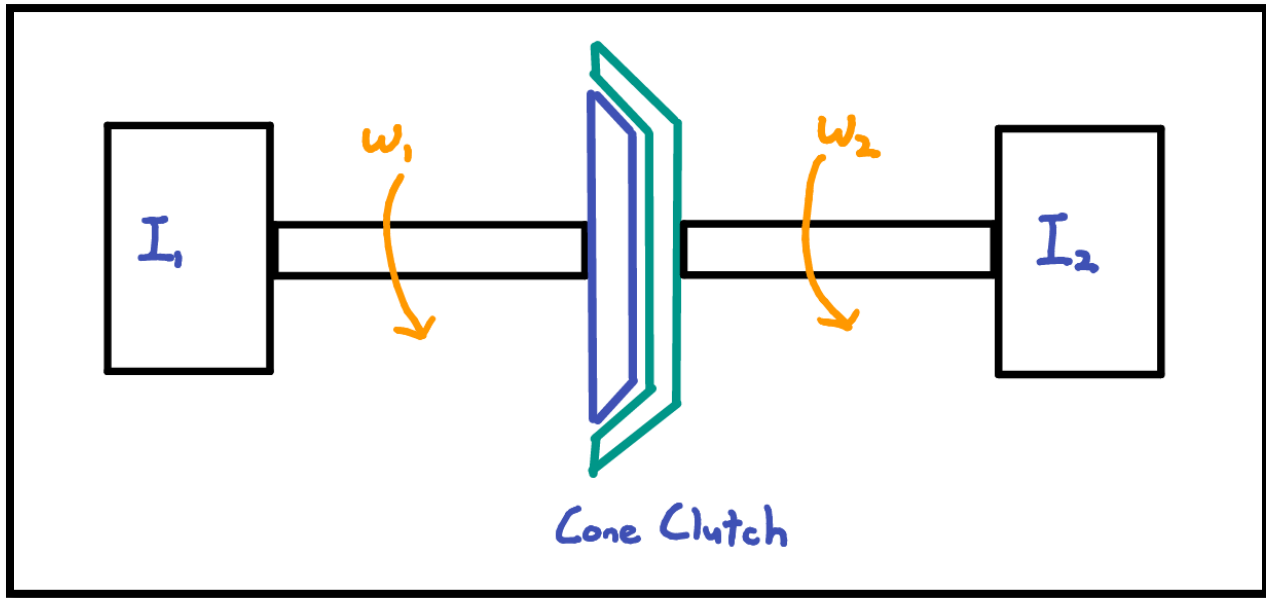


**Figure 21:** Two-inertia system consisting  $I_1$  and  $I_2$

$I_1$  is formed by the bike frame, wheels and all other mechanical components at the side of the cone of the cone clutch, while  $I_2$  is formed by mechanical components at the cup side of the cone clutch.

$I_1$  and  $I_2$  can be calculated as

$$I_1 = \frac{I_e}{n_{sprockets}^2} = \frac{12.1424}{1.6111^2} = 4.6779 \text{ kgm}^2$$

$$I_2 = n_g^2 I_f = 7^2 * 0.1005 = 4.9245 \text{ kgm}^2$$

*Equation 27: Inertia calculation*

where  $n_{sprockets}$  denotes the velocity ratio between 2 sprockets of the brake energy regeneration system and  $n_g$  denotes the velocity ratio of the planetary gearbox.

We also have the initial speeds of half shafts of the cone clutch:

$$\omega_1 = \omega_{rearwheel} * n_{sprockets} = 54.2133 \frac{rad}{s}$$

$$\omega_2 = 0 \frac{rad}{s}$$

*Equation 28: Angular velocity of both side of the shaft*

From Shigley's textbook (p848), the clutch torque required to finish the energy storage process can be written as

$$T = I_1 I_2 \frac{\omega_1 - \omega_2}{t_1(I_1 + I_2)} \quad (1)$$

Where  $t_1$  is the time required to enable the two halves of the clutch to reach the same speed.

Assume that the energy regeneration process lasts for  $t_1 = 4 s$ , which means that the velocity difference between both half of the clutch will be zero after 4 seconds. Then the clutch torque was calculated as  $T = 17.0992 \text{ N m}$  using MATLAB after plugging in all relevant variables.

From Shigley's textbook (p848), the frictional energy loss during the clutch operation is expressed as

$$E = \frac{I_1 I_2 (\omega_1 - \omega_2)^2}{2(I_1 + I_2)} \quad (2)$$

*Equation 29: Energy due to friction loss for cone clutch*

Through Equation 29, the frictional loss during the energy storage process was calculated to be  $E_{energy\ storage\ loss} = 881.9460\ J$  using the corresponding MATLAB code

### Sizing the cone clutch

Assume that the outer diameter of the cone clutch,  $D = 188\ mm$ , the inner diameter of the clutch,  $d = 120\ mm$  and the cone angle of  $\theta = 10\ deg$ . For friction material, the team decides to use sintered metal (dry), which has a friction coefficient  $f=0.3$ , maximum pressure  $P_{max} = 350\ psi = 2413\ kPa$  and maximum velocity,  $V_{max} = 3600\ ft/min$ .

Under the assumption of uniform wear, the cone clutch operating force can be calculated using

$$F = \frac{4T\sin(\alpha)}{f(D+d)}$$

*Equation 30: Cone clutch operating force*

The actual maximum pressure

$$P_a = \frac{2F}{\pi d(D-d)}$$

*Equation 31: Maximum pressure for cone clutch*

Substitute all numerical values from previous calculations and determined clutch parameters into Equations 30, Equation 31, and the cone clutch operating force is calculated to be  $F = 128.5390N$  and the maximum pressure  $P_a = 10.0282\ kPa$ . Apparently, the actual maximum pressure  $P_a=10.0282\ kPa$  is much lower than the allowable pressure of the friction material ( $P_{max} = 350\ psi=2413\ kPa$ ), thus the cone clutch design should be safe.

Now we have parameters of the cone clutch design: the outer diameter D=188 mm, the inner diameter d=120 mm, the cone angle  $\theta = 10 \deg$

Design of the cone clutch is shown below and available in appendix too (**Figure 59**).

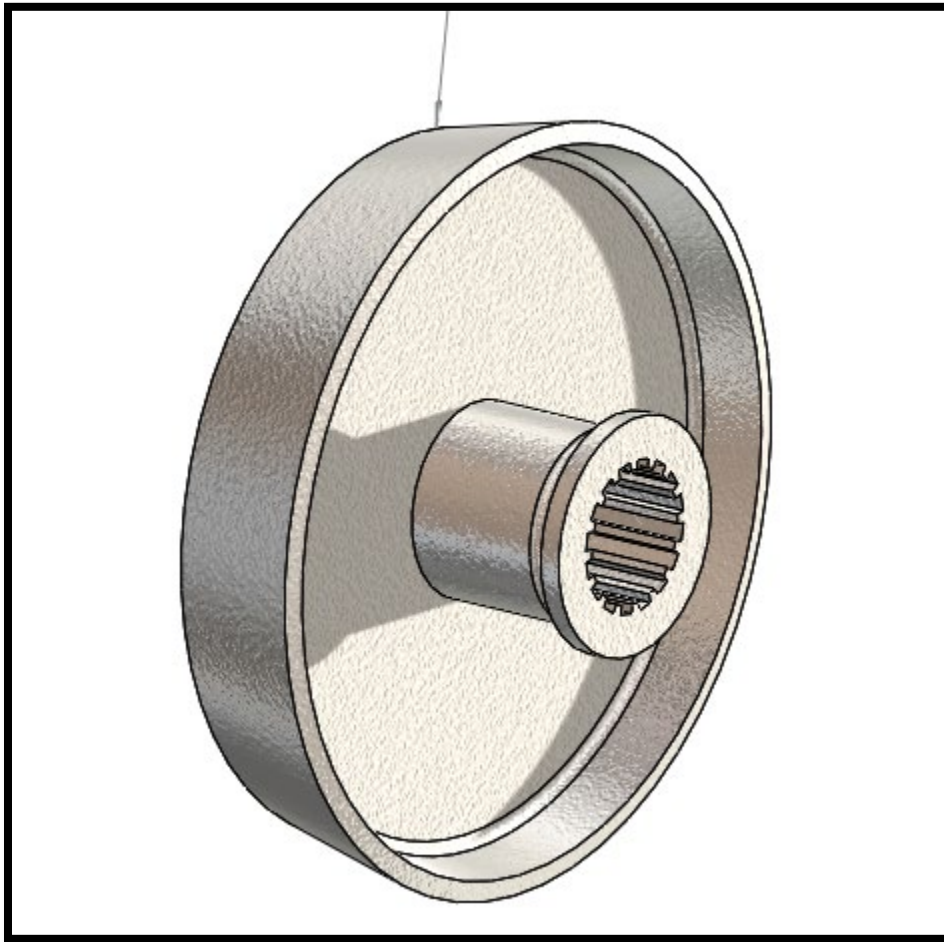


**Figure 22:** CAD model of the cone clutch designed

## Analysis for the cone clutch actuation mechanism

As is shown on **Figure 23**, the cone clutch actuation system consists of a rigid bar 1, compression spring 1 and return spring 2. The rigid link, compression spring 1 and the fork form a slider-crank mechanism to engage or disengage the clutch. Assume that the length of the rigid bar 1 and the spring 1 are the same with the value of  $b = 40\text{mm}$ .

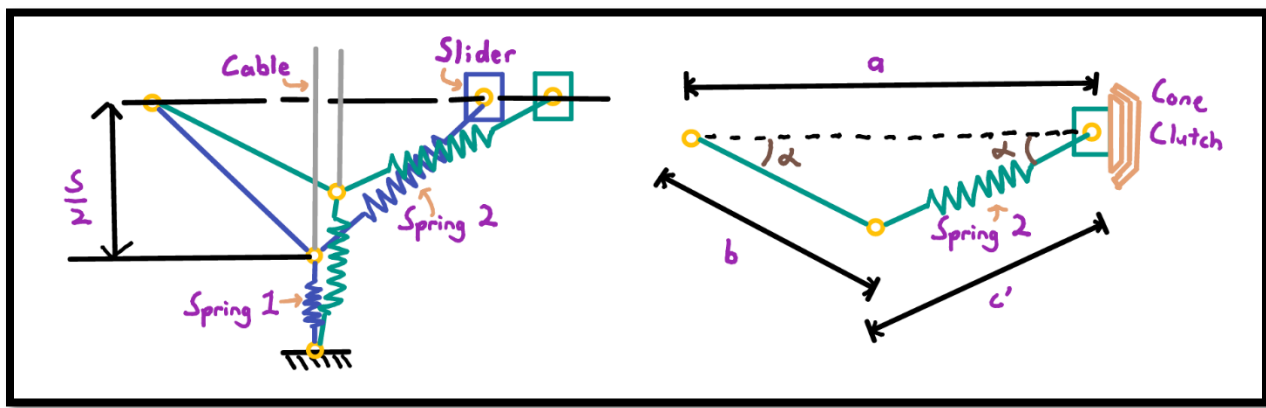


**Figure 23:** Three important position for the three bar linkage

As is shown on **Figure 24**, when bar is located at the initial position  $\alpha = \alpha_0$ , a geometrical relation can be derived as follows,

$$\alpha_0 = 2 \sin^{-1} \left( \frac{s}{4b} \right) \quad (6)$$

**Equation 32:** Geometrical approach to find initial angles of the linkages

Where  $s$  is the motion range of the brake cable, and  $s=20\text{mm}$  measured from an existing bicycle.

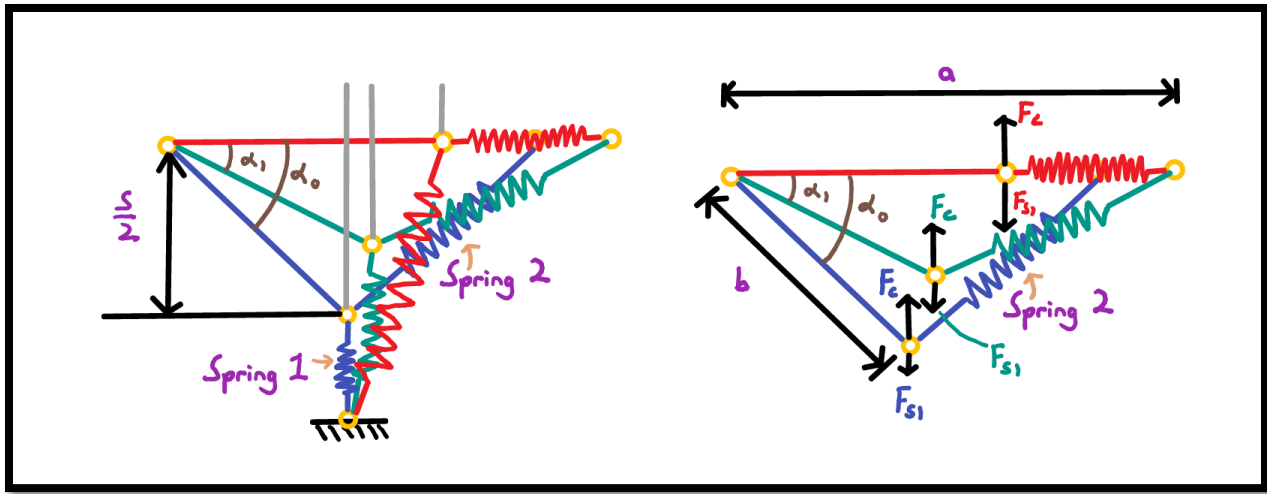


**Figure 24:** Free body diagram of the actuation mechanism at different positions

As is shown on **Figure 24**, the initial position of bar 1 is then calculated to be  $\alpha_0 = 14.3615 \text{ deg}$ .

Bar 1 position  $\alpha_1$  is where the cone reaches the clutch cup and spring 2 starts to become compressed during the energy storage process. Assume  $\alpha_1 = 0.8\alpha_0 = 0.2005 \text{ rad}$ , and the distance between the fixed revolute joint of bar 1 and the clutch engagement position can be expressed as

$$a = 2b\cos(\alpha_1)$$

*Equation 33: Calculate the length of the two movable linkages when they are straight*

which gives  $a = 78.6\text{mm}$  as the result of the corresponding MATLAB program.

When bar 1 and compression spring 2 are collinear, the cone clutch is fully actuated and operates with the maximum torque of 17.0992 Nm. At this instance, spring 2 has the maximum deflection

$$y_2 = 2b - a = 2 * 40 - 78.6 = 1.4\text{mm}$$

*Equation 34: Maximum deflection for spring*

The desired rate of compression spring 2 becomes

$$K_2 = \frac{F}{y_2} = \frac{128.5390\text{N}}{1.4\text{mm}} = 80.185 \text{ N/mm}$$

*Equation 35: Desired spring rate calculation*

### Selection and verification of the fatigue strength of spring 2

From Century Spring website (2018), one 72123 Compression Springs was chosen as spring 2 with parameters shown as follows,

Ends	Closed/Ground - CG
Free Length (mm)	19.0
I. D. (mm)	12.60
Suggested Max Load (N)	369.202
Material	Music Wire - MW
O. D. (mm)	18.29
Rate (N/mm)	82.134
Solid Length (mm)	11.7
Suggested Max Deflection (mm)	4.57
Total Coils	4.13
Wire Dia (mm)	2.84

*Figure 25: Specifications of spring 2*

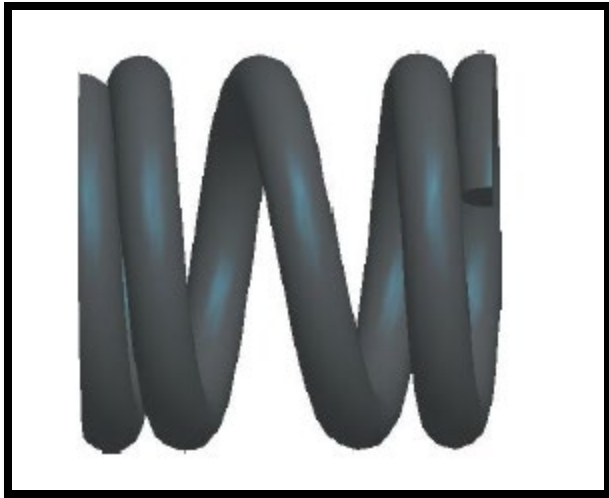


**Figure 26:** CAD model of spring 2

Spring parameters: Free length  $L_0=19$  mm, Inner diameter ID = 12.6mm, Outer diameter OD=18.29 mm, spring rate  $k_2=82.134$  N/mm, solid length  $L_s=11.7$  mm, total coils,  $N_t=4.13$ , wire diameter d = 2.84mm, and the material is music wire

Forces: From previous analysis of cone clutch mechanism, the deflection of compression spring 2 is  $y_2 = 1.4mm$ . Hence the maximum spring force should be  $F_{max} = k_2 y_2 = 131.6625N$ . The compression spring should be able to withstand 128.5390 N of actuation force; therefore, it is appropriate to assume that the spring load fluctuates between 0 and 131.6625N. Hence,  $F_{max} = 131.6625$  N, and  $F_{min} = 0$  N.

From Chapter 10 of Shigley's Mechanical design, we also have the following parameters  $A = 2211 \text{ Mpa} * \text{mm}^m$ ,  $m=0.145$ ,  $S_{sa}=241\text{MPa}$ ,  $S_{sm}=379 \text{ MPa}$ ,  $S_{se}=309.9883 \text{ Mpa}$

Substitute all knowns into the equations below from Shigley's book and use corresponding MATLAB codes to calculate the fatigue safety factor of the spring

$$\text{Mean coil diameter} \quad D = 0.5 * (ID + OD) = 0.0154 \text{ m}$$

$$C = \frac{D}{d} = 5.4384$$

$$\text{Stress Correction factor} \quad K_B = \frac{4C+2}{4C-3} = 1.2666$$

$$\text{Tensile strength} \quad S_{ut} = \frac{A}{d^m} = 1.9005 * 10^9 \text{ Pa}$$

$$\text{Yield strength} \quad S_{sy} = 0.56S_{ut} = 1.0643 * 10^9 \text{ Pa}$$

$$\text{Stability criterion} \quad L_0 < 2.63 \frac{D}{\alpha}$$

Since the spring is supported by 2 parallel plates,  $\alpha = 0.5$ . Then  $L_0 = 19 \text{ mm} < 2.63 \frac{D}{\alpha} =$

$81.2 \text{ mm}$  implies that the compression spring is stable and will not buckle under large value of loads

$$\text{The torsional modulus of rupture} \quad S_{su} = 0.67S_{ut} = 1.2733 * 10^9 \text{ Pa}$$

$$\text{Amplitude of load} \quad F_a = 0.5(F_{max} - F_{min}) = 64.2695 \text{ N}$$

$$\text{The mean of load} \quad F_m = 0.5(F_{max} + F_{min}) = 64.2695 \text{ N}$$

$$\text{Shear stress amplitude} \quad \tau_a = K_B \frac{8F_a D}{\pi d^3} = 1.3977 * 10^8 \text{ Pa}$$

$$\text{The midrange shear stress} \quad \tau_m = K_B \frac{8F_m D}{\pi d^3} = 1.3977 * 10^8 \text{ Pa}$$

Modified Goodman failure criterion

$$\frac{1}{n} = \frac{\tau_a}{S_{se}} + \frac{\tau_m}{S_{su}}$$

*Equation 36: Modified Goodman failure criterion approach to calculate fatigue safety factor for spring used in three bar linkage*

Using the modified Goodman failure criterion above and the fatigue safety factor of the spring is calculated to be,  $n = 1.7836$ . Since the safety factor is greater than 1, compression spring 2 satisfies design requirements.

### Analysis for the return spring 1

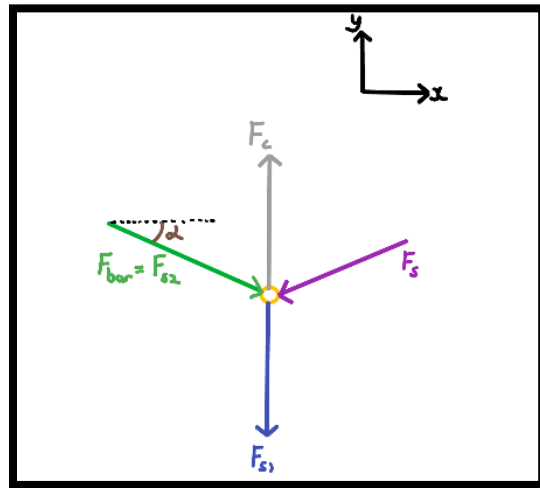


**Figure 27:** Free body diagram of pin

As is shown on the free body diagram for the system of pin 1, which connects link 1, actuation spring 2, return spring 1 and the actuating cable, we have the following force equation at equilibrium.

$$\sum F_y = F_c - F_{s1} - 2F_{s2} * \sin(\alpha) = 0$$

*Equation 37: Force analysis in y-direction for return spring*

Where  $F_c = \text{constant cable force}$

Compression spring force  $F_{s2} = K_2(b - l')$  (11) and  $l'$  is the length of the compression spring assembly.

The extension spring force  $F_{s1} = K_1 b \sin(\alpha)$

Using the geometry relation,  $l'$  can be calculated as

$$l' = \sqrt{a^2 + b^2 - 2ab\cos(\alpha)}$$

*Equation 38: length of the return spring equation*

Combine Equations 37, 38 and (11) and obtain the relation

$$|F_c - F_{s1}| = 2K_2(b - \sqrt{a^2 + b^2 - 2ab\cos(\alpha)})\sin(\alpha)$$

*Equation 39: force differences base on connecting link position (alpha).*

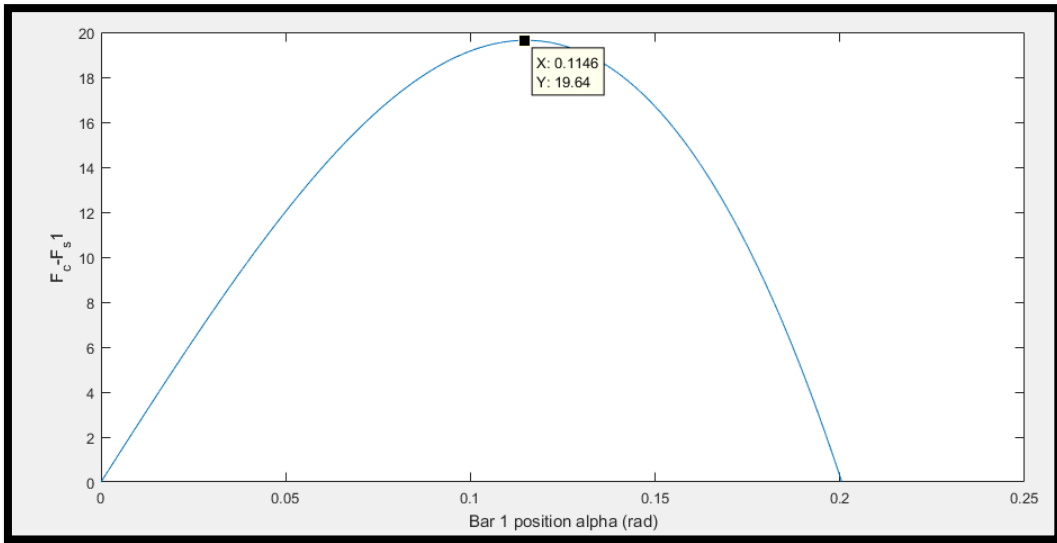


**Figure 28:** Plot of  $|F_c - F_{s1}|$  with respect to the connecting link position  $\alpha$

According to the plot of  $|F_c - F_{s1}|$  with respect to the connecting link position  $\alpha$  as is shown above, the maximum value of  $|F_c - F_{s1}|$  is calculated to be

$$(|F_c - F_{s1}|)_{max} = 19.6407 \text{ N} \quad (14)$$

To ensure that the cable can pull pin 1 and let the mechanism enter and exit the clutch engagement position, which corresponds to the energy storage process, the relation

$$F_c - (F)_{s1\ max} = F_c - K_1 s > 19.6470 \text{ N} \quad (15) \text{ should be satisfied.}$$

In addition, another relation  $F_{s1}(\alpha = -\alpha_1) = K_1 \left( \frac{1}{2} * s + b \sin(\alpha_1) \right) > 19.6470 \text{ N}$  (16) should also be satisfied to let the return spring 1 pull the clutch actuation mechanism back to the original position after finishing the regeneration process. Solve the inequalities (15) (16) to obtain the acceptable range of spring 1 rate:  $K_1 > 1.089 \text{ N/mm}$  (17). Based on this domain, the group is

planning to use a B3-20 extension spring (Century spring) as extension spring 1. Parameters of spring 1 are shown as follows

Initial Tension (N)	8.90
Suggested Max Load (N)	48.930
Length (mm)	63.5
Material	Hard Drawn - HD
O. D. (mm)	7.92
Option	Double Loop
Rate (N/mm)	1.121
Suggested Max Deflection (mm)	33.02
Wire Dia (mm)	1.14

**Figure 29:** Specifications of spring 1

Set the initial tension of spring 1 as  $F_{i1} = 1$  N, then the maximum spring force should be

$$(F_{s1})_{max} = F_{i1} + K_1 s = 44.84 \text{ N}$$

The cable force should be greater than  $F_{Cmin} = (F_{s1})_{max} + 19.6407 = 64.4807$  N. Therefore choose the cable force  $F_c = 64.4807$  N for analysis of the brake handle of the hand brake mechanism.

### Verification of the fatigue strength of spring 1

Spring parameters: Outer diameter OD=7.92 mm, ID=6.78 mm, spring rate  $k_1=1.121$  N/mm, wire diameter d=1.14mm, material: Hard Drawn – HD

From previous analysis of spring 1, the maximum and minimum spring forces should be  $F_{max} = 44.84N$  and  $F_{min} = 0N$ , relatively.

From Chapter 10 of Shigley's Mechanical design, we also have the following parameters:

$A = 1783 \text{ Mpa} * \text{mm}^m$ ,  $m=0.190$ ,  $S_{sa}=241 \text{ MPa}$ ,  $S_{sm}=379 \text{ MPa}$ ,  $S_{se}=309.9883 \text{ Mpa}$ ,  $S_{sa} = 398 \text{ Mpa}$ ,  $S_{sm} = 534 \text{ Mpa}$ ,

Mean coil diameter  $D = OD - d = 0.00678$

$$C = \frac{D}{d} = 5.9474$$

Stress Correction Factor  $K_B = \frac{4C+2}{4C-3} = 1.2405$

Amplitude of load  $F_a = \frac{(F_{max}-F_{min})}{2} = 22.42N$

The mean of load  $F_m = \frac{(F_{max}+F_{min})}{2} = 22.42N$

Tensile Strength  $S_{ut} = \frac{A}{d^m} = 1.7392 * 10^9 \text{ Pa}$

Ultimate Shear Stress  $S_{su} = 0.67 * S_{ut} = 1.1653 * 10^9 \text{ Pa}$

Body-coil fatigue  $\tau_a = \frac{8K_B F_a D}{\pi d^3} = 3.24106 \times 10^8 \text{ pa}$

$$\tau_m = \frac{F_m}{F_a} \tau_a = 3.24106 \times 10^8 \text{ pa}$$

$$S_{se} = \frac{S_{sa}}{1 - (\frac{S_{sm}}{S_{su}})^2} = 503.794 \text{ Mpa}$$

$$(n_f)_{body} = \frac{1}{2} \left( \frac{S_{su}}{\tau_m} \right)^2 \frac{\tau_a}{S_{se}} \left[ -1 + \sqrt{1 + (2 \frac{\tau_m}{S_{su}} \frac{S_{se}}{\tau_a})^2} \right] = 1.33886$$

Coil yielding: as mentioned before, the initial tension of spring 1 is  $F_{i1} = 1N$

$$\tau_i = \left( \frac{F_i}{F_a} \right) \times \tau_a = 14.456 \text{ MPa}$$

$$S_{sm} = \tau_i = 14.456 \text{ MPa}$$

$$r = \frac{\tau_a}{\tau_m - \tau_i} = 1.046685$$

$$S_{sy} = 119.1 \text{ kpsi} = 821165593.6 \text{ Pa}$$

$$(S_{sa})_y = \frac{r}{r+1} \times (S_{sy} - \tau_i) = 412.55541 \text{ MPa}$$

$$(n_y)_{body} = \frac{(S_{sa})_y}{\tau_a} = 1.273$$

*Equation 40: Fatigue strength of return spring verification (Body)*

End-hook bending fatigue

$$D_m = (\text{OD} + \text{ID})/2 = 7.35 \text{ mm}$$

$$r_1 = r_2 = 0.5 * D_m = 3.675 \text{ mm}$$

$$C_1 = 2r_1/d = 6.44737$$

$$C_2 = 2r_2/d = 6.44737$$

$$(K)_A = \frac{4C_1^2 - C_1 - 1}{4C_1(C_1 - 1)} = 1.13056$$

$$(K)_B = \frac{4C_2 - 1}{4C_2 - 4} = 1.13768$$

$$\sigma_a = F_a [(K)_A \frac{16D}{\pi d^3} + \frac{4}{\pi d^2}] = 6.1273 * 10^8 \text{ Pa}$$

$$\sigma_m = \frac{F_m}{F_a} \sigma_a = 6.1273 * 10^8 \text{ Pa}$$

$$S_e = S_{se}/0.577 = 873.127 \text{ MPa}$$

$$(n_f)_A = \frac{1}{2} \left( \frac{S_{ut}}{\sigma_m} \right)^2 \frac{\sigma_a}{S_e} \left[ -1 + \sqrt{1 + (2 \frac{\sigma_m}{S_{ut}} \frac{S_e}{\sigma_a})^2} \right] = 1.17909$$

*Equation 41: Bending Fatigue of return spring verification (End hook)*

End-hook torsional fatigue

$$(\tau_a)_B = (K)_B \frac{8F_a D}{\pi d^3} = 2.97243 * 10^8 \text{ Pa}$$

$$(\tau_m)_B = \frac{F_m}{F_a} (\tau_a)_B = 2.97243 * 10^8 \text{ Pa}$$

$$(n_f)_B = \frac{1}{2} \left( \frac{S_{su}}{(\tau_m)_B} \right)^2 \frac{(\tau_a)_B}{S_{se}} \left[ -1 + \sqrt{1 + (2 \frac{(\tau_m)_B}{S_{su}} \frac{S_{se}}{(\tau_a)_B})^2} \right] = 1.45986$$

*Equation 42: Torsional fatigue of return spring verification (End hook)*

Since corresponding safety factors calculated are greater than 1, design requirement of the spring are satisfied.

The CAD model of the extension spring is shown below

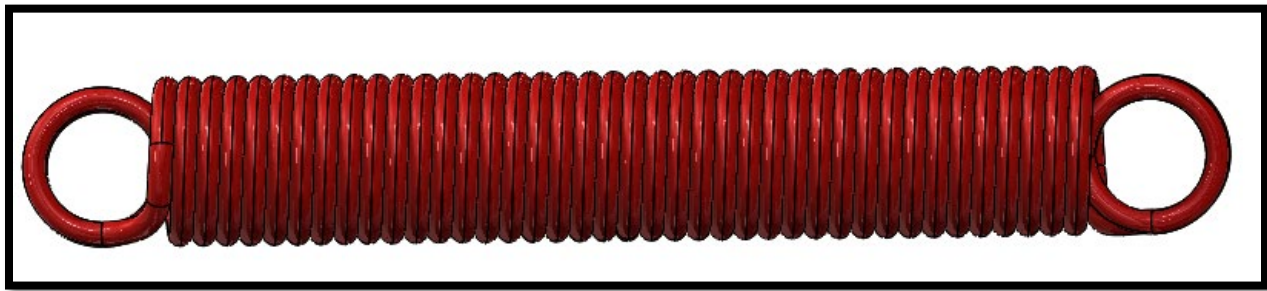


*Figure 30: CAD model of extension spring 1*

## Handbrake:

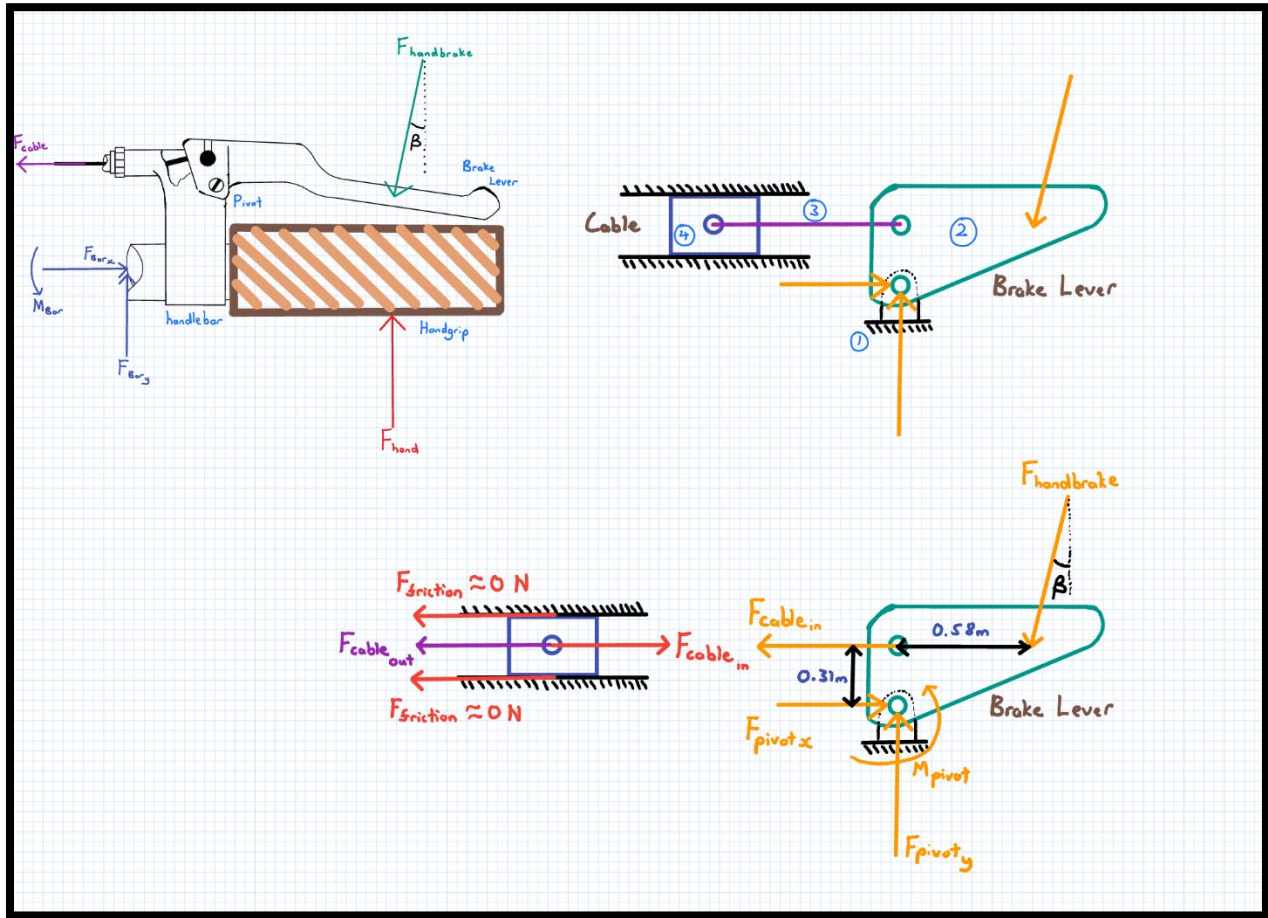


**Figure 31:** Analysis of the hand brake

For the handbrake, it can be model as a triangular bar (**Figure 31**). The handbrake is held in place by a pin which also act as the handbrake's center of rotation. A cable is connected to the upper left hand corner of the handbrake. This cable can be model as a slider sliding back and forward in the handle bar. This assumption is made because, the motion experience by the cable is similar to a slider. The cable is being pulled into the handle bar by the handbrake or pull out of the handle bar by the extension spring used in the three bar linkage structure.

The forces in the free body diagram are  $F_{handbrake}$ = force applied to the handbrake,  $F_{cable\ in}$ = pulling force exerted by the handbrake on to the cable,  $F_{pivot\ x}$ = reaction force by the pivot/pin in the x-direction,  $F_{pivot\ y}$ = reaction force by the pivot/pin in the y-direction and  $M_{pivot}$ =moment at pivot/pin experience by the pivot due to  $F_{handbrake}$ .  $M_{pivot}$  is the moment that will be used to rotate the ratchet wheel below the pin.  $\beta$  is the angle where  $F_{handbrake}$  is being applied.

There are a few assumptions made for this force analysis. First, there is no friction between the slider and the inner surface of the handle bar. Secondly, the handbrake forces (force used to push the handbrake) is assumed to be 70 N.

Based on the free body diagram the following force equation are developed. The objective here is to determine the cable force and the moment experienced by the pivot. These two values will be used in the future calculations.

$$\text{X-direction: } -F_{handbrake} \sin\beta - F_{cable\ in} + F_{pivot\ x} = 0$$

$$\text{Y-direction: } -F_{handbrake} \cos\beta = F_{pivot\ y} = 0$$

$$\text{Moment: } M_{pivot} + (F_{cable\ in} + F_{handbrake} \sin\beta)0.31 - F_{handbrake} \cos\beta(0.58) = 0$$

After calculation,  $F_{cable\ in}=60$  N and  $M_{pivot}=5.71$  Nm

## Ratchet

In this section, various arrangements for the ratcheting mechanism during different stages of regenerative braking will be discussed. In addition, free body diagram of ratchet and pawl at each stage will be shown.

Before beginning the discussion, a few general items will be address for clarity. For the ratcheting mechanism, the spring used is “B4-1 - Compression Springs” from Century Spring. **Figure 32** below shows the important specification for the spring selected.



Standard Finish	Black Oxide - BO
Ends	Closed - C
Free Length (mm)	33.8
I. D. (mm)	4.57
Suggested Max Load (N)	17.793
Material	Music Wire - MW
O. D. (mm)	5.94
Rate (N/mm)	0.893
Solid Length (mm)	13.7
Suggested Max Deflection (mm)	20.07
Total Coils	19.00
Wire Dia (mm)	0.69

**Figure 32:** B4-1 - Compression Springs picture and specification table

As shown in **Figure 32** the spring rate (K) for this spring is 8.93 (N/cm); the maximum deflection is 2.007 cm and the maximum recommended load is 17.793 N (Century Spring Corp. (n.d.)). . No stress analysis is done on this mechanism as it is only a complimentary item to the regenerative system. It does not affect the effectiveness of the regenerative braking system in place.

Four different analysis will be done on this mechanism, each representing different arrangement for ratcheting mechanism at different stages of regenerative braking. The four stages are before

regenerative braking (handbrake at  $\theta_0$ ), during regenerative braking (handbrake at  $\theta_1, \theta_2$ ), after friction braking (handbrake at  $\theta_{1.5}$ ), and during boosting (using the energy stored).

### Analysis of ratcheting mechanism when at position $\theta_0$

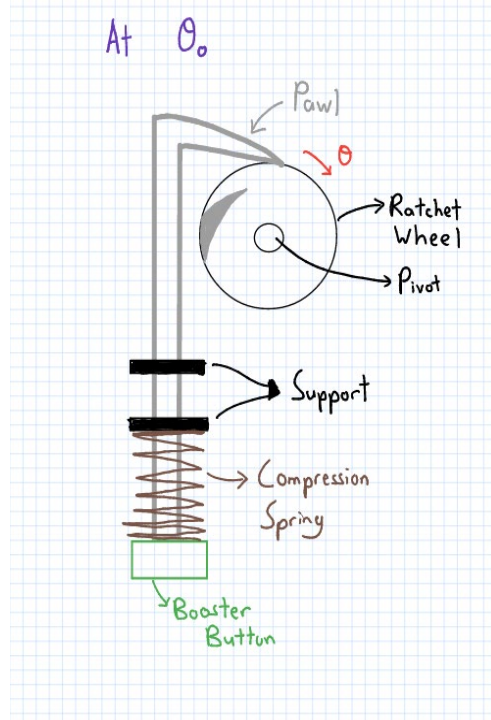


**Figure 33:** Ratcheting Mechanism when at position  $\theta_0$

When the handbrake is at position  $\theta_0$  (either idle or normal riding), the ratcheting mechanism will maintain the arrangement shown in **Figure 32**. In this scenario, the cyclist is not exerting any force on to the handbrake, which means that the ratcheting mechanism remains stationary. In other words, no external moment acting on the ratchet.

With that said, the free body diagram will look like the one shown below. The free body diagrams for ratchet and pawl are drawn separately for clarity.

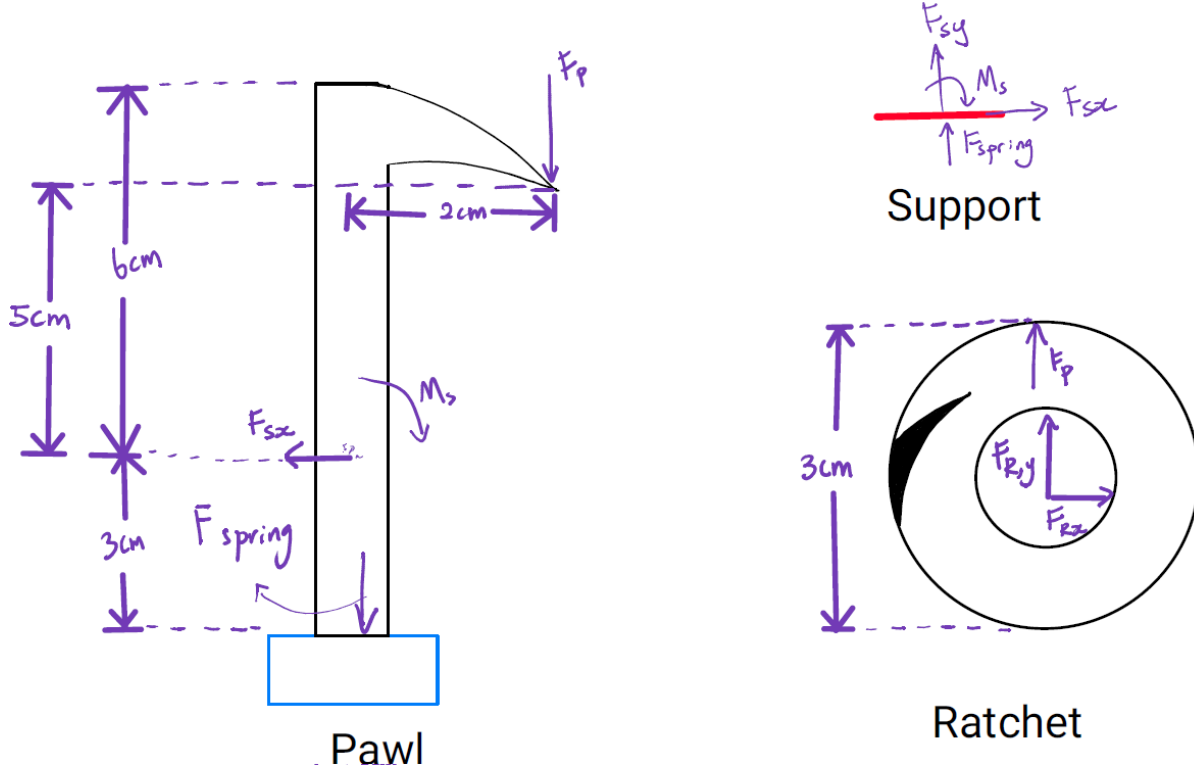


**Figure 34:** Free body diagram for ratchet and pawl at position  $\theta_0$

For the ratchet, the only external force acting on it is the force  $F_p$  which is caused by the spring pushing the tip of the pawl onto the ratchet. The other forces  $F_{r,y}$  and  $F_{r,x}$  are the reaction forces due to the pin holding the ratchet in place.

Moving on to the pawl, the tip experienced a reaction force  $F_p$  as the spring pushes it down onto the ratchet. The support on the pawl experiences a reaction force in the x-direction,  $F_{sx}$  and a moment,  $M_s$ . There is no reaction force in the y-direction because the pawl can slide up and down on the support. Lastly, a spring force will act on the button. These forces will be consistent throughout all arrangements at different stages.

Three force balancing equation are form for each component. The unknowns in this case are  $F_{ry}$ ,  $F_{rx}$ ,  $F_p$ ,  $M_s$ , and  $F_{sx}$ . The known variable is  $K=8.93$  and  $\Delta x = 0.378$ . The following are the equations used for calculation.

Spring Force:

$$F_{spring} = k\Delta x$$

where  $K$  and  $\Delta x$  is based on the specification

Force equations for pawl:

X-direction:  $F_{sx} = 0$

Y-direction:  $F_p + F_{spring} = 0$

Moment:  $M_s + 2F_p = 0$

Force equation for ratchet:

Y-direction:  $F_{ry} + Fp = 0$

X-direction:  $F_{rx} = 0$

There is no moment component.

*Equation 42: Force analysis when ratchet and pawl at position  $\theta_0$*

Ultimately, the variables come out to be as follow,

Variable	Value
$F_p$	3.3755 N
$F_{rx}$	0 N
$F_{ry}$	3.3755 N
$F_{sx}$	0 N
$F_{sy}$	3.3755 N
$F_{\text{spring}}$	-3.3755 N
$M_s$	5.5021 Ncm

**Table 1:** Values of unknowns for ratchet and pawl at position  $\theta_0$

### Analysis of ratcheting mechanism when at position $\theta_{1.5}$

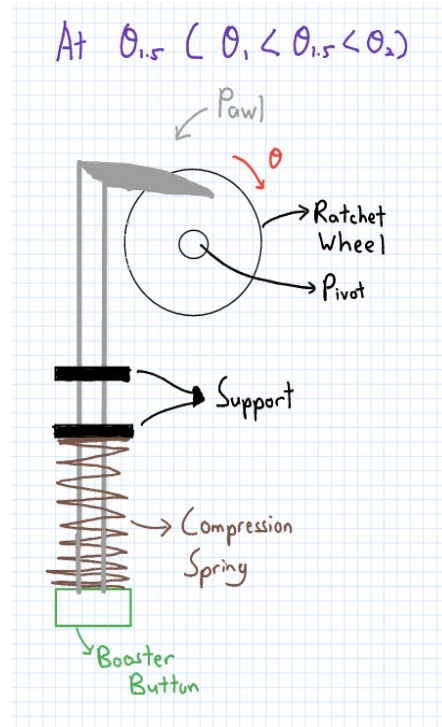


**Figure 35:** Ratcheting Mechanism when at position  $\theta_{1.5}$

In this case, the cyclist has already completed both the regenerative braking as well as frictional braking. The pawl is stuck in the ratchet (**Figure 35**) to prevent the handbrake from reaching  $\theta_1$  and start reengaging the cone clutch. There will be a moment created by the handbrake trying to spring back to its original position acting on the ratchet. That moment will be called  $M_{hb}$ .

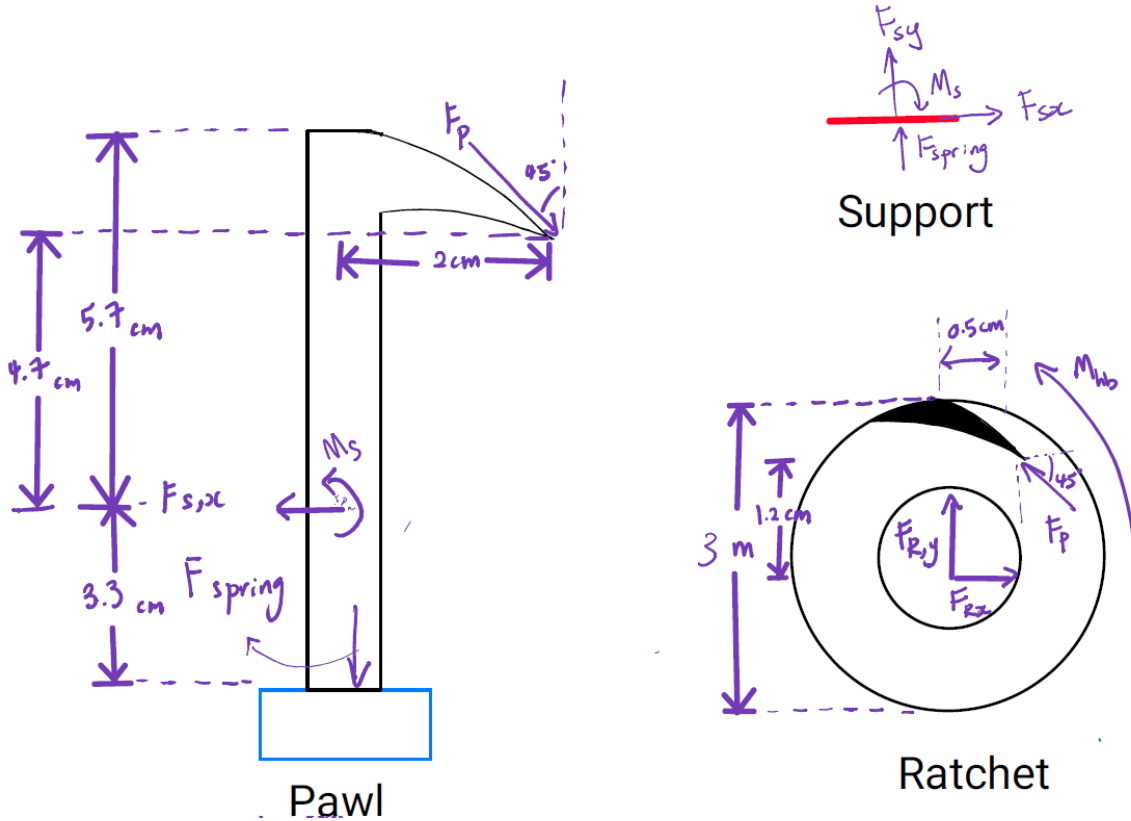


**Figure 36:** Free body diagram for ratchet and pawl at position  $\theta_{1.5}$

For the ratchet, this time there is a external moment,  $M_{hb}$  as mentioned. Other than that, the force  $F_p$  is acting at an angle of 45 degree instead of parallel to the y-direction.

The unknown in this case is  $F_{ry}$ ,  $F_{rx}$ ,  $F_p$ ,  $M_s$ ,  $F_{sy}$ , and  $F_{sx}$ . The knowns are  $M_{hb} = 5.71$  (Nm) and  $F_{spring} = 9.84$ . These are calculated from  $K = 8.93$  and  $\Delta x = 0.078$ .

Spring Force:  $F_{spring} = k\Delta x$

Force equations for pawl:

$$X\text{-direction: } F_p \sin(45) - F_{sx} = 0$$

$$\text{Moment: } M_s + 2\cos(45)F_p + 4.7\sin(45)F_p = 0$$

Force equation for ratchet:

Y-direction:  $F_{ry} + \sin(45)F_p = 0$

X-direction:  $F_{rx} - \cos(45)F_p = 0$

Moment:  $-M_{hb} - \cos(45)F_p - 0.5\sin(45)F_p = 0$

Force equation for support:

X-direction:  $F_{xy} - F_{spring} - F_p \cos(45) = 0$

*Equation 43: Force analysis when ratchet and pawl at position  $\theta_{1.5}$*

Variable	Value
$F_p$	-538.3 N
$F_{rx}$	-380.7 N
$F_{ry}$	380.7 N
$F_{sx}$	-380.7 N
$F_{sy}$	-311.0 N
$F_{spring}$	0.697 N
$M_s$	2.4096 Nm

*Table 2: Values of unknowns for ratchet and pawl at position  $\theta_{1.5}$*

## Analysis of ratcheting mechanism when handbrake is push down.

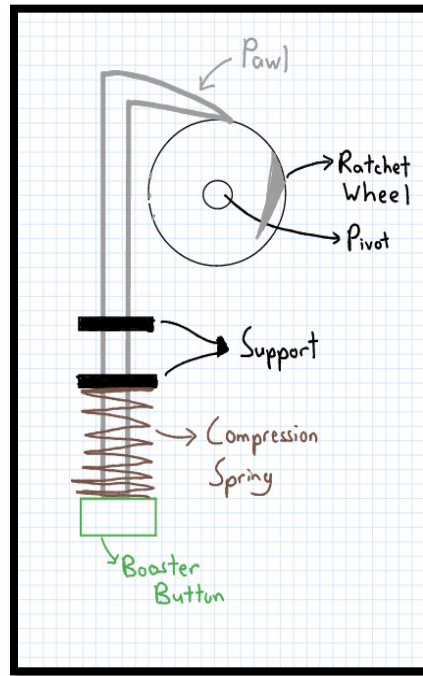


**Figure 37:** Ratcheting Mechanism when handbrake is push down.

In this scenario, the cyclist is pushing down the handbrake. This can happen in either regenerative braking or friction braking. Since the cyclist is pushing the handbrake a moment is applied to the ratchet wheel. The moment will again be set as  $M_{hb}$ .

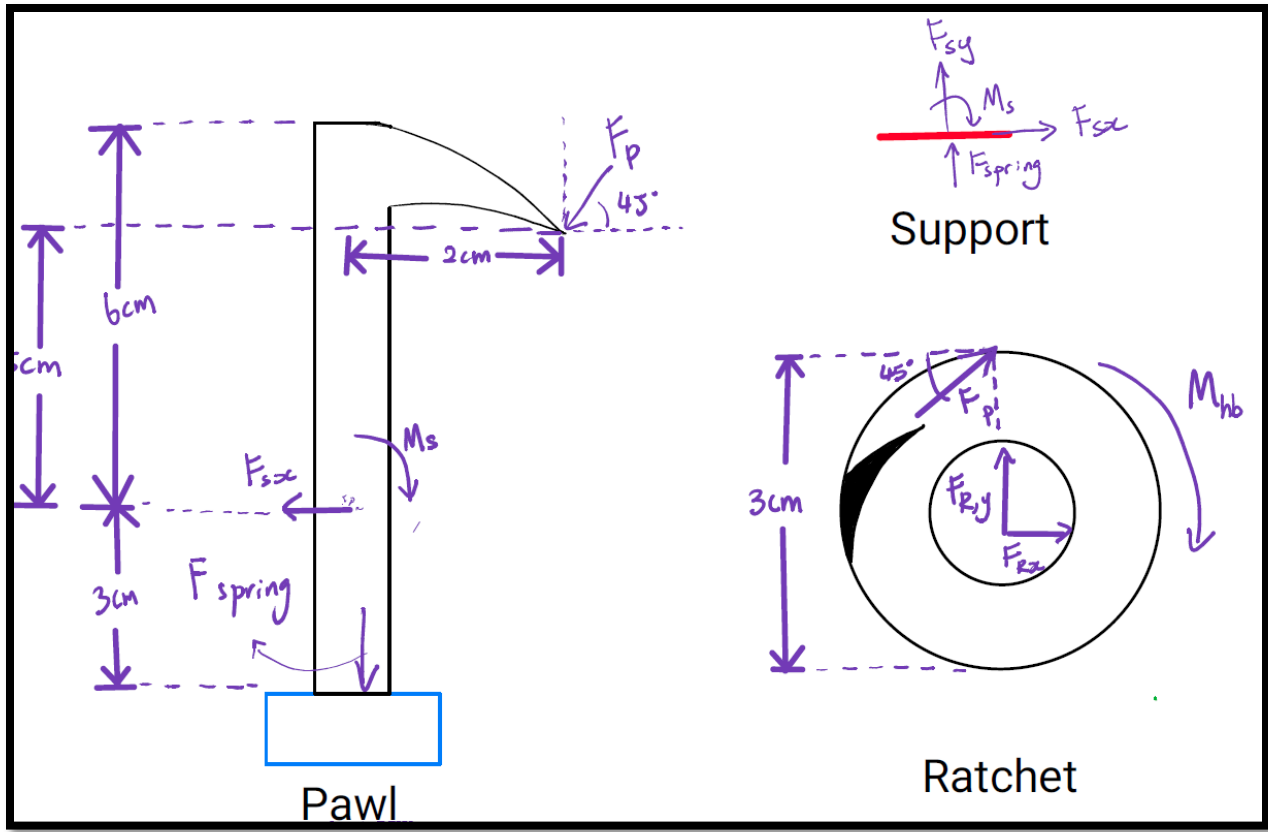


Figure 38: Free body diagram for ratchet and pawl for when the handbrake is push down.

There is no difference between the free body diagram in this scenario compare to the one for when handbrake is at  $\theta_{1.5}$ , except that the  $F_p$  is facing the opposite direction due to the moment  $M_{hb}$  going clockwise instead of counter clockwise.

The unknowns in this are  $F_{ry}$ ,  $F_{rx}$ ,  $F_p$ ,  $M_s$ ,  $F_{sy}$ , and  $F_{sx}$ . The known is  $M_{hb}$ .  $M_{hb}$  is the moment induce by the handbrake and that is calculated to be 5.71 (Nm).

$$\text{Spring Force:} \quad F_{spring} = k\Delta x$$

Force equations for pawl:

$$\text{X-direction:} \quad F_p \cos(45) + F_{sx} = 0$$

$$\text{Moment:} \quad M_s + 2\sin(45)F_p - 5\cos(45)F_p = 0$$

Force equation for ratchet:

$$\text{Y-direction: } F_{ry} + \sin(45)F_p = 0$$

$$\text{X-direction: } F_{rx} + \cos(45)F_p = 0$$

$$\text{Moment: } M_{hb} + 1.5\cos(45)F_p = 0$$

Force equation for support:

$$\text{Y-direction: } F_{sy} - F_{spring} - F_p \sin(45) = 0$$

*Equation 44: Force analysis when ratchet and pawl when handbrake is pushed down*

Variable	Value
$F_p$	-538.3 N
$F_{rx}$	380.7 N
$F_{ry}$	380.7 N
$F_{sx}$	380.7 N
$F_{sy}$	-377.3 N
$F_{spring}$	337.6 N
$M_s$	-11.42 Nm

*Table 3: Values of unknowns for ratchet and pawl for when the handbrake is push down.*

## Analysis of ratcheting mechanism when button is pushed

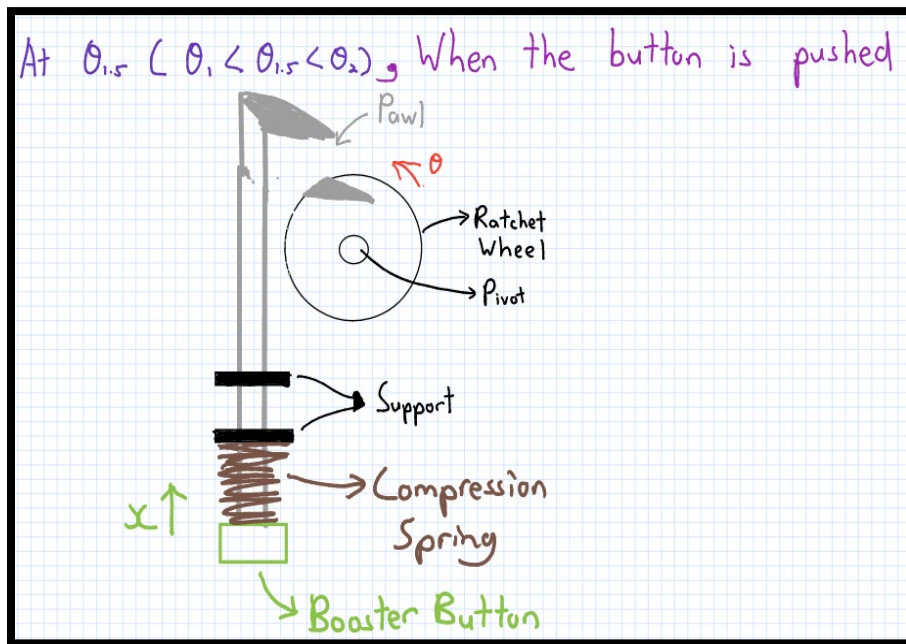


**Figure 39:** Ratcheting Mechanism when button is pushed

In this case, the button is pushed to engage the clutch and used the energy stored in the flywheel. Because the pawl is raised. There will not be any contact forces between the pawl and the ratchet, leaving only external forces on the ratchet be the moment created from the handbrake springing back to its original position, that force is denoted by  $M_{hb}$ .

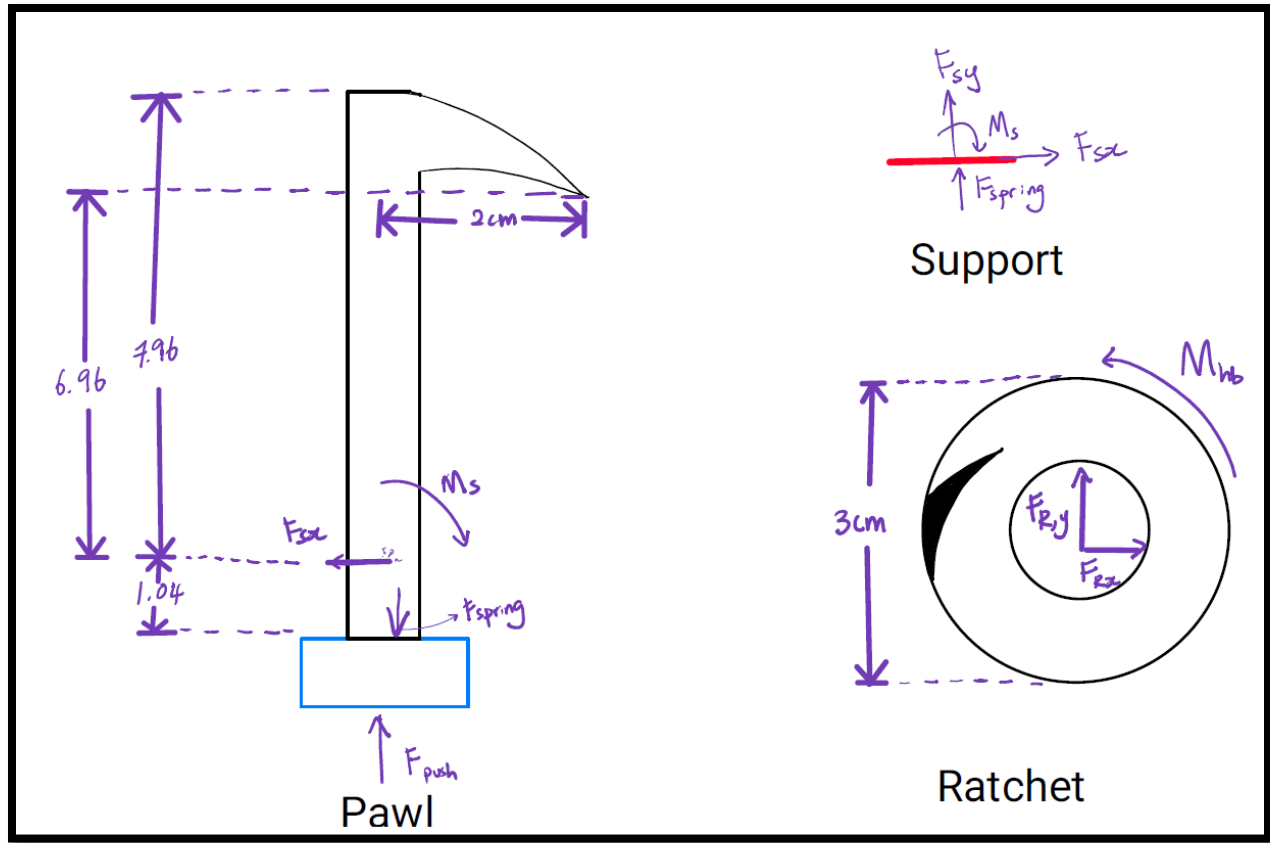


**Figure 40:** Free body diagram for ratchet and pawl for when the button is pushed.

For the ratchet, as mentioned the only external force is the moment, the reaction forces remained the same.

For the pawl, a new external force is introduced. A force is used to raise the pawl away from the ratchet and that force is denoted by  $F_{push}$ . Again, the other internal forces remain the same.

The unknowns are  $F_{ry}$ ,  $F_{rx}$ ,  $M_s$ ,  $F_{sx}$  and maximum value for  $F_{push}$ . The knowns are  $M_{hb}=5.71 \text{ Nm}$  and  $k$  value of  $8.93 \text{ Ncm}^{-1}$  and  $\Delta x$  of  $2.007 \text{ cm}$ .  $2.007 \text{ cm}$  is the maximum deflection for the spring, because any more than that will cause it to be shorter than the specified free length, which is physically impossible.

Spring Force:

$$F_{spring} = k\Delta x$$

Force equations for pawl:

Y-direction:  $F_{push} + F_{spring} = 0$

X-direction:  $F_{sx} = 0$

Moment:  $M_s = 0$

Force equation for ratchet:

Y-direction:  $F_{ry} = 0$

X-direction:  $F_{rx} = 0$

No need for moment balance equation.

Force equations for support:

Y-direction:  $F_{sy} - F_{spring} = 0$

*Equation 45: Force analysis when ratchet and pawl when button is pushed*

Variable	Value
$F_p$	0 N
$F_{push}$	17.92251 N
$F_{rx}$	0 N
$F_{ry}$	0 N
$F_{sx}$	0 N
$F_{spring}$	17.92251 N
$M_s$	0 Ncm

*Table 4: Values of unknowns for ratchet and pawl for when the button is pushed*

## Selection of bearings

EcoBoost group decided to choose deep groove bearings to support the shaft 1 and shaft 2 located at both sides of the cone clutch.

## Static Analysis for shaft 1

As shown on the figure of the cone clutch (**Figure 41**), since there is a spline fit between the cone and the cone shaft 1, the thrust from the cone cannot be transmitted to the cone shaft, thus the cone shaft 1 carries radial loads only, and the free body diagram of the cone shaft is shown as follows.

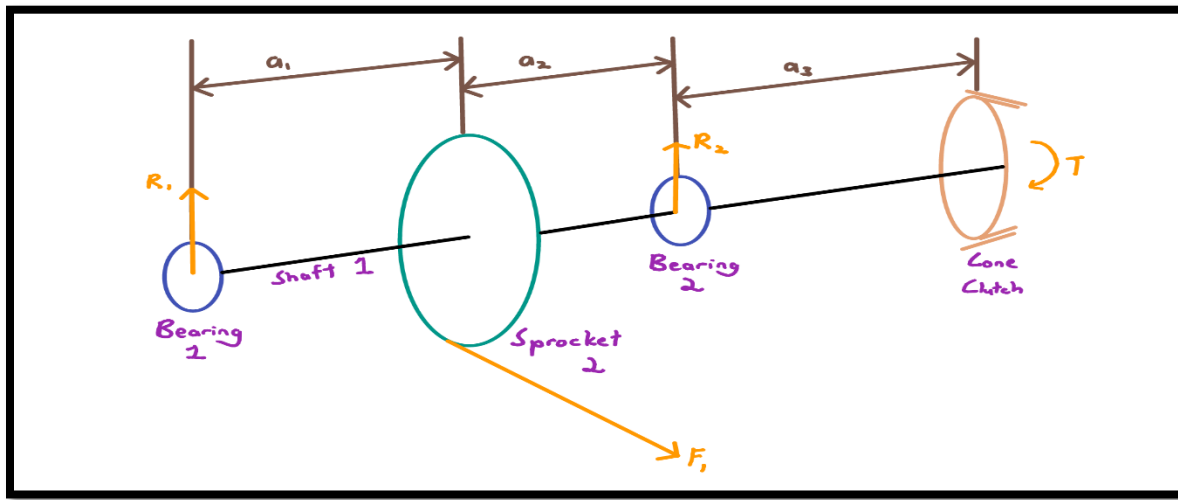


**Figure 41:** Free body diagram of shaft 1

$$a_1 = 16.9 \text{ mm}, \text{ distance between bearing 1 and sprocket}$$

$$a_2 = 24.4 \text{ mm}, \text{ distance between bearing 2 and sprocket 2}$$

Initial conditions:

$$\text{Pitch radius of sprocket 2 : } r_2 = (0.5 * (79.65 + 34.16 * 2) * 10^{-3}) * 0.5 = 0.037 \text{ m}$$

$$\text{Maximum cone shaft speed: } w_{\text{cone}} = 54.2133 \frac{\text{rad}}{\text{s}} = 517 \text{ rpm}$$

$$\text{Maximum cup shaft speed : } w_{\text{cup}} = 37.8392 \frac{\text{rad}}{\text{s}} * n_{\text{planetary gear}} = 264.8744 \frac{\text{rad}}{\text{s}}$$

$$= 2529.36 \text{ rpm}$$

From previous cone clutch capacity calculations, maximum shaft cone shaft torque  $T = 17.0992$

Nm. Therefore, the tension on sprocket 2 should be  $F_2 = \frac{T}{r_2} = 462.2342 \text{ N}$

## Strength analysis for shaft 1

The free body diagram, shear force and bending moment diagrams of shaft 1 are shown as follows:

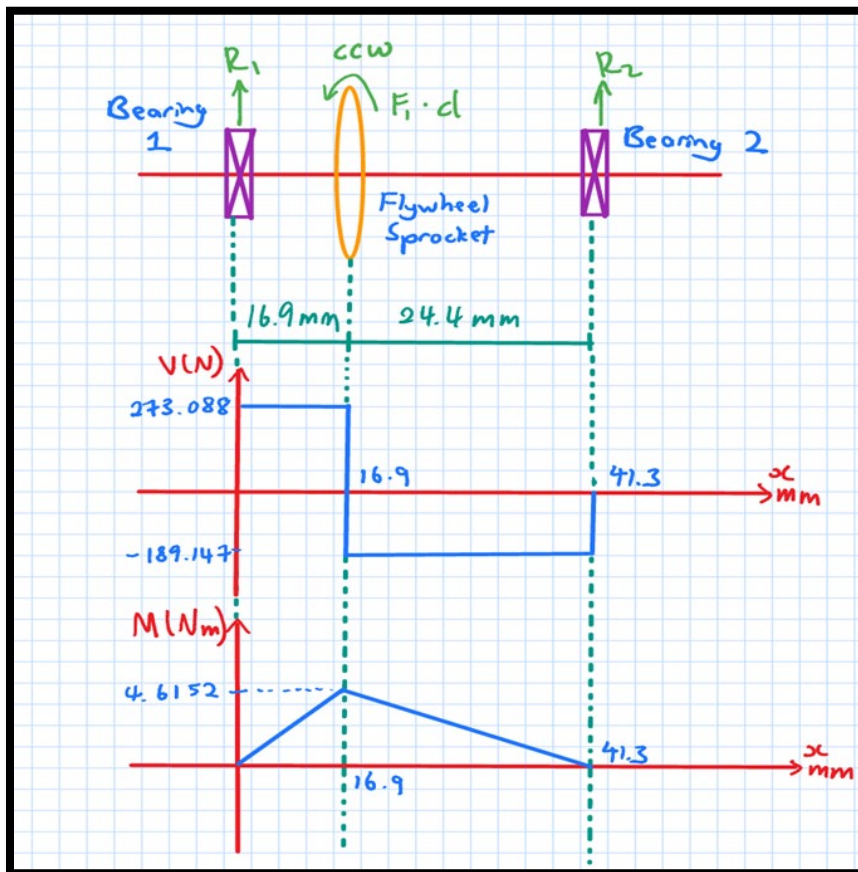


**Figure 42:** Free body diagram, shear force and bending moment diagrams of shaft 1

Initial conditions:  $S_{ut} = 105$  kpsi;  $S_y = 82$  kpsi; Small diameter  $d = 10$  mm; Large diameter  $D = 12$  mm; Notch radius  $r = 0.5$  mm;  $D/d = 1.2$ ;  $r/d = 0.05$ ;

## Calculate the fatigue factor of safety

From Chapter 7 of Shigley's Mechanical design,  $K_t = 1.95$  (Fig. A-15-9);  $K_{ts} = 1.6$  (Fig. A-15-8);  $q = 0.68$  (Fig. 6-20);  $q_{shear} = 0.72$  (Fig. 6-21) (*Budynas et al, 2015*)

$$K_f = 1+q*(K_t - 1) = (1+0.68(1.95-1)) = 1.646;$$

$$K_{fs} = 1+q_{shear}*(K_{ts} - 1) = (1+0.72(1.6-1)) = 1.432;$$

$$S'_e = 0.5*S_{ut} = 0.5*(105) = 52.5 \text{ kpsi};$$

$$k_a = a*S_{ut}^b = 2.7(105)^{-0.265} = 0.787;$$

$$k_b = \left(\frac{d}{7.62}\right)^{-0.107} = \left(\frac{10}{7.62}\right)^{-0.107} = 0.9713;$$

$$k_c = k_d = k_f = 1;$$

With a reliability of 99%,  $k_e = 0.814$ ,

$$S_e = k_a k_b k_e S'_e = 0.787 * 0.9713 * 0.814 * 52.5 = 32.6672 \text{ kpsi};$$

Use maximum bending moment and torque,  $M=4.6152 \text{ Nm} = 40.847962 \text{ lbf*in}$ ;  $T = 17.0992 \text{ Nm} = 151.340673 \text{ lbf*in}$ ;  $d = 10 \text{ mm} = 0.393701$ ;

From Equation 7-7 (*Budynas et al, 2015*)

$$\frac{1}{n} = \frac{\frac{16}{pi}}{d^3} * \left( \sqrt{4 * (K_f * M_a)^2 + 3 * (K_{fs} * T_a)^2} \frac{1}{S_e} + \sqrt{4 * (K_f * M_m)^2 + 3 * (K_{fs} * T_m)^2} \frac{1}{S_{ut}} \right) =$$

$$\frac{\frac{16}{pi}}{0.393701^3} * \left( \sqrt{4 * (1.646 * 40.847962)^2} \frac{1}{32667.2} + \sqrt{3 * (1.432 * 151.340673)^2} \frac{1}{105000} \right) =$$

$$0.64191$$

$$n = 1.55785 \quad DE - Goodman$$

From Equation 7-9,

$$\frac{1}{n} = \frac{\frac{8\sqrt{4*(1.646*40.847962)^2}\frac{1}{pi}}{0.393701^3}}{32667.2} * \left( 1 + \sqrt{1 + \left( \frac{2\sqrt{3*(1.432*151.340673)^2} * \frac{32667.2}{\sqrt{4*(1.646*40.847962)^2}}}{105000} \right)^2} \right) = 0.51605$$

$$n = 1.9378 \quad DE - Gerber$$

## Calculate the yielding factor of safety

Using von Mises maximum stress equation:

$$\sigma'_{max} \sqrt{\left( 32 * K_f * \frac{M_m + M_a}{pi} \right)^2 + 3 * \left( 16 * K_{fs} * \frac{T_m + M_a}{pi} \right)^2} =$$

$$\sqrt{\left( 32 * 1.646 * \frac{40.847962}{0.0393701^3} \right)^2 + 3 * \left( 16 * 1.432 * \frac{151.340673}{0.0393701^3} \right)^2} = 33.277 \text{ kpsi}$$

$$n_y = \frac{S_y}{\sigma_{max'}} = \frac{82}{33.277} = 2.464$$

Equation 46: Shaft 1 safety factor calculation

## Static Analysis for Shaft 2

As is shown on the free body diagram of shaft 2, it is fixed with the flywheel and mounted located between bearing 3 and bearing 4. And geometrical parameters of the shaft are provided as follows

$$a_1 = 36.945 \text{ mm}, a_2 = 22.985 \text{ mm}$$

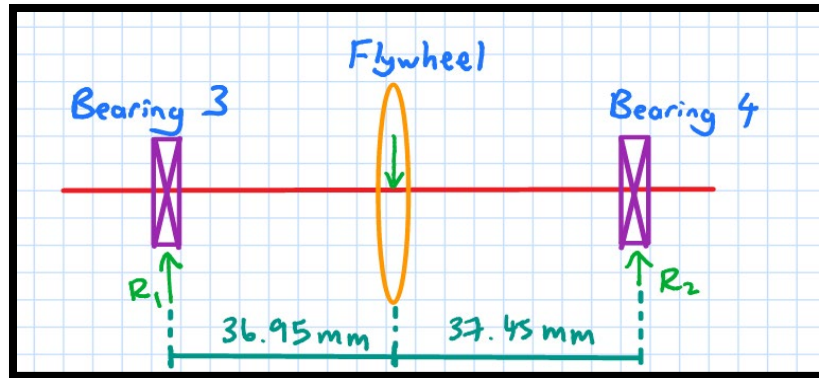


**Figure 43:** Free body diagram of shaft 2

Since there is no bending moment transmitted through the planetary gearbox, shaft 2 transmits torque only because of no axial or radial loads. However, radial loads might occur during vertical impact conditions. Assume a linear impact and the maximum impact force satisfies the following equation.

$$\frac{1}{2} F_{max}s = \frac{1}{2}mv^2$$

**Equation 47:** Relationship of linear impact and maximum impact force

Where  $F_{max}$ =impact force,  $v$ =mass center velocity of flywheel before impact

We also assume the  $s= 6 \text{ in}$  and  $v=\sqrt{gs}$

Substitute the flywheel  $m=9.0046 \text{ kg}$  into equations above and the maximum impact force is calculated to be  $F= 92.48 \text{ N}$ , which is the radial load  $F=180.43 \text{ N}$

Then reaction forces of bearing 3 and 4 can be calculated using equations below:

$$F_{R1} = \frac{a_2}{a_1 + a_2} F$$

$$F_{R2} = \frac{a_1}{a_1 + a_2} F$$

*Equation 48: Forces acted by the bearing on to the shaft 2*

Substitute values of  $a_2$  and  $a_1$  into equations above to obtain the load of bearing 3 and 4 as is shown below

	Axial load	Radial load
Bearing 3	$F_{a1} = 0$	$F_{r1} = 69.2 \text{ N}$
Bearing 4	$F_{a2} = 0$	$F_{r2} = 111.23 \text{ N}$

*Table 5: Bearing loads corresponding to shaft 2*

## Strength analysis for shaft 2

The free body diagram, shear force and bending moment diagram of shaft 2 are shown as follows

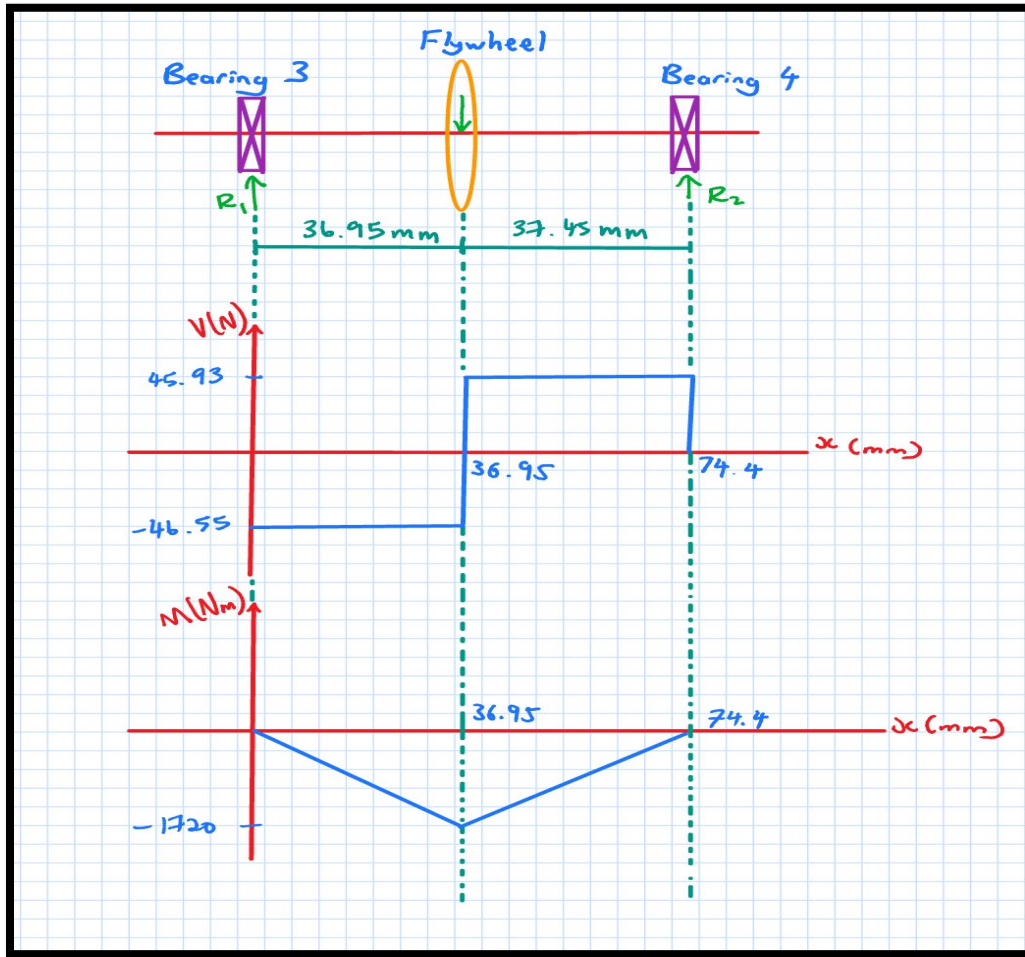


**Figure 44:** The free body diagram, shear force and bending moment diagram of shaft 2

According to free body diagram of shaft 2 (**Figure 44**):

$$\Sigma M = 92.48 * 36.95 - R_2 * (36.95 + 37.45) = 0$$

$$R_2 = 45.93 N$$

$$\Sigma F = R_1 + R_2 - F = 0$$

$$R_1 = 92.48 - 45.93 = 46.55$$

*Equation 49: Moment analysis of shaft 2*

According to the bending moment diagram,

$$M_{max} = 46.55 * 36.95 = 1720 \text{ Nmm}$$

Safety factor for shaft 2 was calculated using Goodman's method:

Parameters for Goodman's method was obtained from Shigley's book:  $K_t=1.6$ ,  $K_{ts}=1.4$ ,  $q=0.8$ ,  $q_{shear}=0.9$ ,  $S_{ut}=565 \text{ MPa}$  (Budynas et al, 2015)

$$K_f = 1 + 0.8(1.6 - 1) = 1.48$$

$$K_f = 1 + 0.9(1.4 - 1) = 1.36$$

$$S'_e = 0.5 * 565 = 282.5 \text{ MPa}$$

$$K_a = 2.7 + 565^{-0.265} = 0.5036$$

$$K_b = \left(\frac{10}{0.3}\right)^{-0.107} = 0.88$$

$$S_e = 1.48 * 1.36 * 282.5 = 568.6 \text{ MPa}$$

$$\frac{1}{n} = \frac{16}{\pi * 1000} * (1/568.2 * (4 * 1.48 * 1720)^2 + 3 * (1.36 * 2442)^2))^{1/2}$$

$$n = 14.53$$

*Equation 50: Safety factor of shaft 2*

Factor of safety for the 1045 steel shaft is 14.53, which is greater than 1. The designed product is safe to use.

## Selection of bearings

Ecoboost group decided to choose deep groove bearings to support the shaft 1 and shaft 2 located at both sides of the cone clutch.

### Calculations of Load on Bearings Supporting Shaft 1

Since bearing 1 and 2 withstand no axial load, bearing loads can be calculated and presented in the following table (Table 6) (Budynas et al, 2015)

For bearing 1, the axial load  $F_{a1} = 0$

$$\text{The radial load } F_{r1} = \frac{a_2}{a_1+a_2} F_2 = 273.0875 \text{ N}$$

For bearing 2, the axial load  $F_{a2} = 0$

$$\text{The radial load } F_{r2} = \frac{a_1}{a_1+a_2} F_2 = 189.1467 \text{ N}$$

*Equation 51: Force acted on shaft 1 by bearings*

	Axial load	Radial load
Bearing 1	$F_{a1} = 0$	$F_{r1} = 273.0875 \text{ N}$
Bearing 2	$F_{a2} = 0$	$F_{r2} = 111.23 \text{ N}$

*Table 6: Bearing loads corresponding to shaft 1*

## Selection of deep groove bearings for bearing 1

The initial conditions for bearing 1 selection are shown as follows:

Shaft speed  $n = 517 \text{ rpm}$ ,  $F_r = 273.0875 \text{ N}$ ,  $F_a = 0 \text{ N}$ ,  $a=3$  for ball bearings. Assume load factor  $L_F=1.2$  for light impact applications. Also assume the reliability of bearing is 90% associated with design life of  $L_D = 25 \text{ khr}$  and  $k_{rel} = 1$ .

From Table 11-1 of Shigley's book,  $F_a/C_0 = 0$  (1) (Budynas et al, 2015)

Use  $\frac{F_a}{C_0} = 0.014$  and  $e=0.19$  to obtain equivalent load correction factors  $X_1 = 1, Y_1 = 0$ .

The equivalent ball bearing load can then be calculated as

$$F_e = X_1 V F_r + Y_1 F_a \quad (2) \text{ (equation 11-12 from Shigley's book) (Budynas et al, 2015)}$$

*Equation 52: Equivalent ball bearing load (bearing 1)*

For inner race rotation,  $V=1$ . Hence the equivalent bearing load becomes

$$F_e = X_1 F_r + Y_1 F_a = 273.0875 \text{ N}$$

The bearing rated life in hours  $L_R(\text{hours}) = 10^6 \text{ rev} \frac{\text{min}}{517 \text{ rev}} \frac{\text{hr}}{60 \text{ min}} = 32.2373 \text{ hours}$  (3)

Catalog C10 rating of bearing 1 should be

$$C_{10} = L_F * F_e \left( \frac{L_D}{K_{rel} L_R(\text{hours})} \right)^{\frac{1}{a}} = 3.0108 * 10^3 \text{ N} \quad (4)$$

*Equation 53: C10 rating of bearing 1*

Choose 6003ZZ single row deep groove bearing from the catalog provided by AST bearing company (AST, 2018). According to the spec sheet, deep groove bearing 6003ZZ has  $C_{10}=6000\text{N}$  and  $C_0=3250\text{ N}$ , substitute the 2 parameters back into equations (1) through (4) as the second iteration to obtain the following results

$$F_e = 273.0875 \text{ N}, C_{10} = 3.0108 * 10^3 \text{ N}$$

From the catalog, 6003ZZ single row deep groove bearing is still selected with the adjusted service life being

$$L_D = k_{rel} L_R \left( \frac{F_r}{F_e} \right)^a = 341905 \text{ hours}$$

*Equation 54: service life of bearing 1*

Specifications and the CAD model of the bearing 1 are shown as follows

<b>Specifications</b>		
Bearing Type	Shielded	
Bore Dia (d)	10.000	mm
Outer Dia (D)	26.000	mm
Width (B)	8.000	mm
Radius (min) (rs)	0.30	mm
Dynamic Load Rating (Cr)	4,550	N
Static Load Rating (Cor)	1,950	N
Max Speed (Grease)	31,000	rpm
Max. Shaft Shoulder Dia. Inner (Ui)	12.9	mm
Min. Housing Shoulder Dia., Outer (Uo)	22.40	mm
Ball Qty	7	
Ball Dia (Dw)	4.762	mm
Weight (g)	19.00	grams
Precision	A1	
Standard Clearance	C0	
Material	52100 Chrome steel (or equivalent)	

**Figure 45:** Specifications of bearing 1 (AST 6003ZZ deep groove bearing, from AST website)

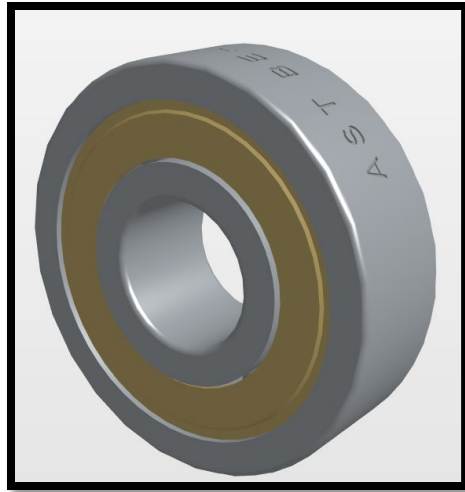


**Figure 46:** CAD model of bearing 1 (AST 6003ZZ deep groove bearing, from AST website)

## Selection of deep groove bearings for bearing 2

The initial conditions for bearing 2 selection are shown as follows:

Shaft speed  $n = 517$  rpm,  $F_r = 189.1467$  N,  $F_a = 0$  N,  $a=3$  for ball bearings. Assume load factor  $L_F=1.2$  for light impact applications. Also assume the reliability of bearing is 90% associated with design life of  $L_D = 25$  khr and  $k_{rel} = 1$ .

Utilize the same equation from previous analysis for bearing 1, we obtain

$$\frac{F_a}{C_0} = \frac{0}{C_0} = 0$$

$$X_1 = 1, Y_1 = 0$$

$$F_e = X_1 F_r + Y_1 F_a = 189.1467 \text{ N}$$

*Equation 55: Equivalent ball bearing load (bearing 2)*

$$L_{R(\text{hours})} = 10^6 \text{rev} \frac{\text{min}}{517 \text{ rev}} \frac{\text{hr}}{60\text{min}} = 32.2373 \text{ hours}$$

Catalog C10 rating of bearing 2 should be

$$C_{10} = LF * F_e \left( \frac{L_D}{K_{rel} L_R(\text{hours})} \right)^{\frac{1}{\alpha}} = 2.0853 * 10^3 N$$

*Equation 56: C10 rate of bearing 2*

Choose 6001ZZ single row deep groove bearing from the catalog provided by AST bearing company (AST, 2018). According to the spec sheet, deep groove bearing 6001ZZ has  $C_{10} = 5100N$  and  $C_0 = 2400 N$ , substitute the 2 parameters back into equations (1) through (4) as the second iteration to obtain the following results

$$F_e = 273.0875 N, C_{10} = 2.0853 * 10^3 N$$

From the catalog, 6003ZZ single row deep groove bearing is still selected with the adjusted service life being

$$L_D = k_{rel} * L_R * \left( \frac{F_r}{F_e} \right)^\alpha = 631935 \text{ hours}$$

*Equation 57: Service life of bearing 2*

Specifications and the CAD model of the bearing 2 are shown as follows:

Specifications		
Bearing Type	Shielded	
Bore Dia (d)	12.000	mm
Outer Dia (D)	28.000	mm
Width (B)	8.000	mm
Radius (min) (rs)	0.30	mm
Dynamic Load Rating (Cr)	5,100	N
Static Load Rating (Cor)	2,400	N
Max Speed (Grease)	27,000	rpm
Max. Shaft Shoulder Dia. Inner (Ui)	17.2	mm
Min. Housing Shoulder Dia., Outer (Uo)	25.50	mm
Ball Qty	8	
Ball Dia (Dw)	4.762	mm
Weight (g)	22.00	grams
Precision	A1	
Standard Clearance	C0	
Material	52100 Chrome steel (or equivalent)	

*Figure 47: Specification of bearing 2 (AST 6003ZZ deep groove bearing, from AST website)*

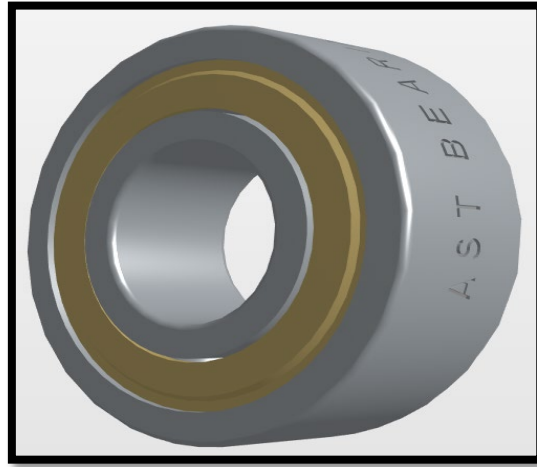


**Figure 48:** CAD model of bearing 2 (AST 6003ZZ deep groove bearing, from AST website)

## Selection of deep groove bearings for bearing 3 and 4

The group decides to use the same model of deep groove ball bearing to function as the bearing 3 and 4. Since bearing 4 has a greater radial load than bearing 3, bearing 4 is chosen to conduct corresponding bearing selection calculations.

The initial conditions for bearing 4 selection are shown as follows:

Shaft speed  $n = 2529.36$  rpm,  $F_r = 111.23$  N,  $F_a = 0$  N,  $a=3$  for ball bearings. Assume load factor  $L_F=1.2$  for light impact applications. Also assume the reliability of bearing is 90% associated with design life of  $L_D = 25$   $khr$  and  $k_{rel} = 1$ .

From Table 11-1 of Shigley's book,  $\frac{F_a}{C_0} = \frac{0}{C_0} = 0$  (1)

Use  $\frac{F_a}{C_0} = 0.014$  and  $e=0.19$  to obtain equivalent load correction factors  $X_1 = 1, Y_1 = 0$ .

The equivalent ball bearing load can then be calculated as

$$F_e = X_1 V F_r + Y_1 F_a \quad (2) \quad (\text{equation 11-12 from Shigley's book}) (\text{Budynas et al, 2015})$$

For inner race rotation,  $V=1$ . Hence the equivalent bearing load becomes

$$F_e = X_1 F_r + Y_1 F_a = 111.23 \text{ N}$$

*Equation 58: Equivalent ball bearing load (bearing 3 and 4)*

$$\text{The bearing rated life in hours } L_{R(\text{hours})} = 10^6 \text{ rev} \frac{\text{min}}{2529.36 \text{ rev}} \frac{\text{hr}}{60 \text{ min}} = 6.5893 \text{ hours} \quad (3)$$

Catalog C10 rating of bearing 1 should be

$$C_{10} = LF * F_e \left( \frac{L_D}{K_{rel} L_{R(\text{hours})}} \right)^{\frac{1}{a}} = 2.0818 * 10^3 \text{ N} \quad (4)$$

*Equation 59: C10 rate for bearing 3 and 4*

Choose 6003ZZ single row deep groove bearing, which is the same as the bearing model used for bearing 1, from the catalog provided by AST bearing company (AST, 2018). According to the spec sheet, deep groove bearing 6003ZZ has  $C_{10} = 6000 \text{ N}$  and  $C_0 = 3250 \text{ N}$ , substitute the 2 parameters back into equations (1) through (4) as the second iteration to obtain the following results

$$F_e = 273.0875 \text{ N}, C_{10} = 3.0108 * 10^3 \text{ N}$$

From the catalog, 6003ZZ single row deep groove bearing is still selected with the adjusted service life being

$$L_D = k_{rel} * L_R * \left( \frac{F_r}{F_e} \right)^a = 1,034,251 \text{ hours}$$

*Equation 60: Desired life for bearing 3 and 4*

The specification sheet and the CAD model of the 6003ZZ Bearing has already been presented in **Figure 47**, **Figure 48** and **Figure 81**.

## Wire Rope Stress Analysis and Safety Factor

As we calculated that the cable force,  $F_c = 64.4807$  N, the wire rope stress analysis could be calculated easily given that the bicycle brake cable was a SHIMANO Stainless Steel Universal Brake Cable with a wire diameter,  $d$  of 1.6 mm which is about 0.064 inch and the length of the cable bought is 2.05 m long. The tensile stress of the wire rope could be calculated as shown below:

$$\sigma = \frac{F_c}{A_w} = \frac{64.4807}{\frac{\pi}{4}(d^2)} = \frac{64.4807}{\frac{\pi}{4}(0.0016^2)} = 32.07007 MPa$$

*Equation 61: Tensile stress for wire rope*

The safety factor of the wire rope could be found if the Ultimate Tensile Strength of the wire rope is given. However, several bike cable testing was done by students at the University of Pennsylvania, and the students found that the stainless steel bike cable with a diameter of 0.064" could withstand approximately 300 lbf as shown in the **Figure 49** shown below (*University of Pennsylvania, 2013*).

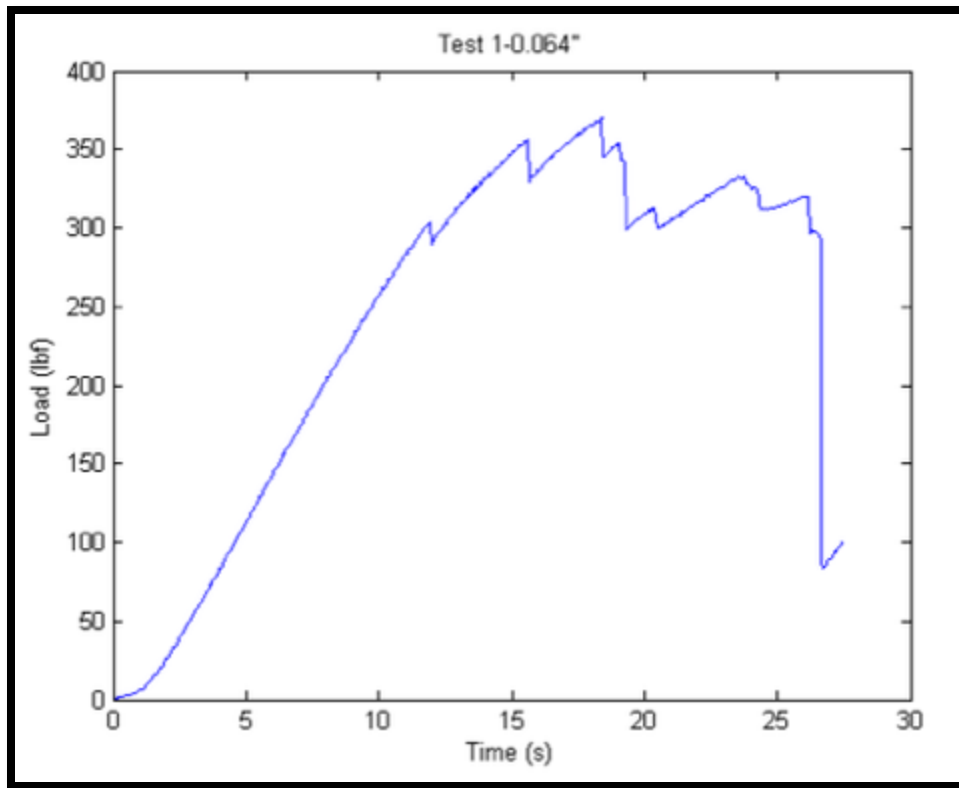


**Figure 49:** Tensile Stress Testing of the 0.064 " Diameter Bike Cable

From the **Figure 49**, it was assumed that the ultimate tensile force of the 0.064 inch diameter wire rope of the bicycle cable,  $F_u = 300 \text{ lbf} = 1334.47 \text{ N}$  because it could only withstand up to 300 lbf before breaking. With the experimental ultimate tensile force for the stainless-steel bicycle wire rope with a diameter of 1.6 mm or 0.064 inch, the factor of safety could be determined as shown below:

$$\eta_{wire} = \frac{F_u}{F_c} = \frac{1334.47}{64.4807} = 20.696$$

*Equation 62: factor of safety for wire rope*

Since the calculated safety factor of the bicycle wire rope,  $\eta_{wire}$  is 20.696 which is greatly more than one, the durability of the bicycle brake wire rope for the regenerative braking system design operation is high. Hence, it was safe to use, and it would not break easily.

## 5. Conclusions

Despite months of work and numerous modifications, the team deems that this design is leaning towards being unviable, due to having more disadvantages than advantages. To start off, the entire regenerative braking system weight slightly more than the bicycle itself. This making for a terrible riding experience. The cyclist needs to put out a lot more energy to move the bicycle than he or she would when riding a bicycle without this regenerative braking system.

Secondly, the efficiency calculated is low, 0.12. This means that only 12% of the energy used to move the bike can be used for kick starting the bicycle. This combine with that fact that the bicycle weight about 20 kg. It becomes a chore to move the bicycle to a sufficient speed to store enough energy for kick starting a 20kg bicycle with a regenerative system that has 0.12 efficiency to a decent speed. This will be an extremely tiring process.

Lastly, the entire regenerative braking system itself is large. It requires a lot of room to fit it on to the bicycle. This decreases the viability significantly, because heavy modification needs to be done on the bicycle frame to make room for the system. In addition, the bulkiness of the system might affect the comfort of riding, since the cyclist leg might constantly run into the system.

As for advantages, this design is simple. There are no complex actuation mechanism or energy storage methods involve. It is a simple cone clutch plus flywheel energy storage design. The simplicity combine with the fact that components are typically held together by a few nuts and bolts, offers a great amount of flexibility in both modification and repairs. Other can easily understand the working principle behind this design and modify the design or repair it. The

flexibility offer by this design allows others to use this design as a skeleton for their own regenerative braking system.

If there are more time, the team will consider spring as an option instead. After doing this project, the team found out that flywheel needs to be large and heavy in order to achieve good efficiency (larger moment of inertia). On the other hand, spring will be better choice simply because of its low weight and small size. The factor that governs how effective a spring is at storing energy is spring rate, instead of moment of inertia. Spring rate is not heavily governed by weight and size. This leads to two benefits alone which already solve the two major issue associated with using a flywheel, hard to move the bicycle due to weight and limited leg room due to size.

## 6. Lessons Learned

There are a lot stuff to be learned from this one semester long project. The most important one is to consider every detail possible. The team suffers from a consistent trend where the team would find something wrong with the design after submitting the report. This is due to the negligent of smaller details and realization of the bigger picture. For example, the team did not consider how this regenerative design would be mounted on the bicycle or be held together when first started brainstorming design. In the intermediate report, the team found out that the three bar linkage had a glaring flaw associated with it (will not provide enough contact between the cup and cone for the cone clutch). Then scrambling to find a solution to fix it.

In addition, the team learns that it is important to spend more time at the beginning to come out with a good and detail design, because the team encounter situation where the chosen design is less than ideal but is too late into the semester to rethink a new design. If the team had a better and more detail design at the start of the semester, the team would need less time coming up with ways to compensate for the short coming of the design.

Another important skill the team learned is machine component selection. The team learn how to use the knowledge learned in class and apply it in a design project. Most of the components selected in this design project is based on optimization calculation. These optimization calculation are done by applying concepts learn from class. Next, choosing the one component needed from a catalog with thousands of options is daunting task. However, through several trial and error, the team manage to figure out ways to do selection quick and effectively by identifying what are the important parameters to constraint in the filter function.

Other than technical skills, the team also learned the importance of communication. Working in a group of six is difficult. The team struggled at first trying to allocate work load evenly, but eventually put through with no trouble. At the beginning some members are extremely free while others are bombarded with endless amount of work. This is solve later through communication, learning to ask for help when there is really too much at hand. Sometimes it is difficult for others to know how much a person is doing especially when that person didn't say anything as well.

This is overall a great project. Begin able a get a taste of how a real design project might be. However, there are rooms for improvement. For example, more guidance is needed at the beginning, because the class is still unfamiliar with many of the essential machine component for this project.

## 7. Appendix

### Computer-Aided Design 2-Dimensional Drawing

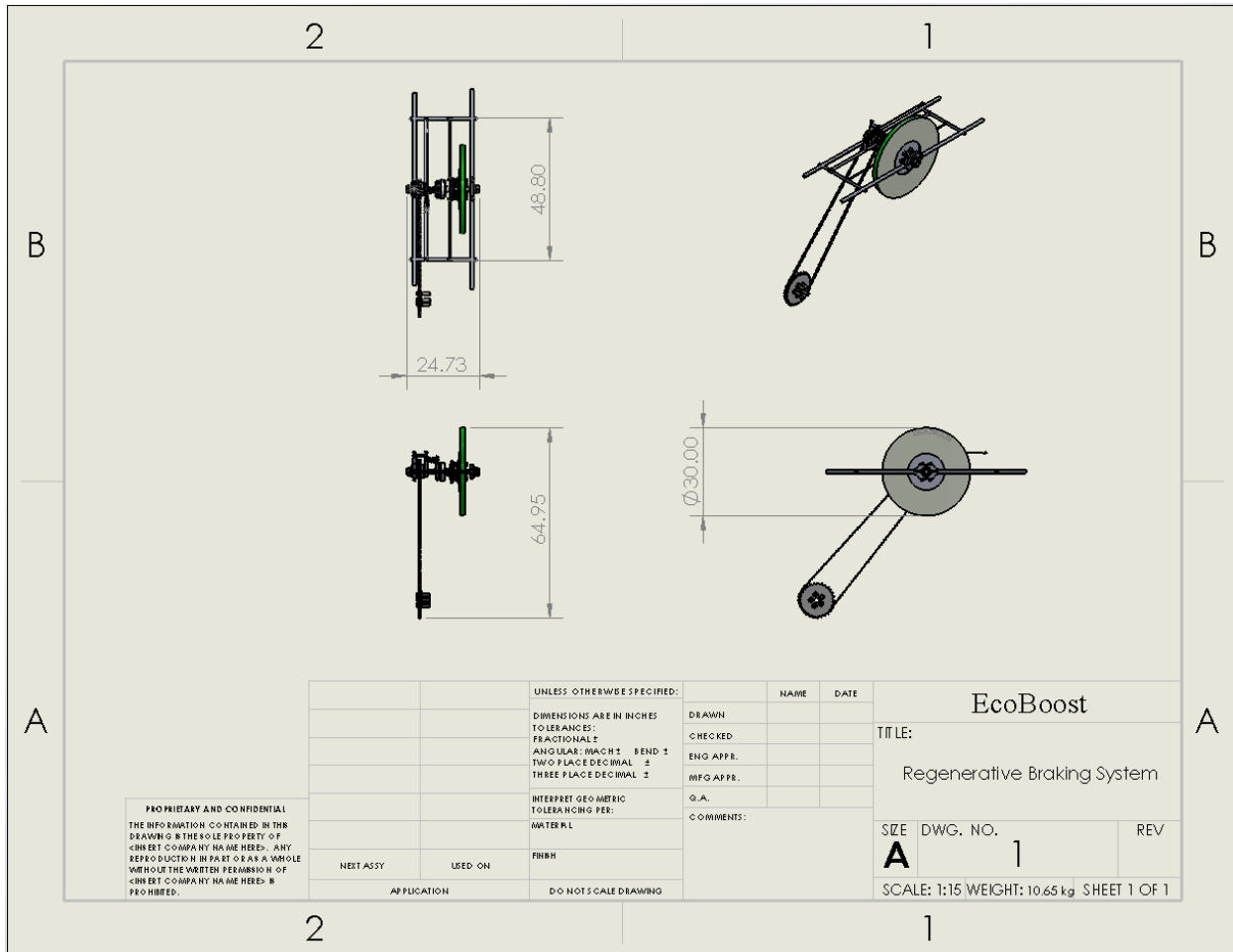


**Figure 50: Regenerative Braking Design 2D Drawing**

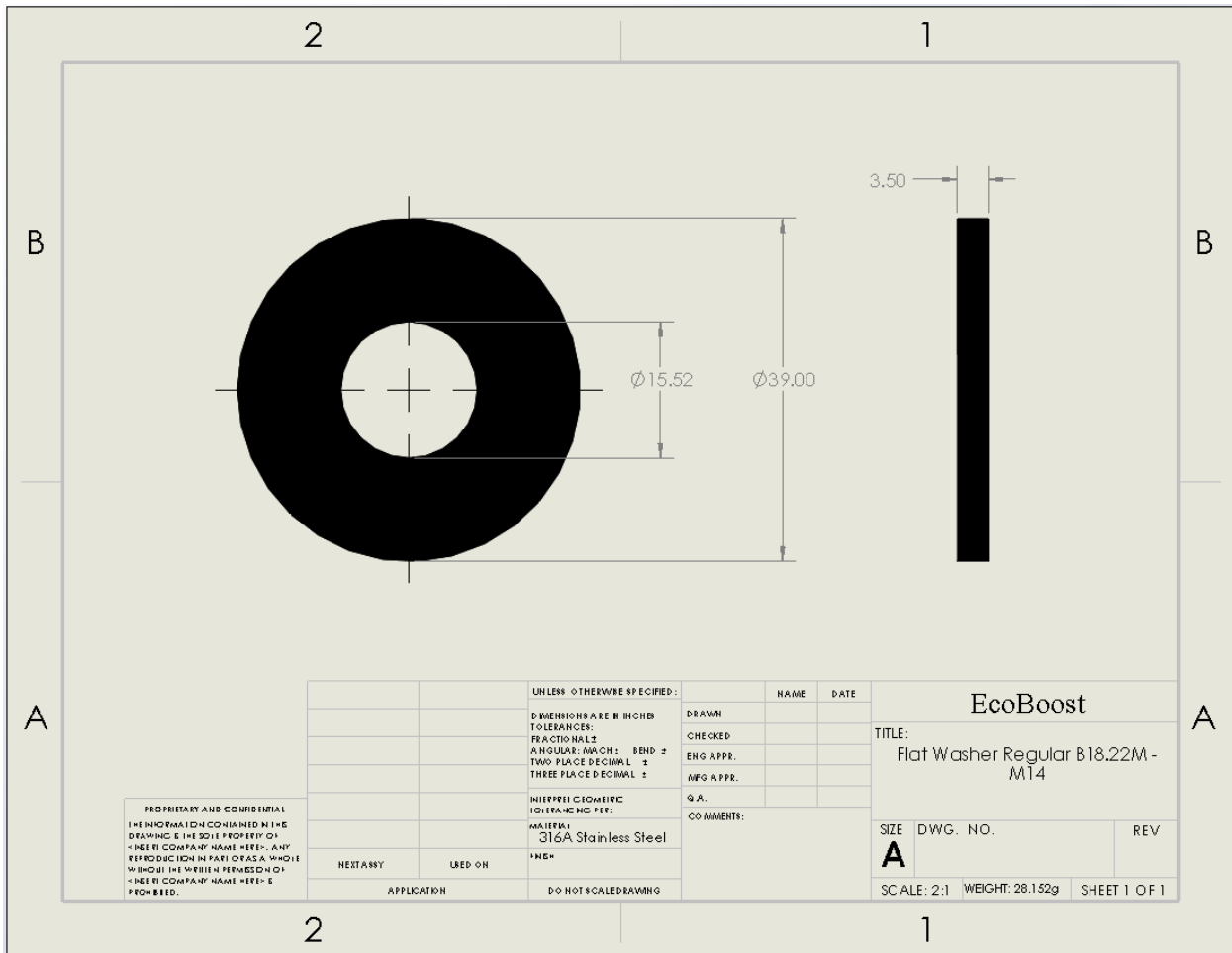


**Figure 51: B18.22M-M14 Washer 2D Drawing**

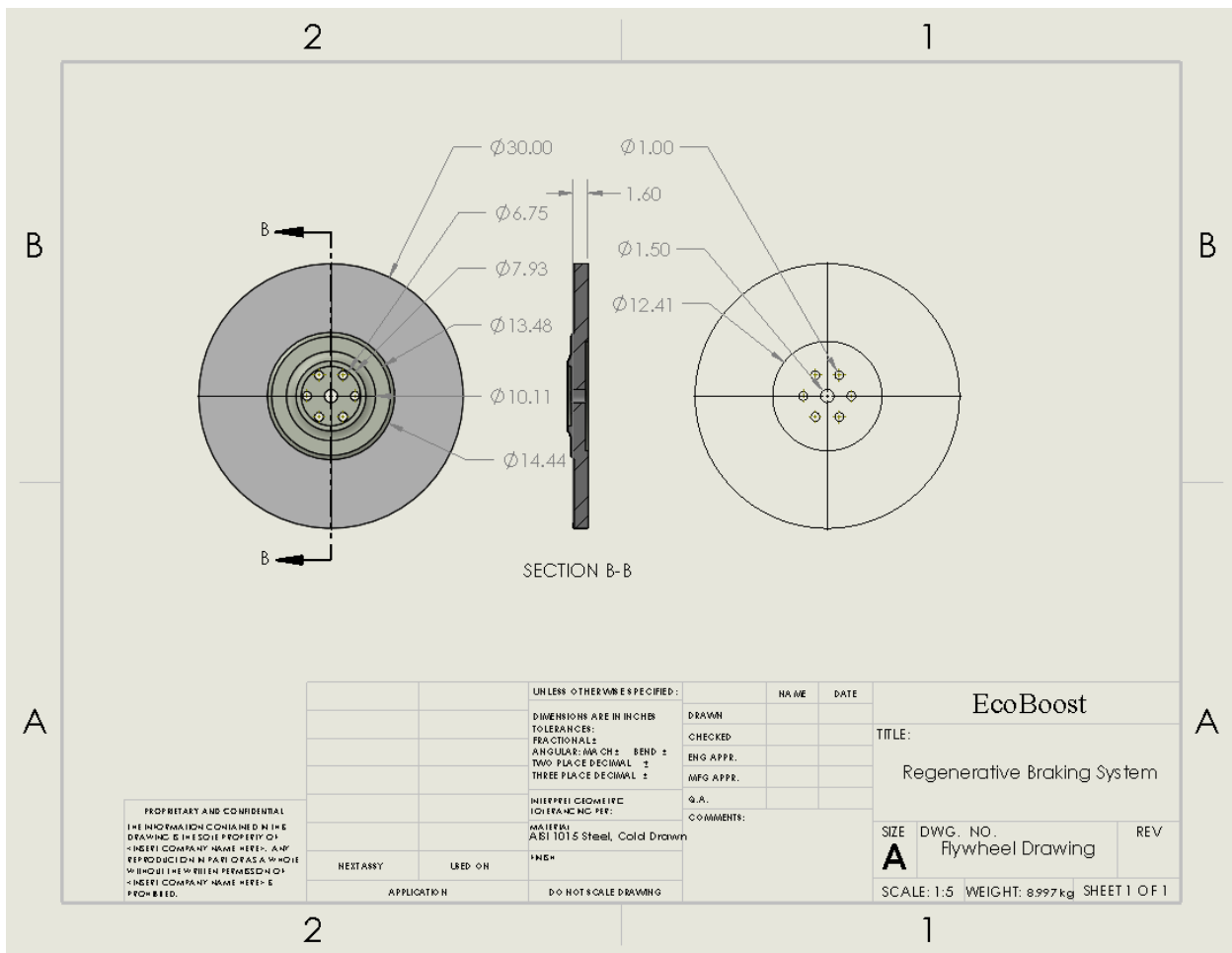


**Figure 52: Flywheel Drawing**

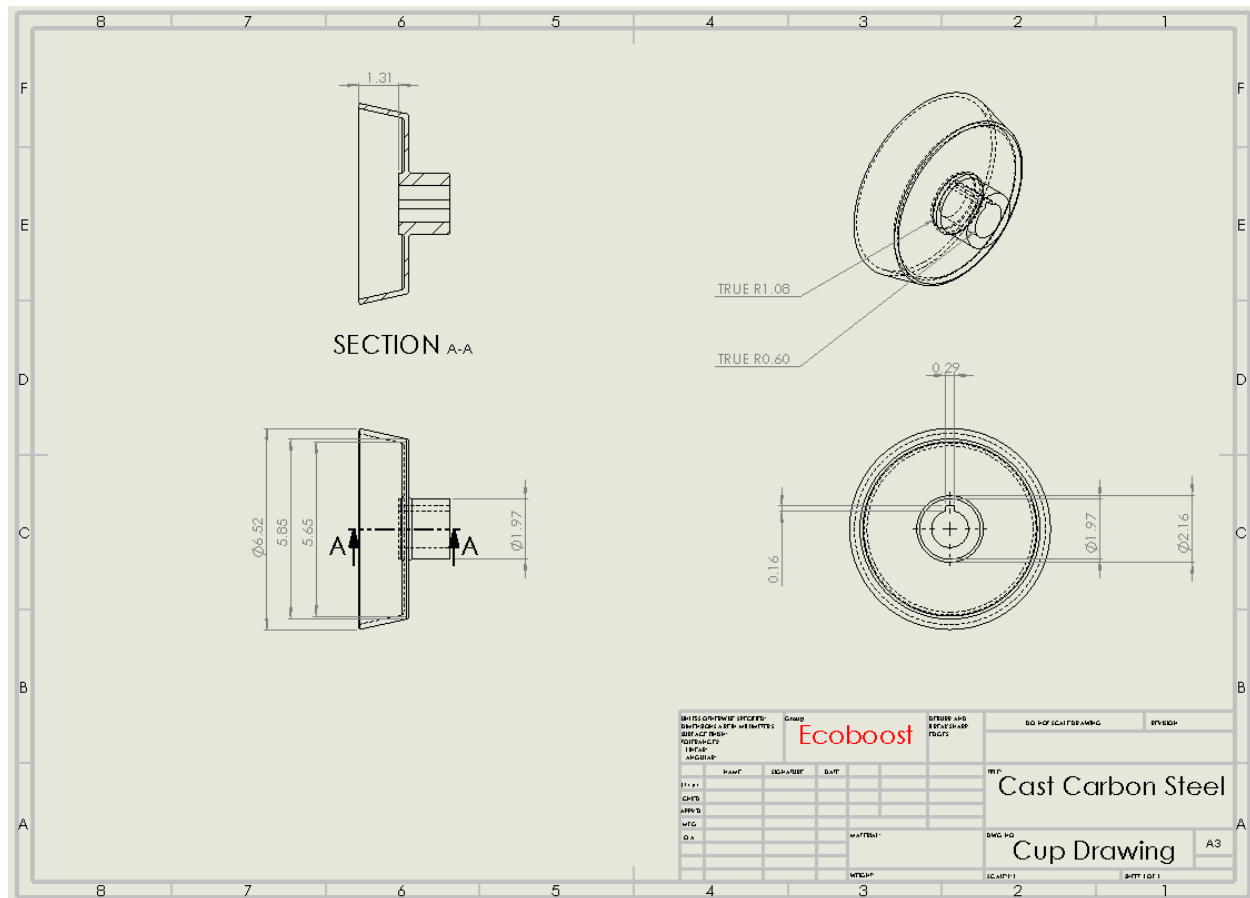


**Figure 53: Cup drawing**

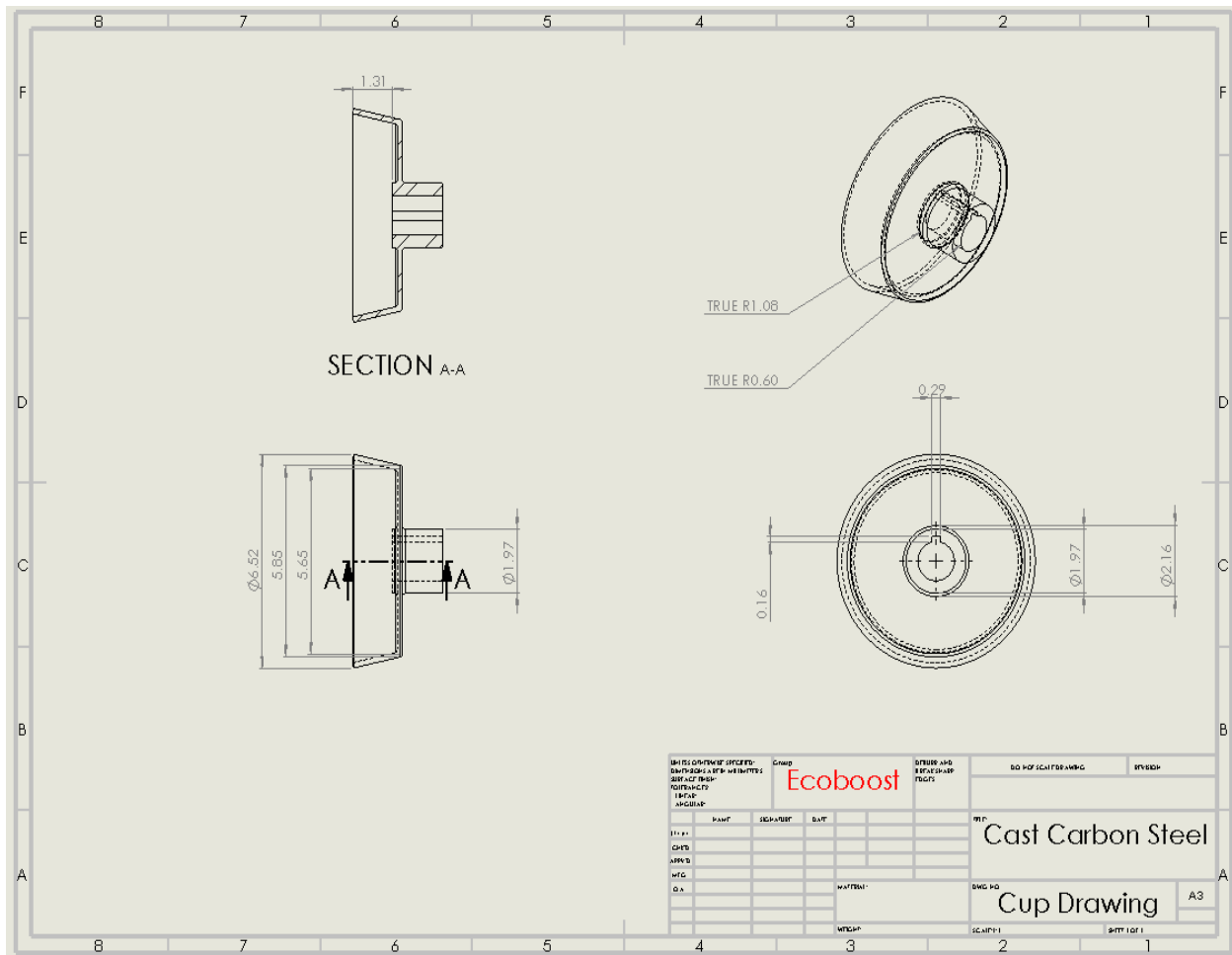


**Figure 54: Driven shaft drawing**

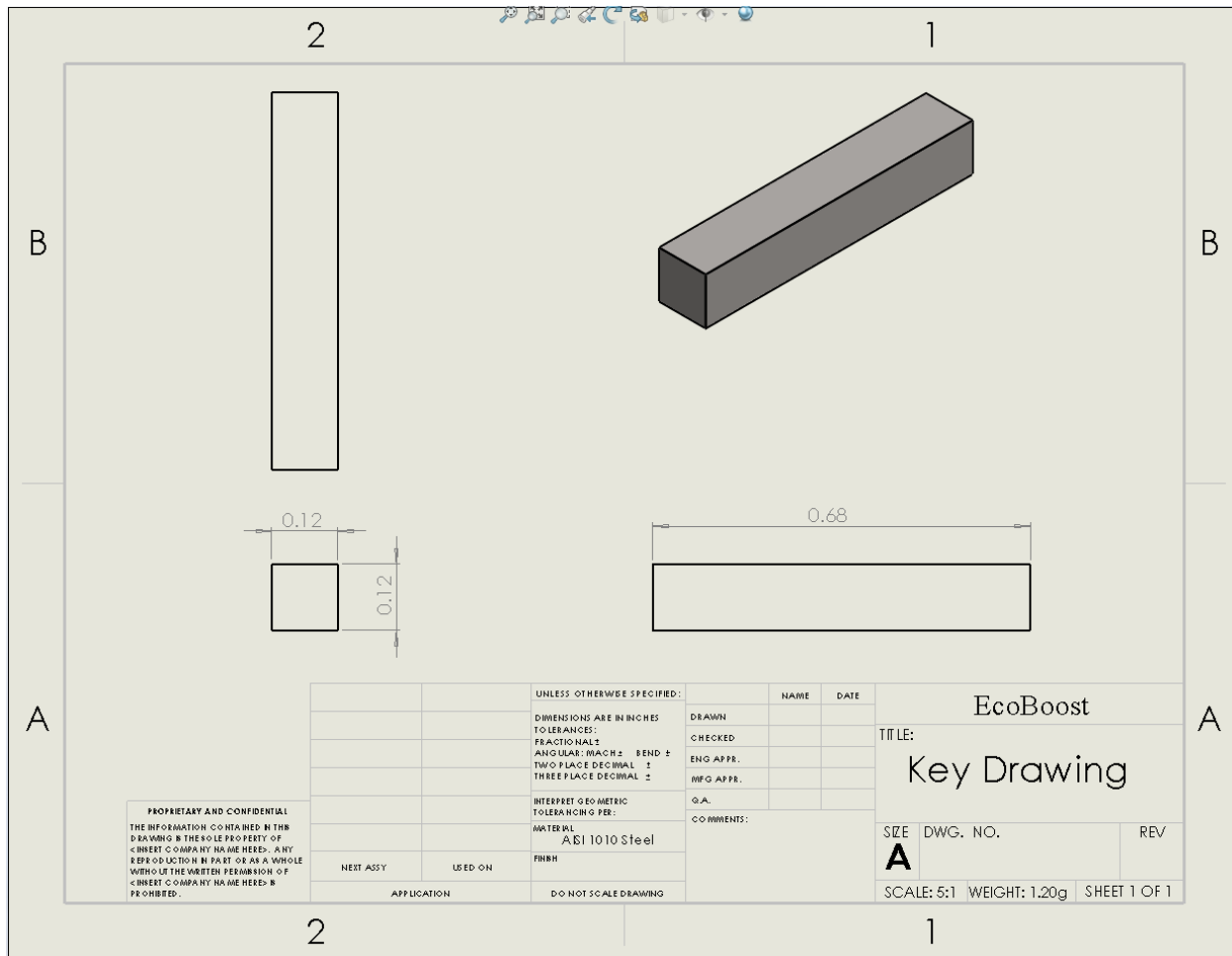


**Figure 55: Key drawing**

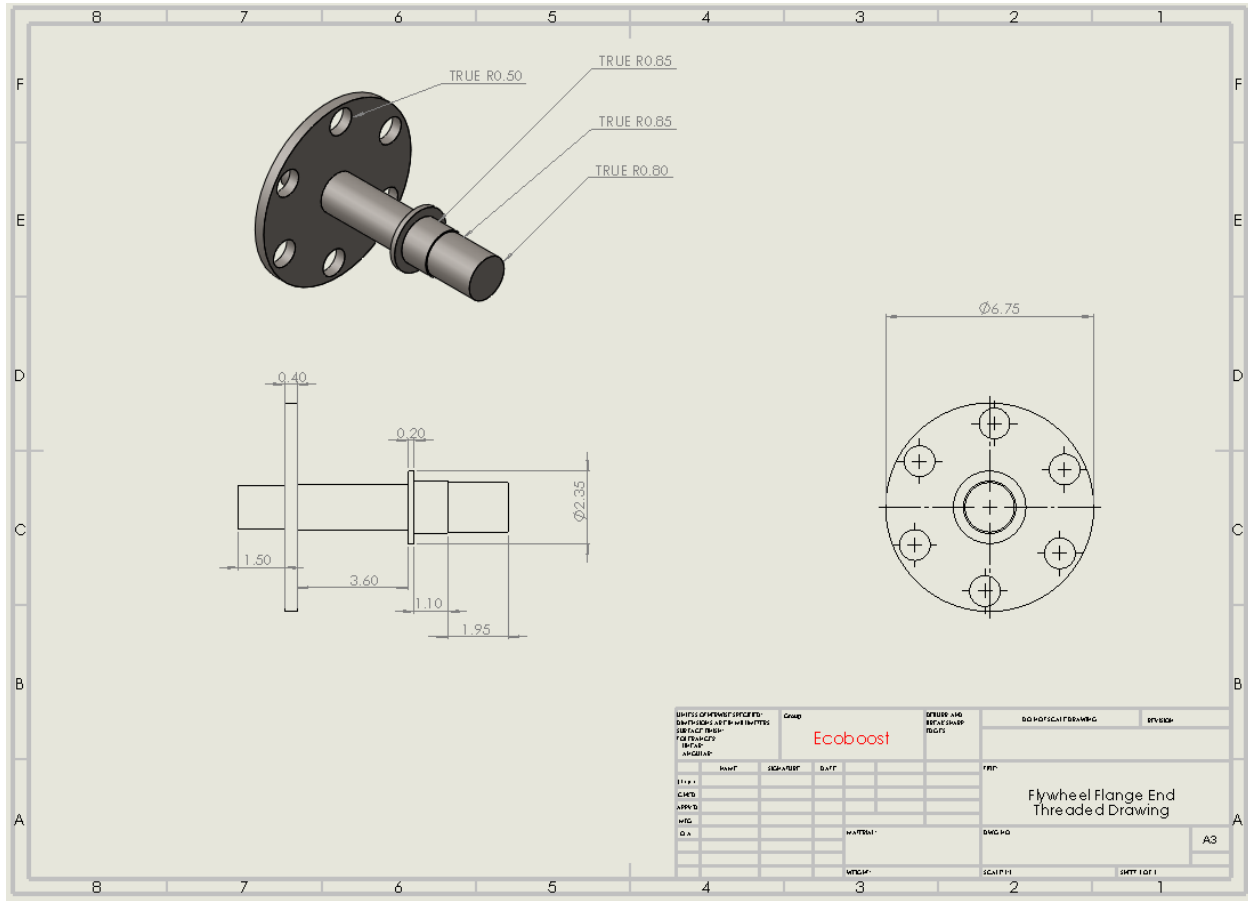


**Figure 56:** Flywheel Flange End Threaded Drawing

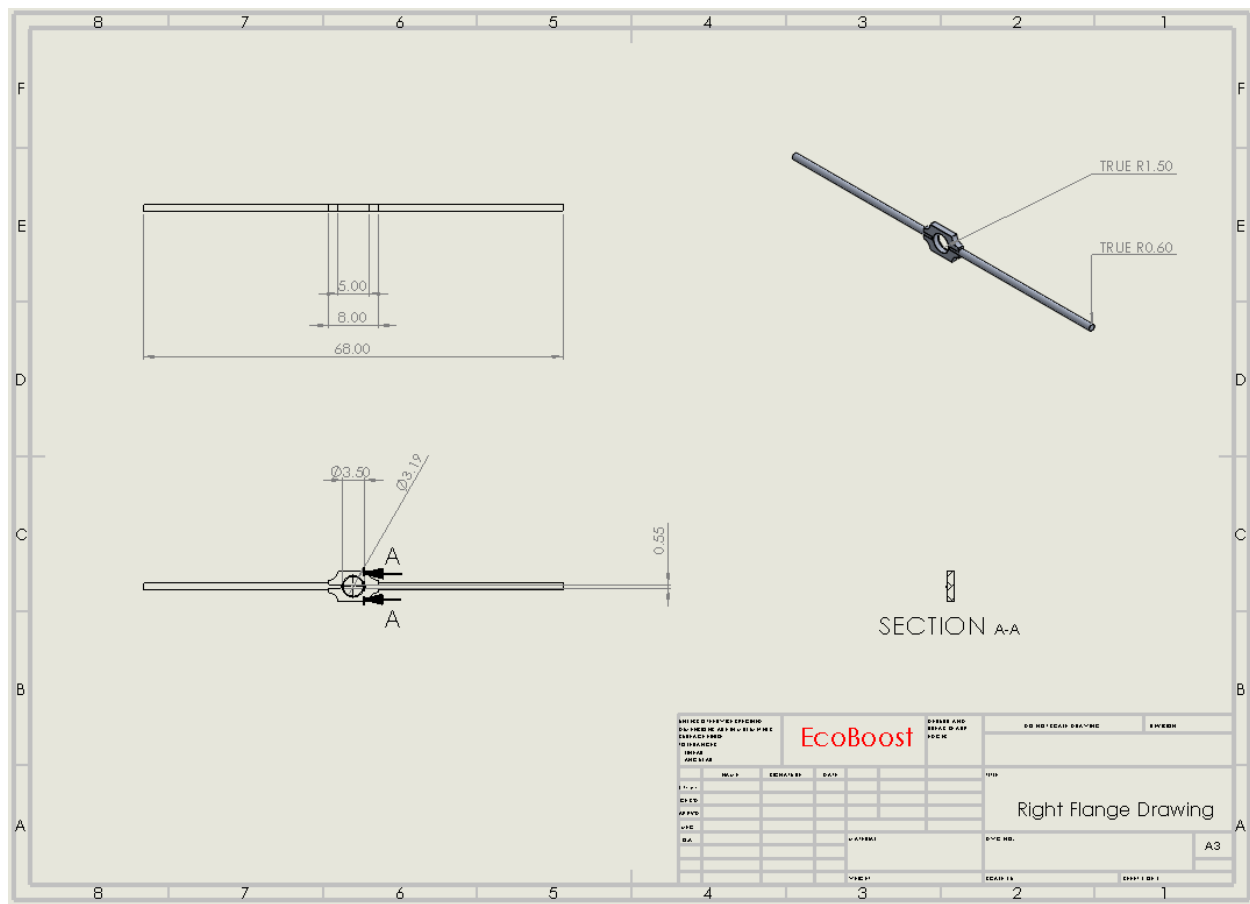


**Figure 57: Right Flange Drawing**

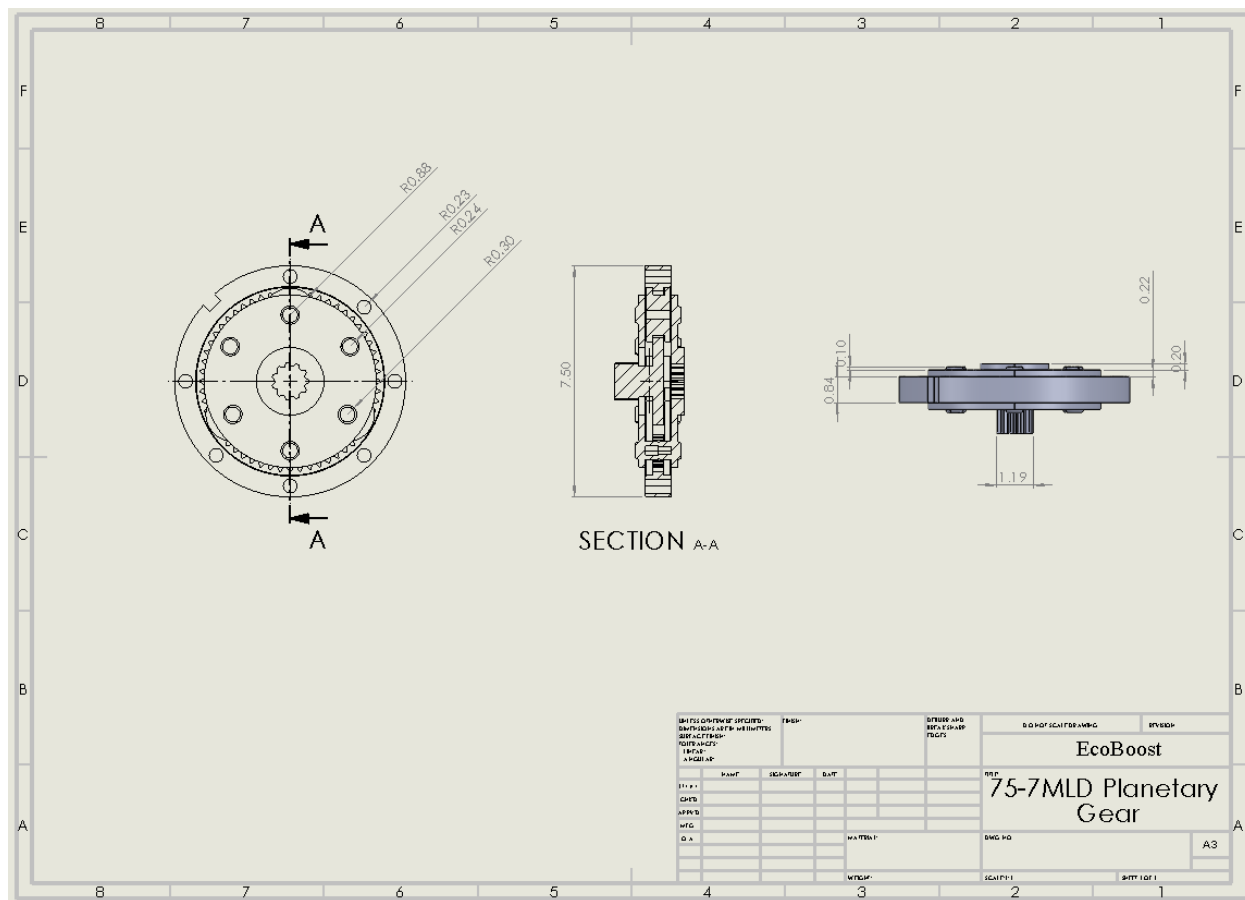


**Figure 58: 75-7 MLD drawing**

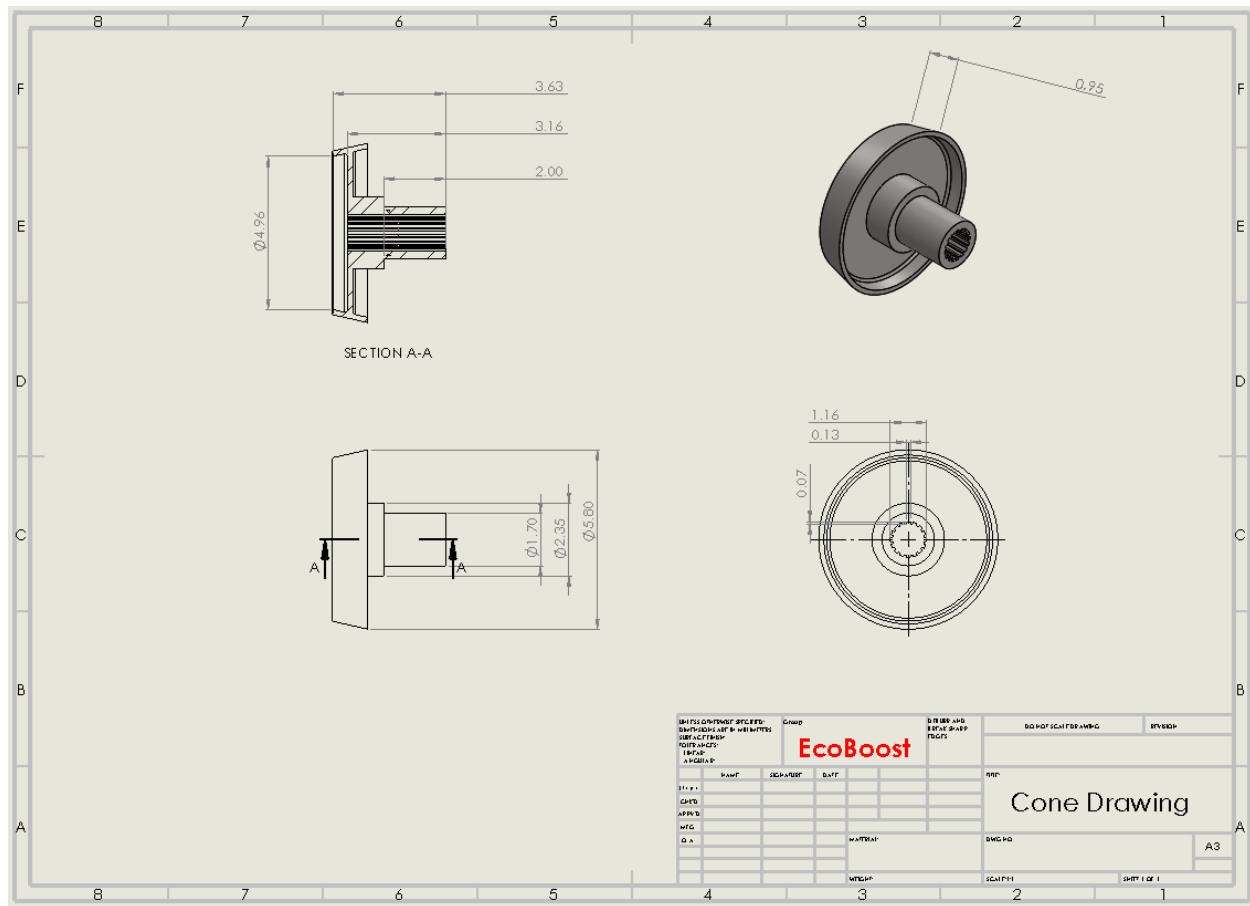


**Figure 59: Cone drawing**

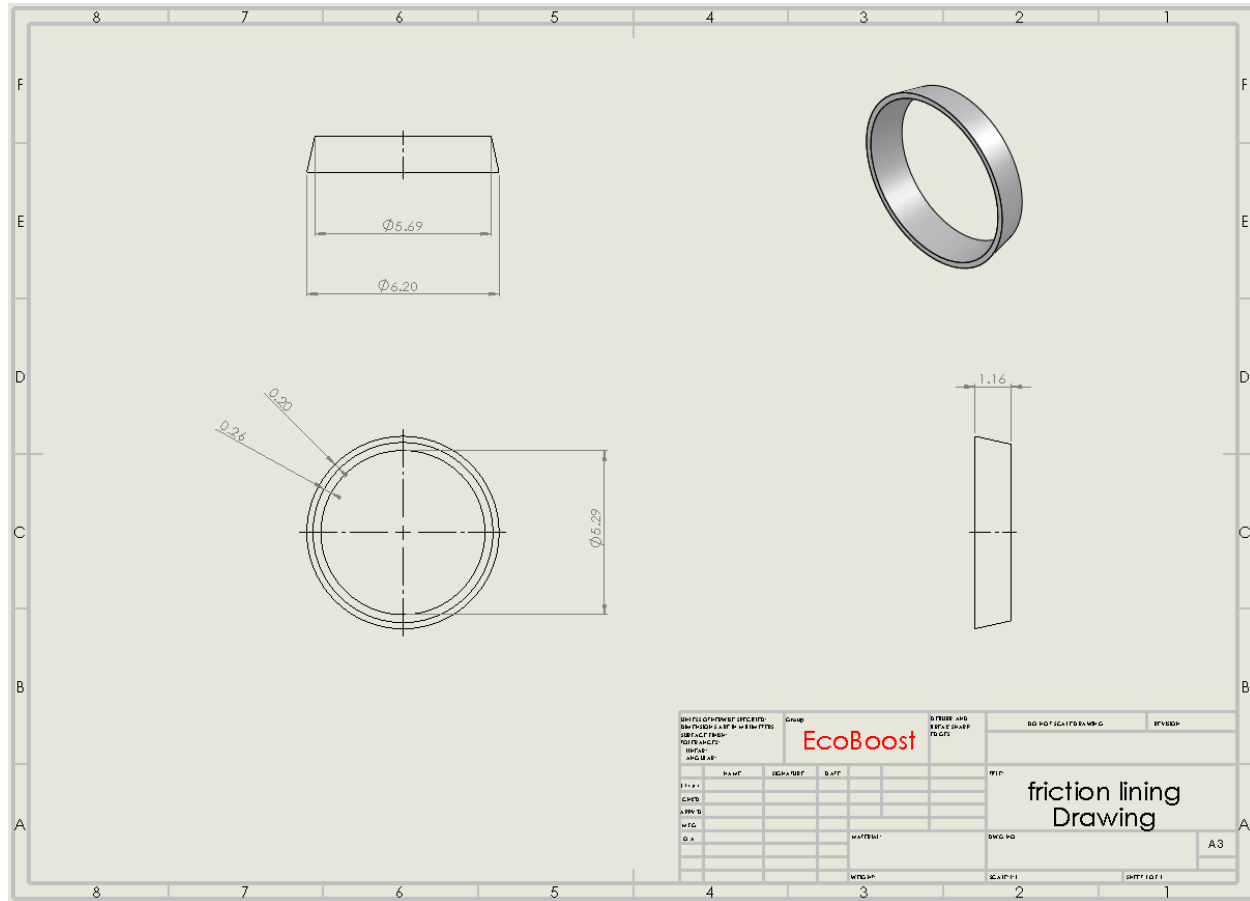


**Figure 60: Friction line drawing**

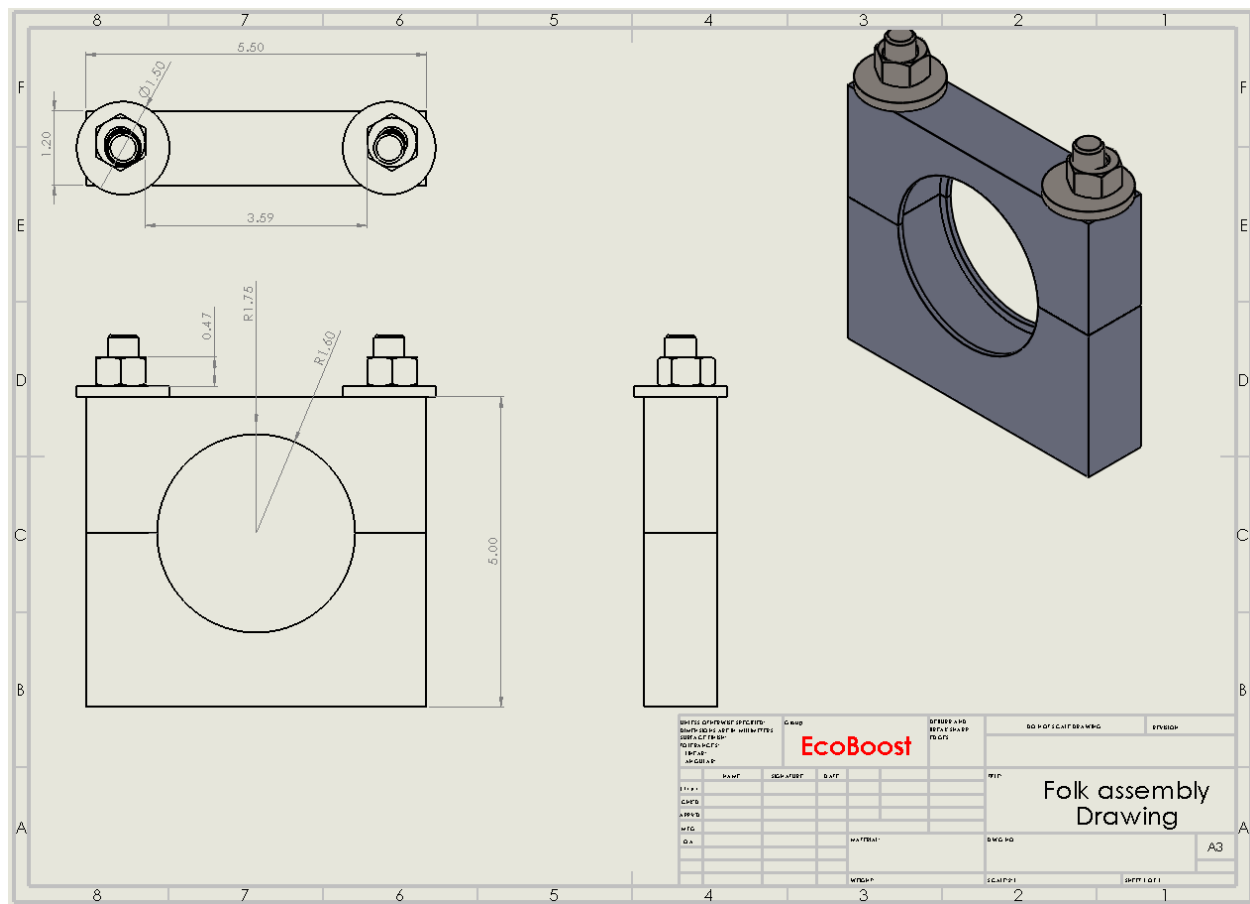


**Figure 61:** Folk assenby drawing

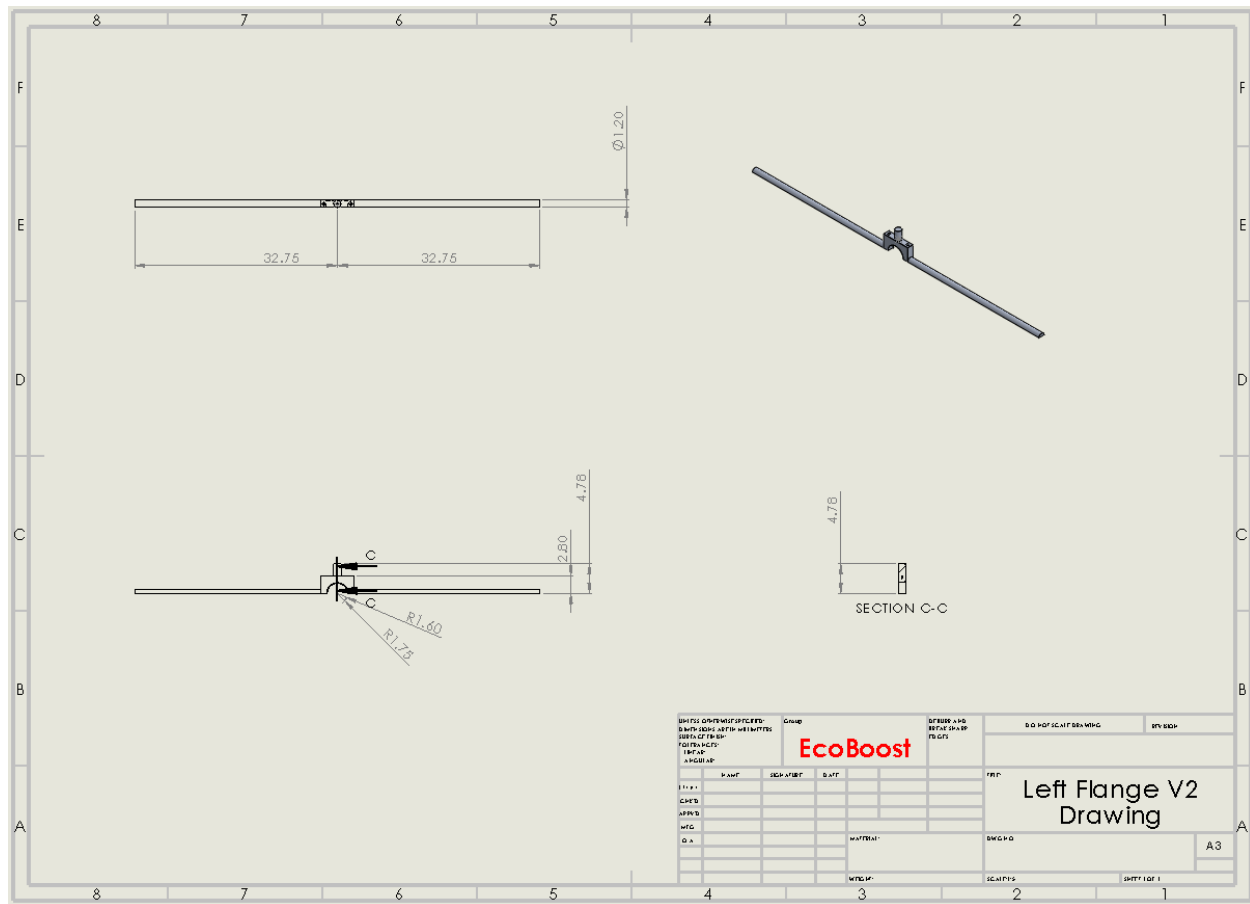


**Figure 62: Left Flange V2 Drawing**

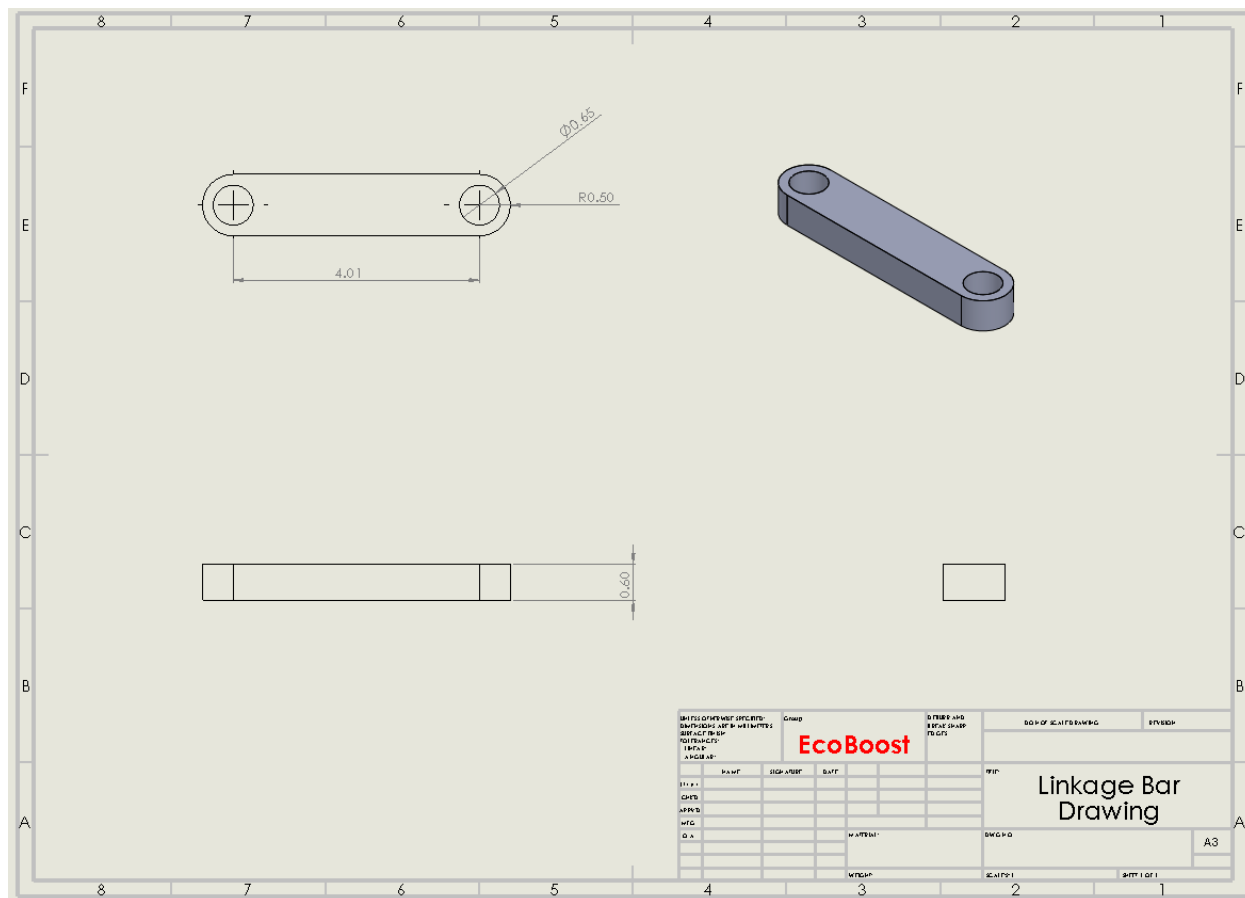


*Figure 63: Linkage bar drawing*

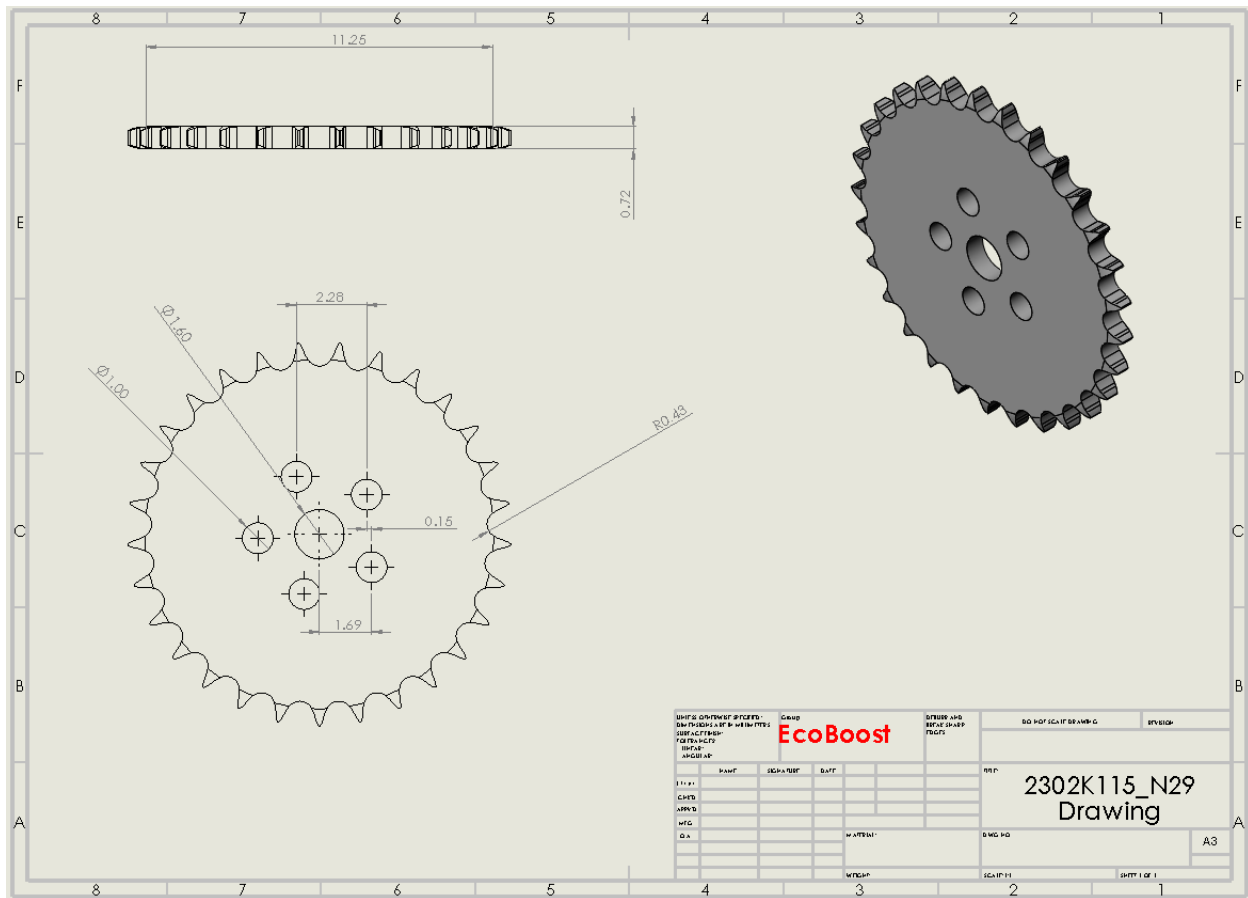


**Figure 64: 2302K115 Rear Wheel Sprocket with 29 Teeth Drawing (After Machined)**

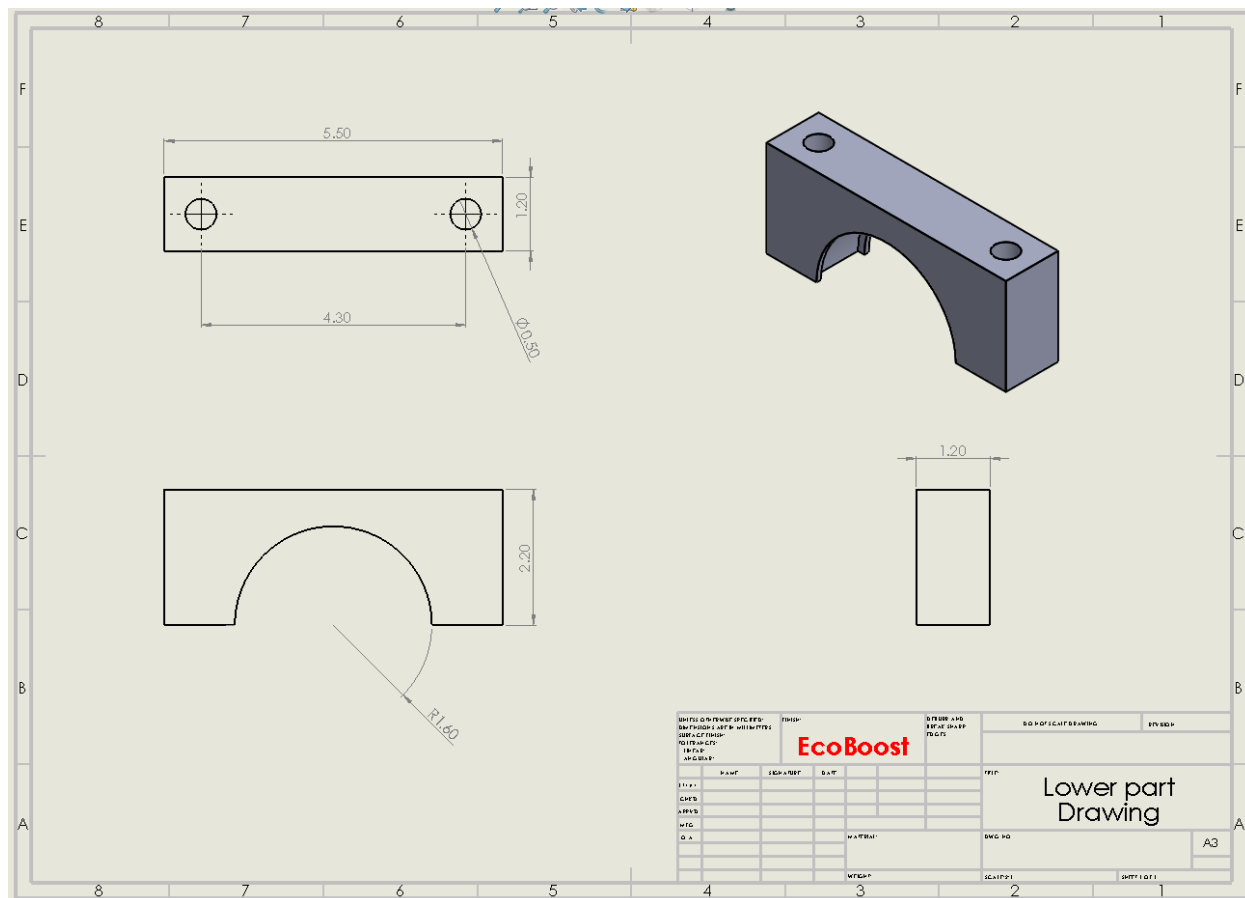


**Figure 65: Lower part**

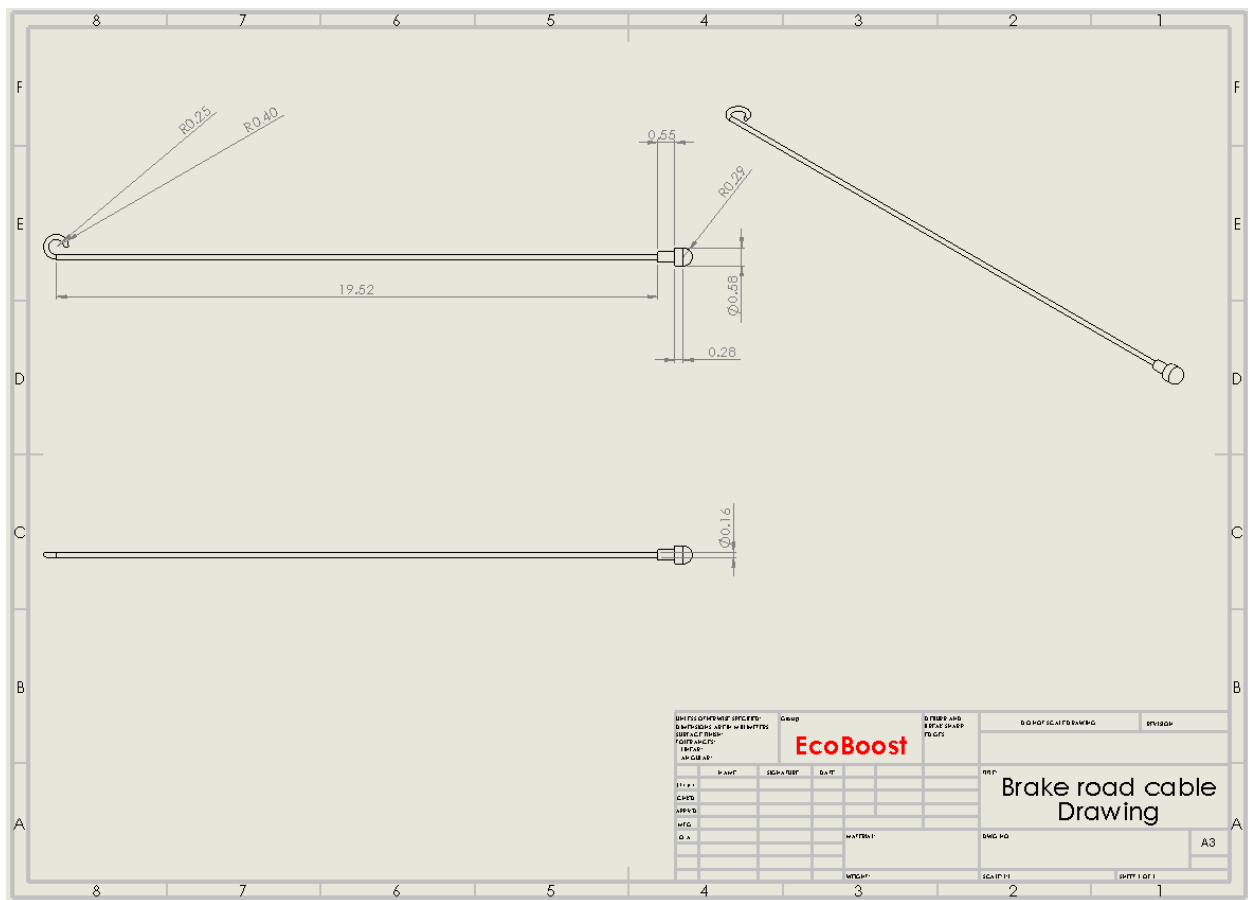


**Figure 66: Brake Road Cable Drawing**

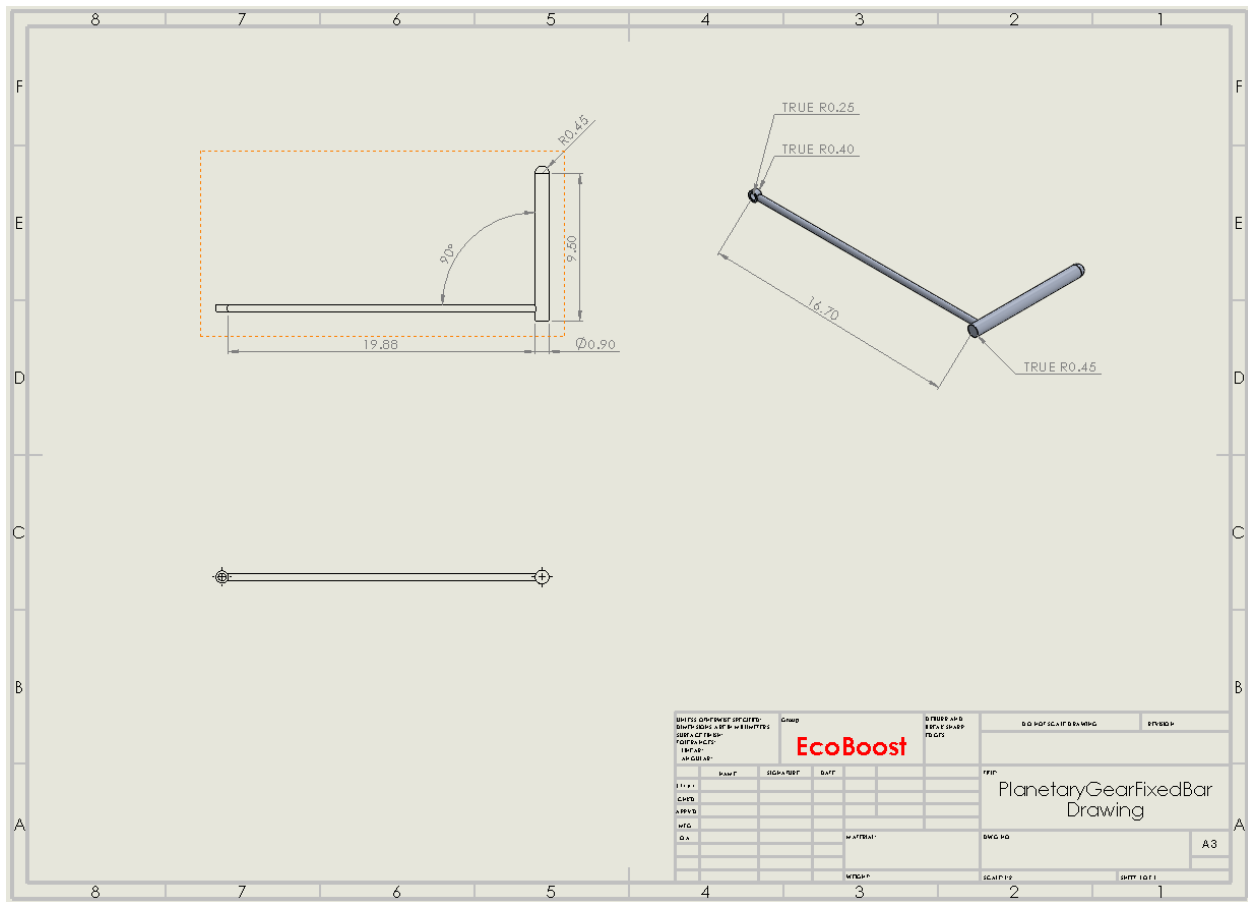


**Figure 67: PlanetaryGearFxedBar**

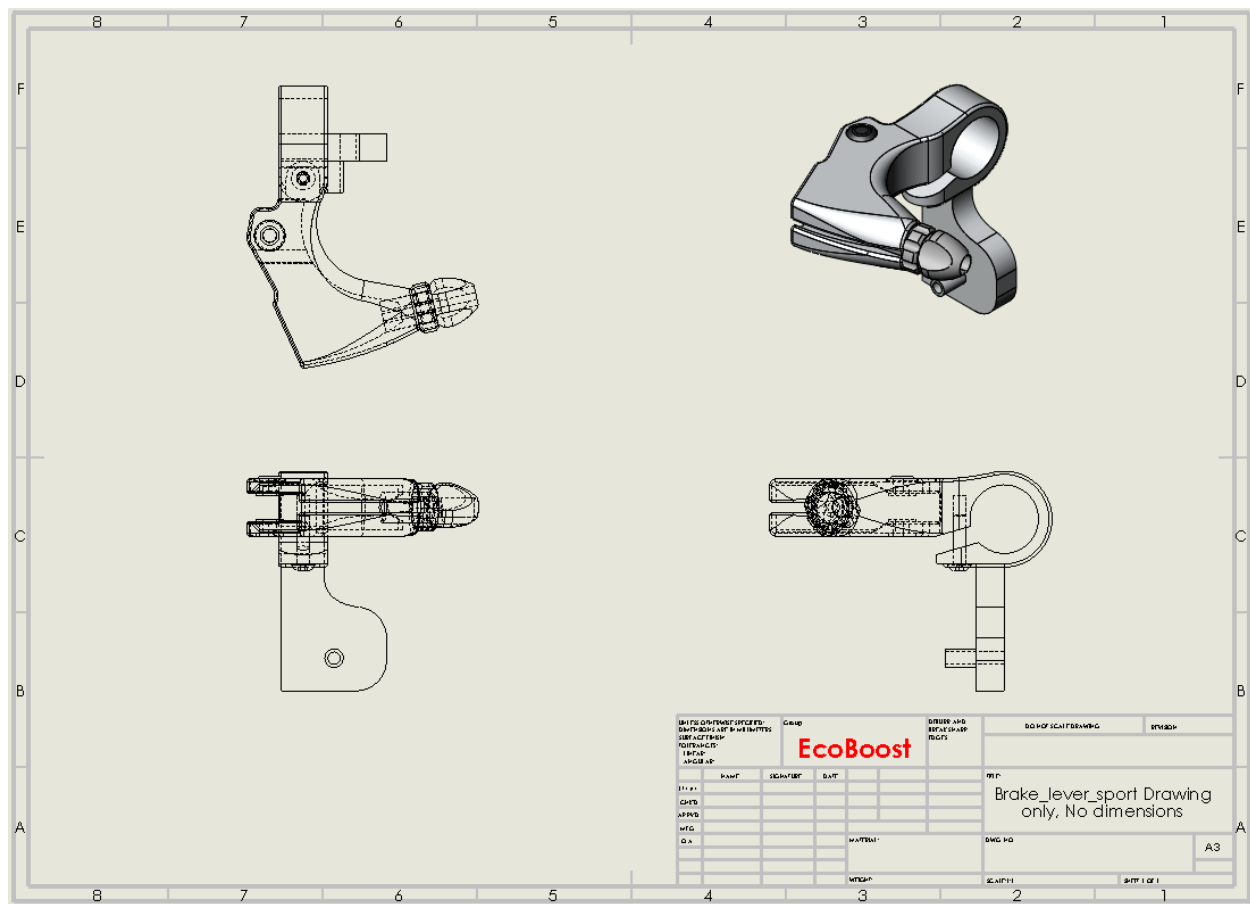


**Figure 68: Brake lever sport Drawing**

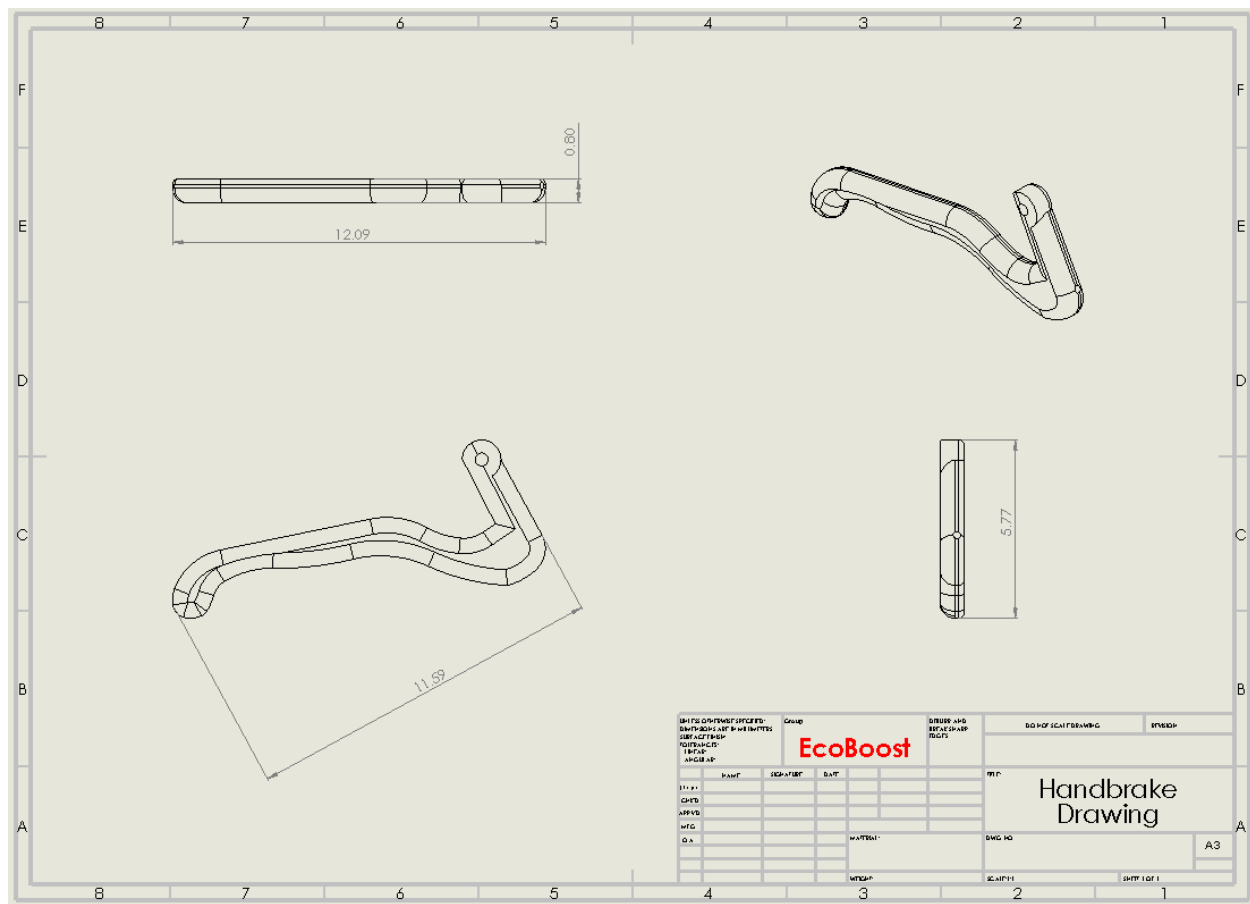


**Figure 69: Handbrake Drawing**

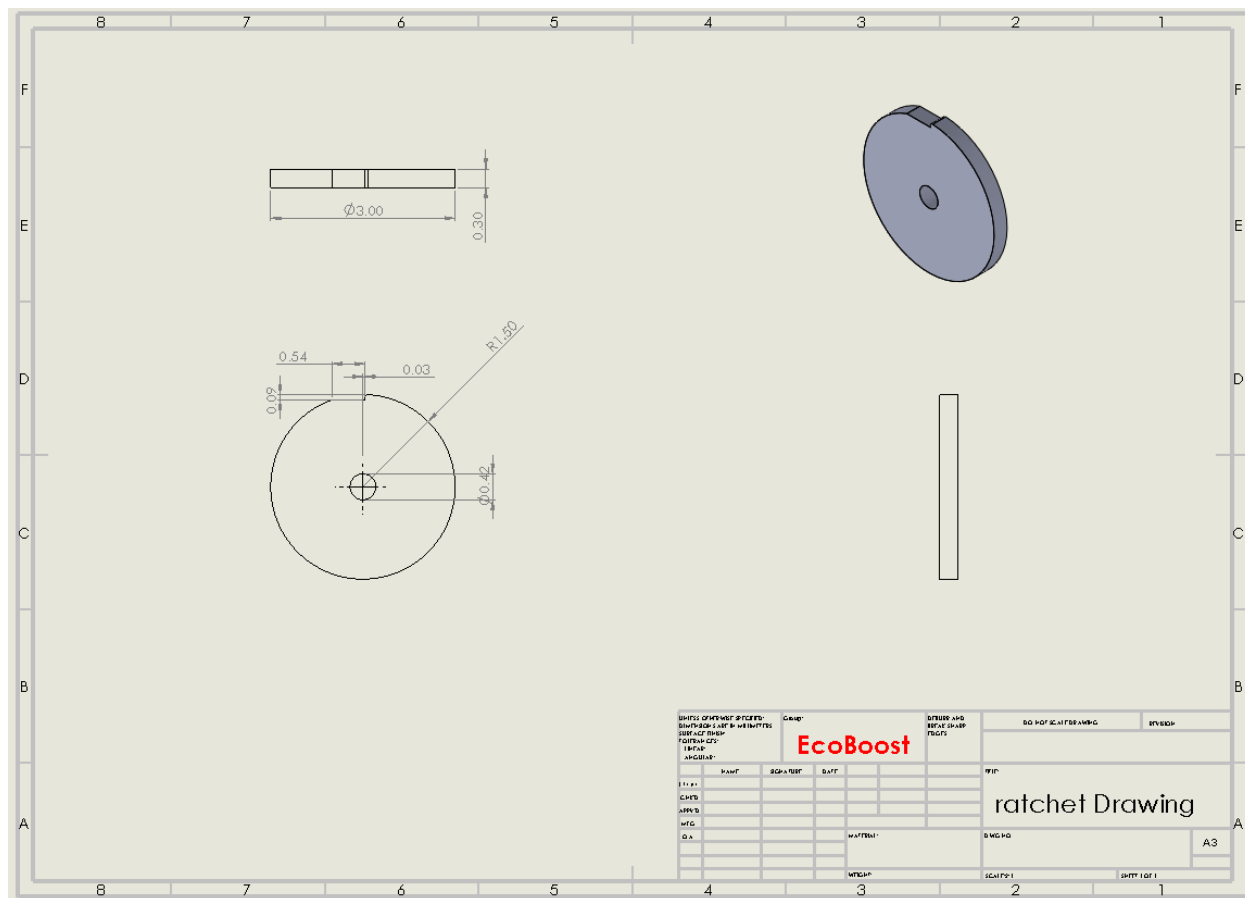


**Figure 70: Ratchet drawing**

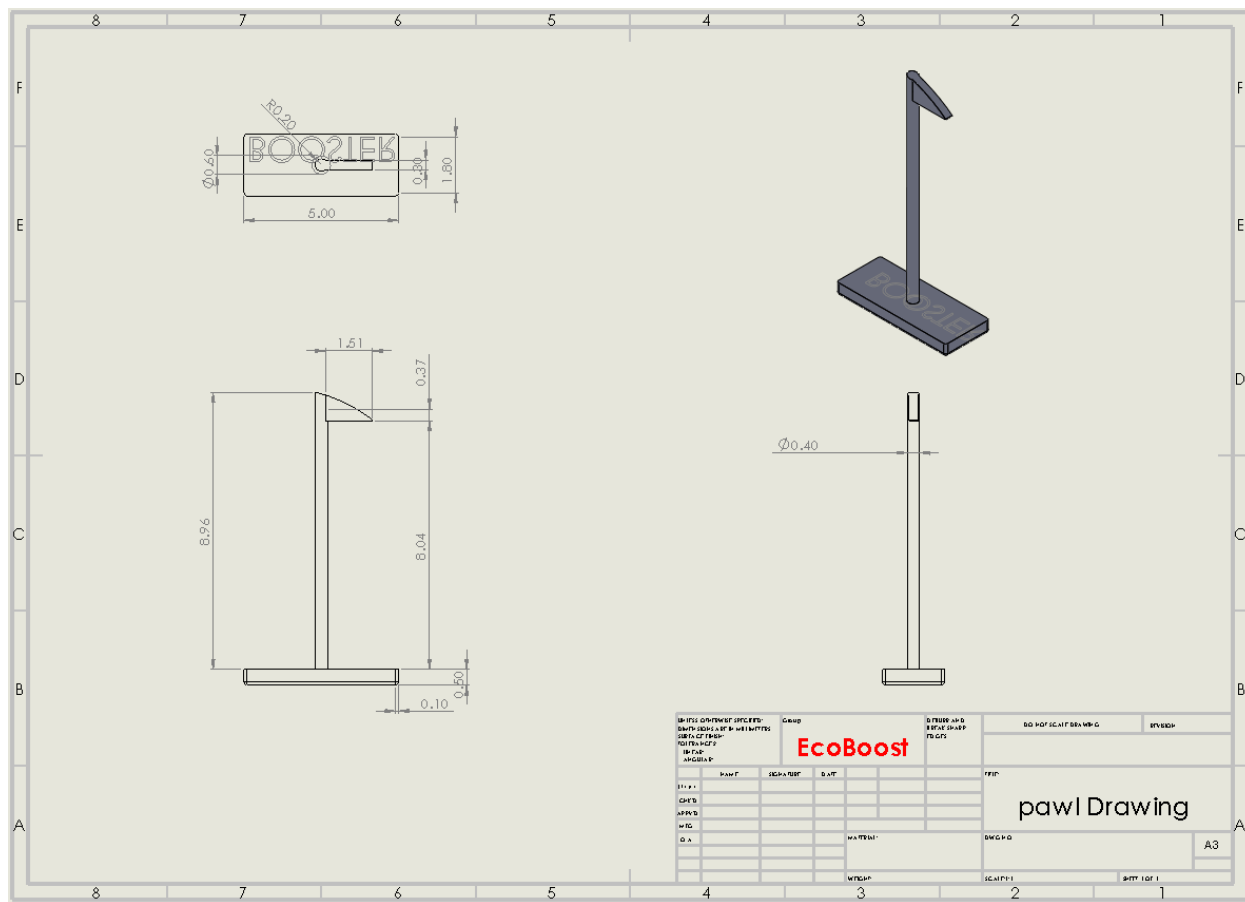


**Figure 71: Pawl drawing**

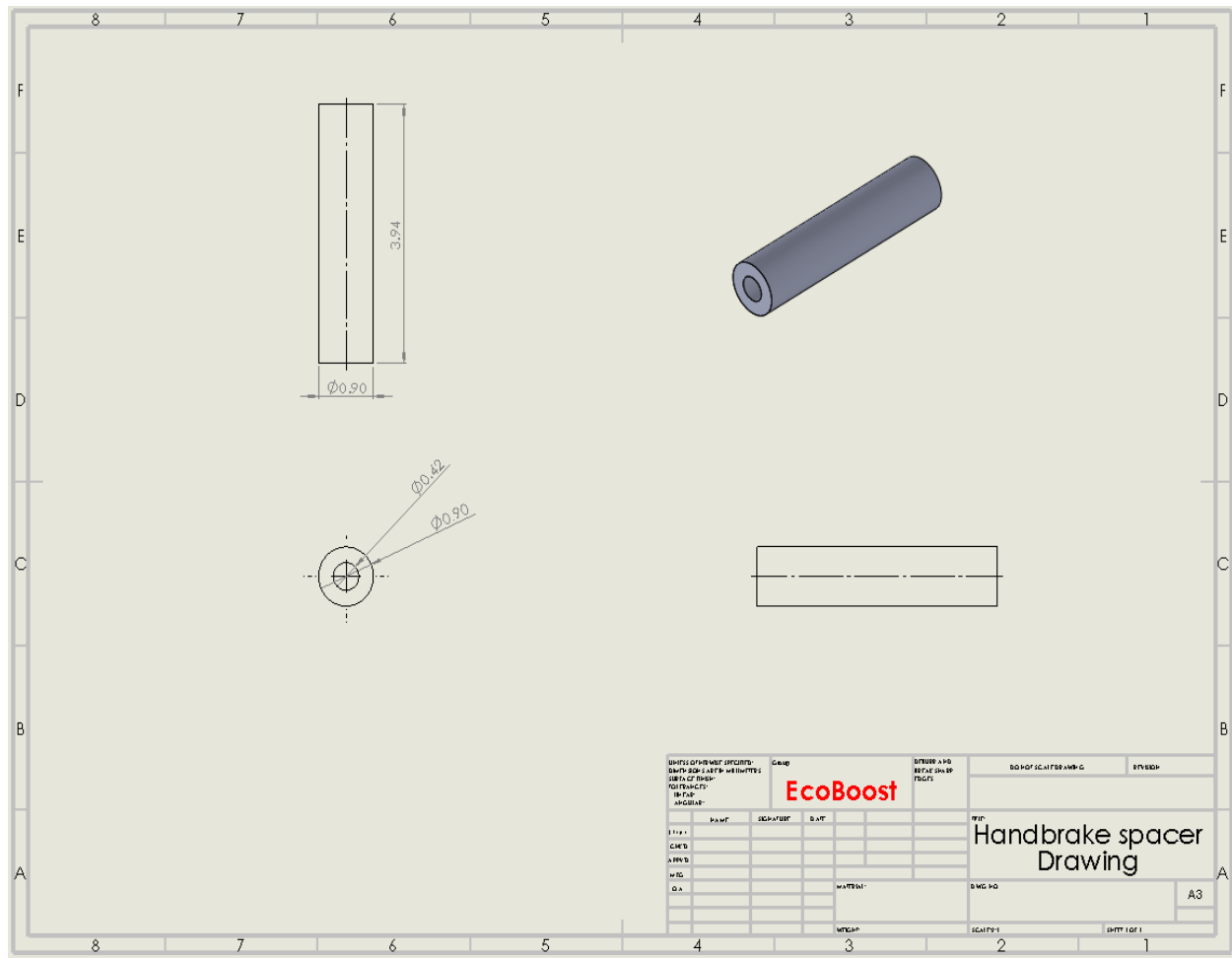


**Figure 72:** Handbrake spacer drawing

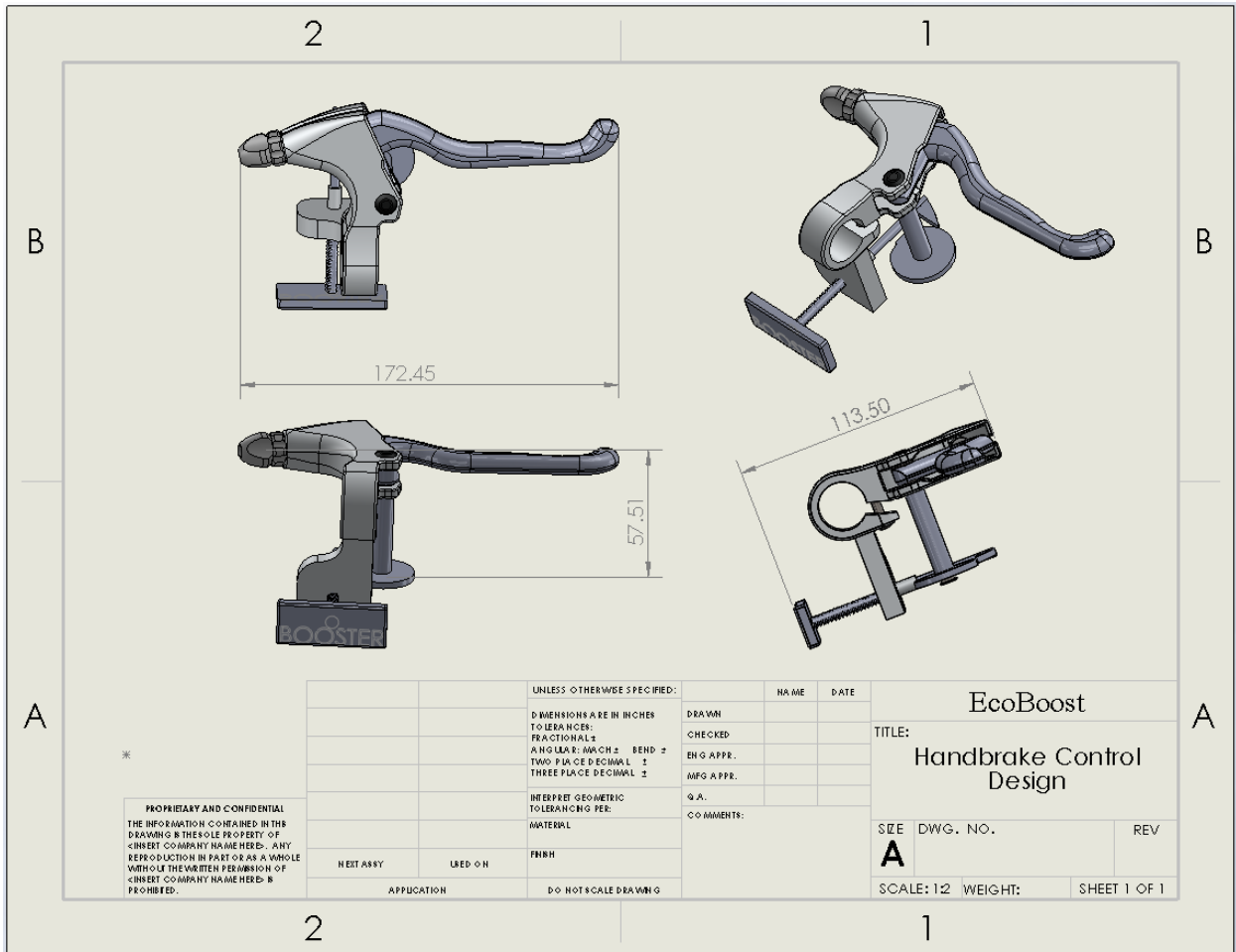


**Figure 73: Handbrake Control Design 2D Drawing**

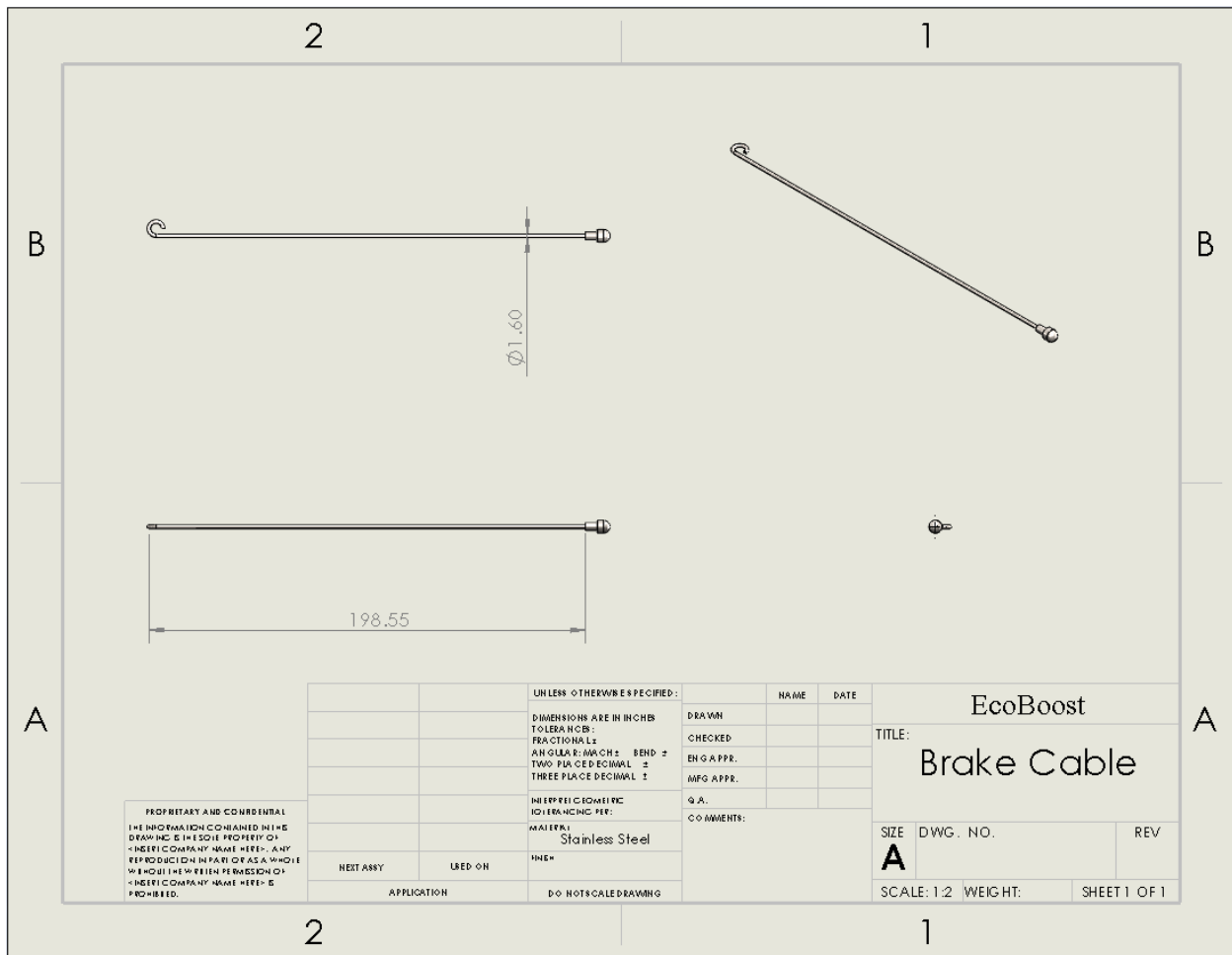


**Figure 74: Handbrake Brake Cable 2D Drawing**

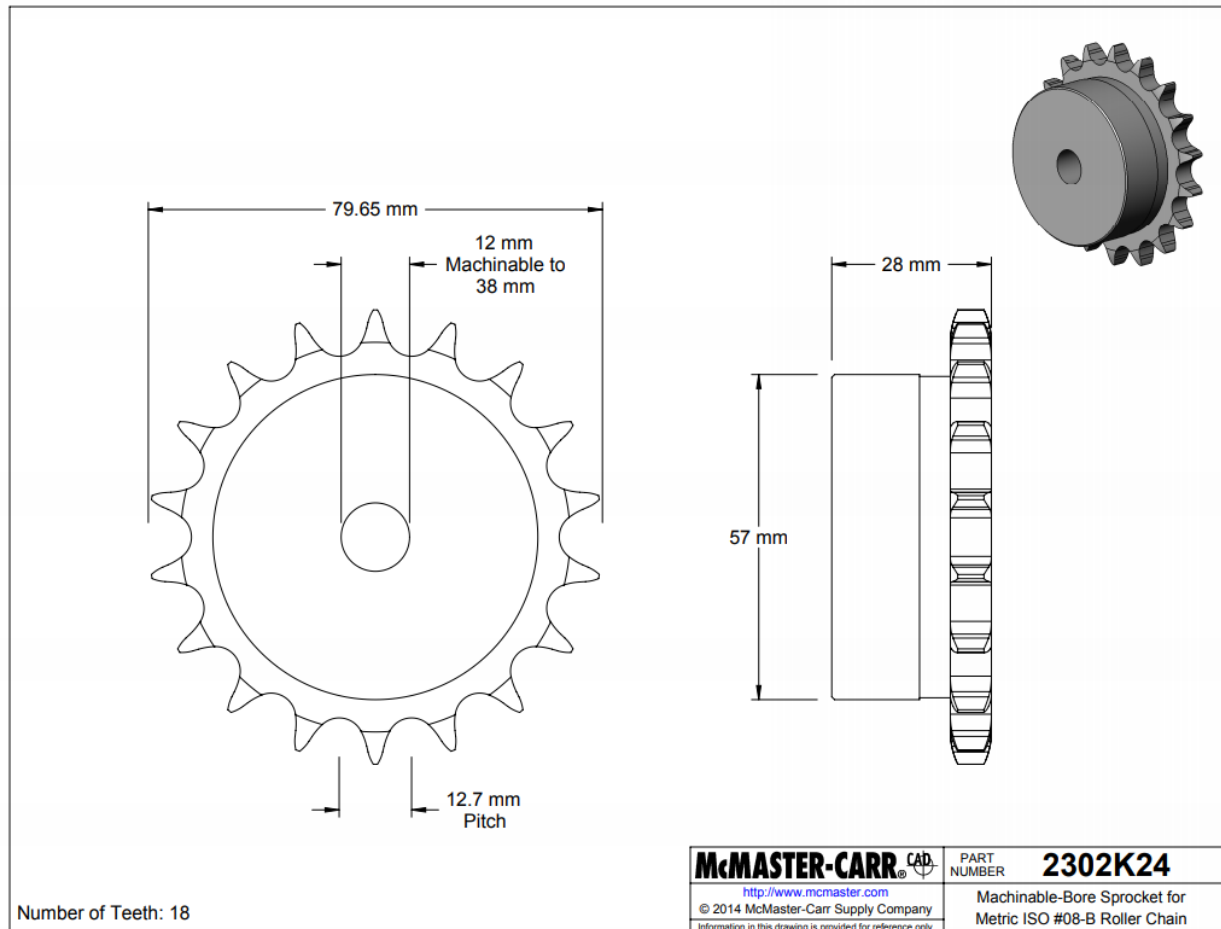


**Figure 75:2302k115 Sprocket with 29 Teeth Drawing (Before Machined)**

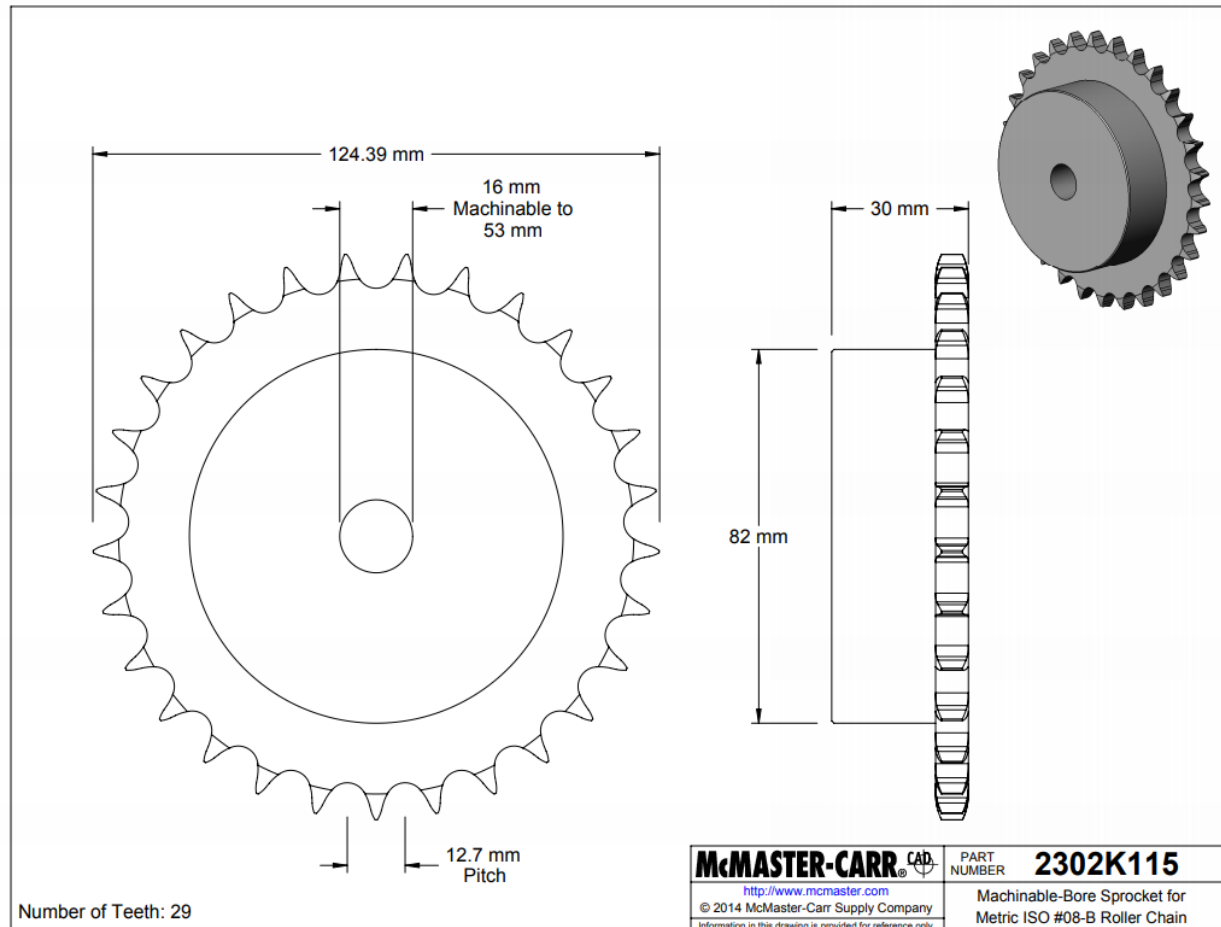


**Figure 76:** 2302k115 Sprocket with 29 Teeth Drawing (Before Machined)

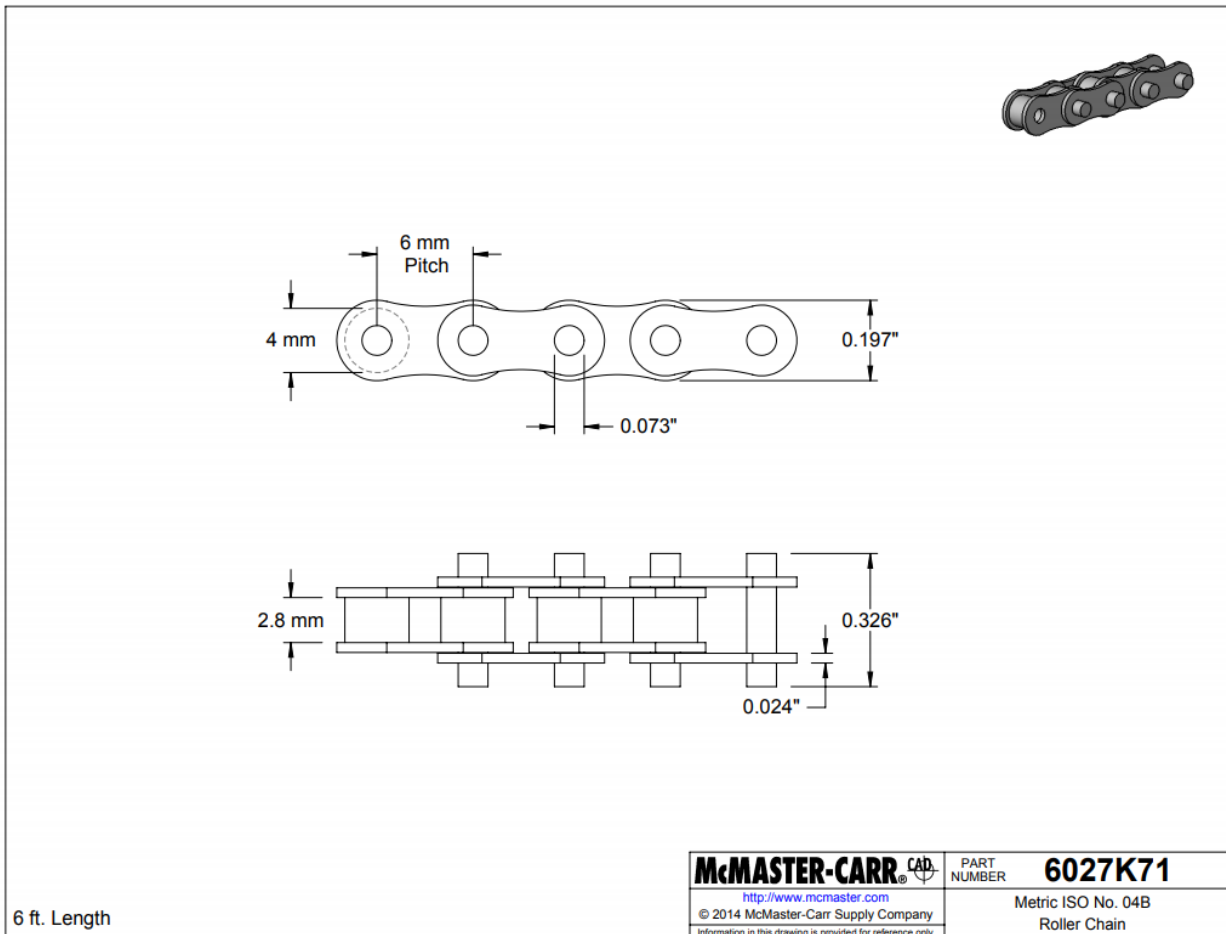


**Figure 77:** 6027K71 Roller Chain 2D-Drawing (Before Machined)

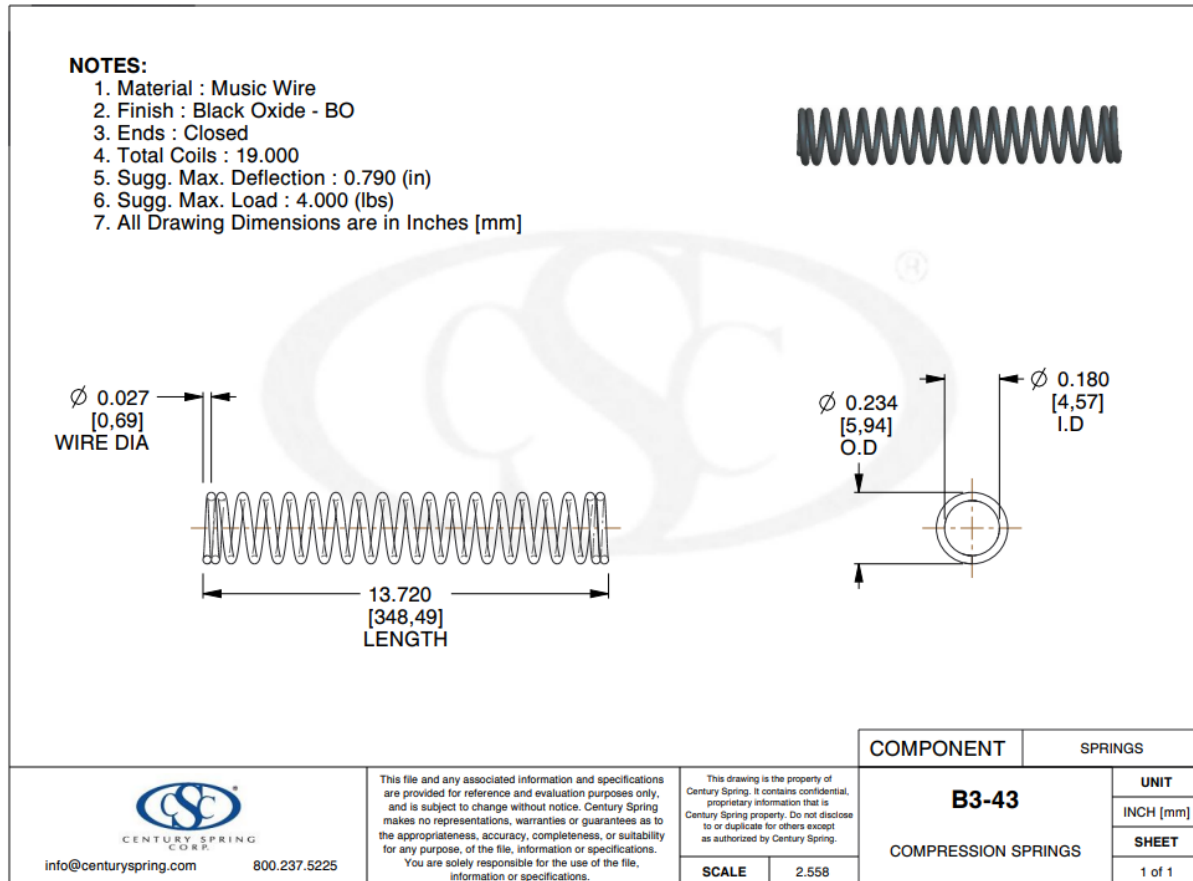


**Figure 78 :B3-43 Compression Spring for the Ratchet Wheel Mechanism 2D-Drawing**

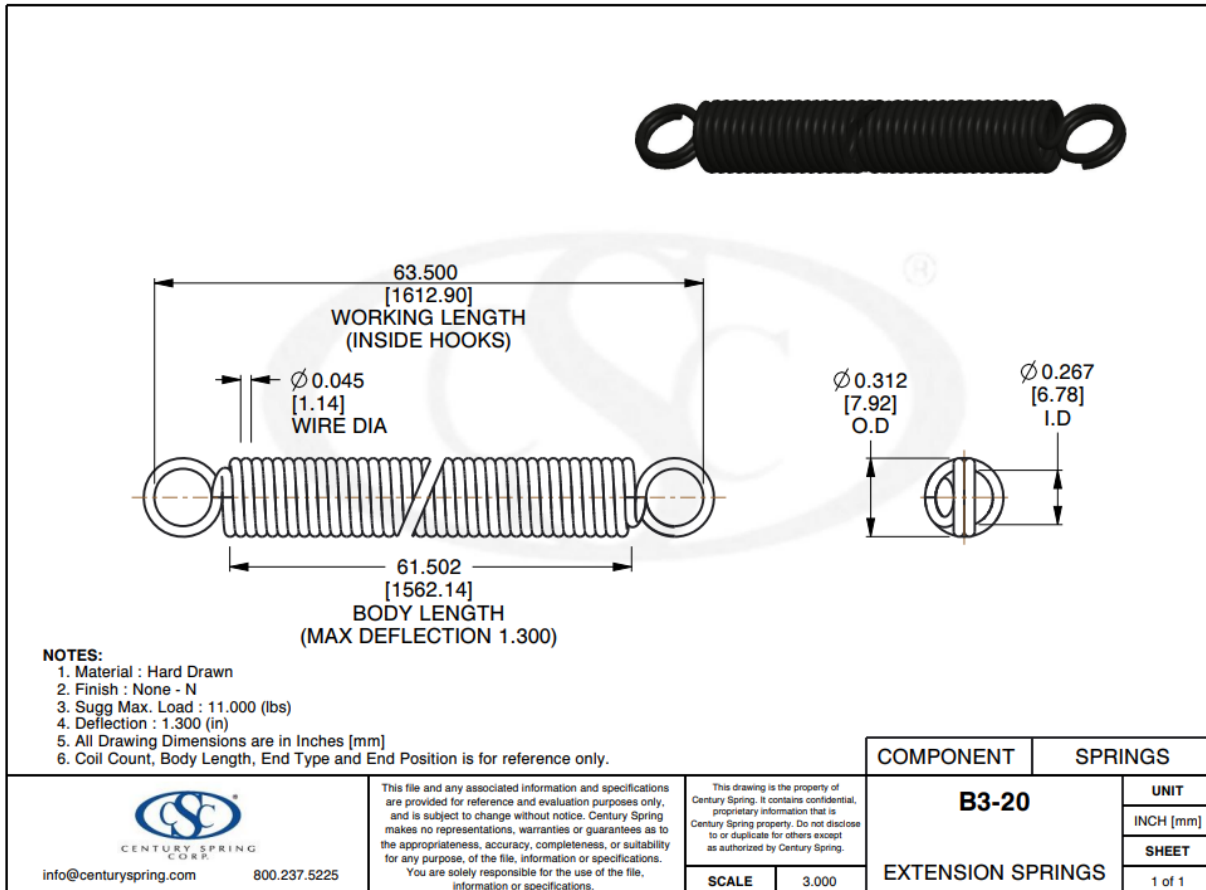


**Figure 79 :B3-20 Extension Spring for the Three Bar Linkages 2D-Drawing**

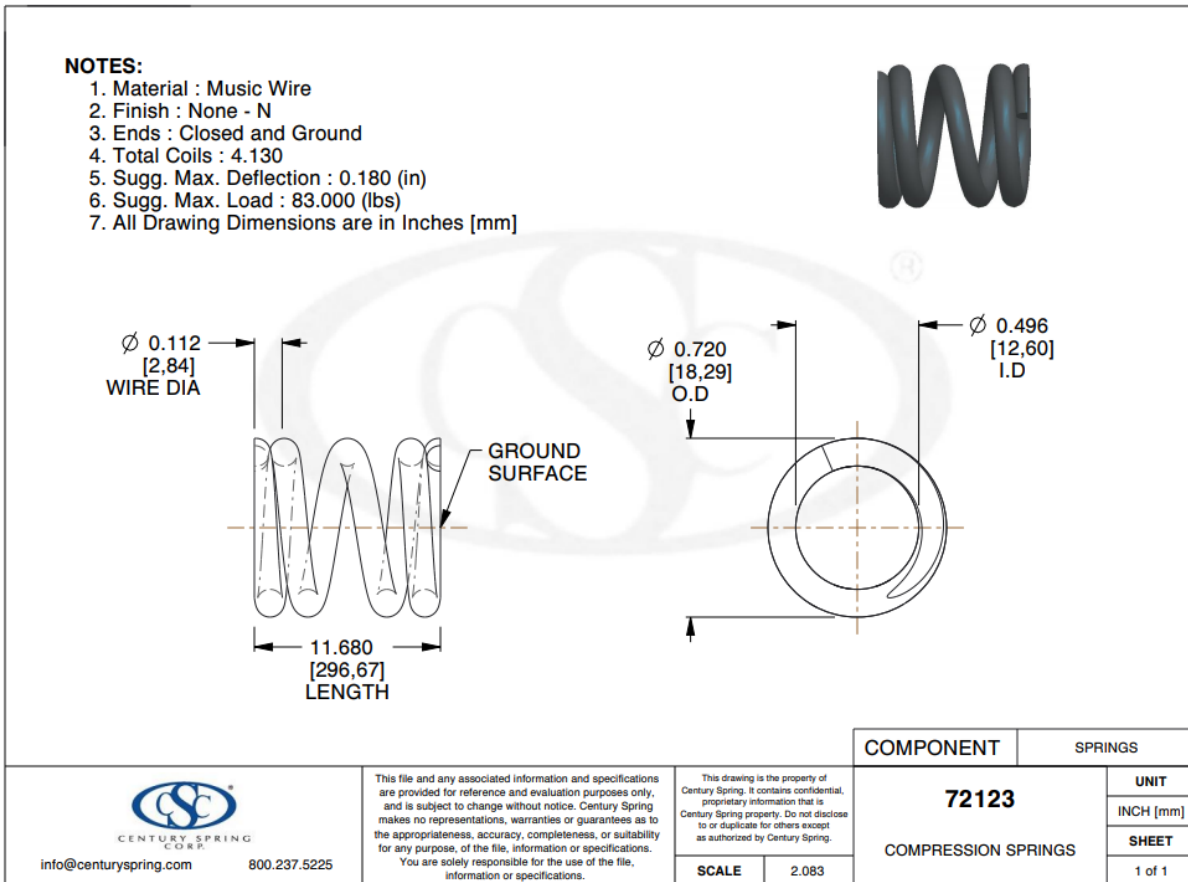


*Figure 80: 72123 Compression Spring for the Three Bar Linkages 2D-Drawing*

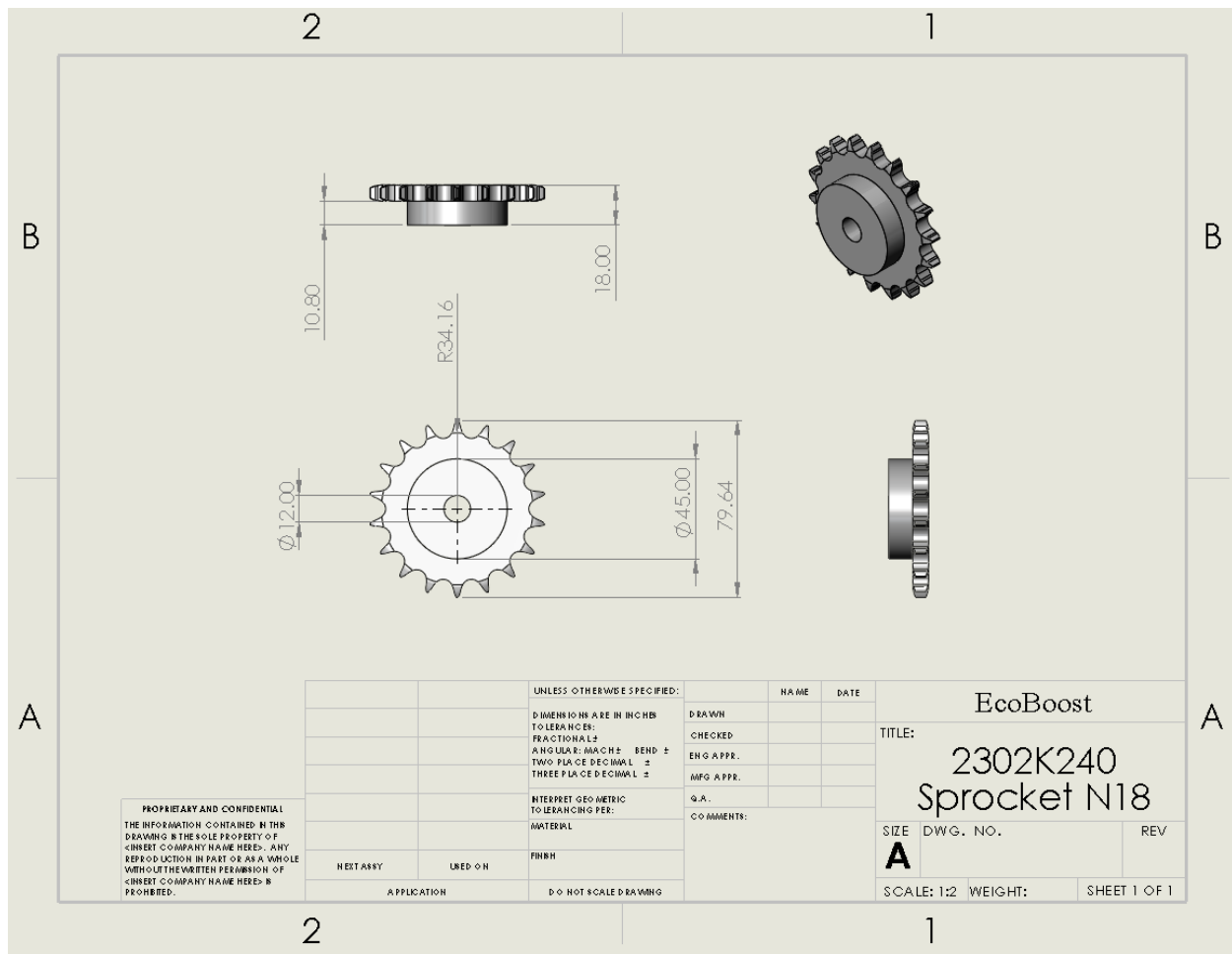
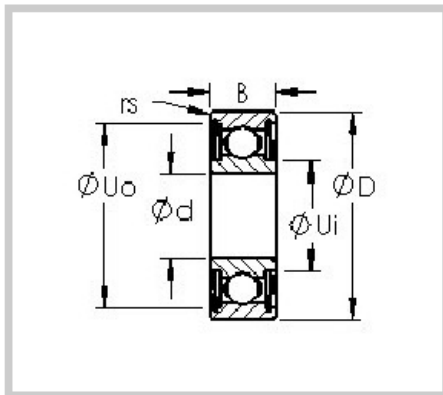


**Figure 81: 2302K240 Machined Sprocket with 18 Teeth 2D-Drawing**

# Technical Specification Sheets



Part Number: 6000ZZ  
Single Row Deep Groove



## Product Details

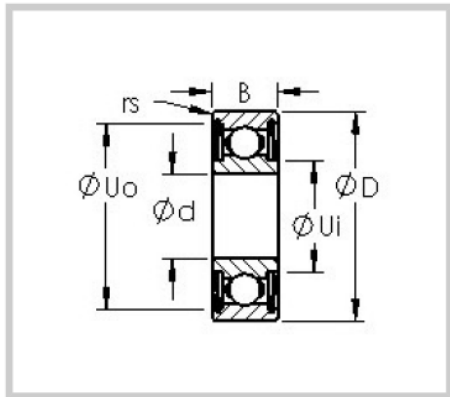
### Specifications

Bearing Type	Shielded	
Bore Dia (d)	10.000	mm
Outer Dia (D)	26.000	mm
Width (B)	8.000	mm
Radius (min) (rs)	0.30	mm
Dynamic Load Rating (Cr)	4,550	N
Static Load Rating (Cor)	1,950	N
Max Speed (Grease)	31,000	rpm
Max. Shaft Shoulder Dia. Inner (Ui)	12.9	mm
Min. Housing Shoulder Dia., Outer (Uo)	22.40	mm
Ball Qty	7	
Ball Dia (Dw)	4.762	mm
Weight (g)	19.00	grams
Precision	A1	
Standard Clearance	C0	
Material	52100 Chrome steel (or equivalent)	

\* ABEC Grades 1, 3, 5, 7, and 9 are available.

\* Two metal shields = (ZZ), also available with a single metal shield = (Z).

*Figure 82: 6000ZZ Single Row Deep Groove Bearing Technical Specs*



Part Number: 6003ZZ  
Single Row Deep Groove



## Product Details

---

### Specifications

Bearing Type	Shielded	
Bore Dia (d)	17.000	mm
Outer Dia (D)	35.000	mm
Width (B)	10.000	mm
Radius (min) (rs)	0.30	mm
Dynamic Load Rating (Cr)	6,000	N
Static Load Rating (Cor)	3,250	N
Max Speed (Grease)	21,000	rpm
Max. Shaft Shoulder Dia. Inner (Ui)	23.5	mm
Min. Housing Shoulder Dia., Outer (Uo)	31.85	mm
Ball Qty	10	
Ball Dia (Dw)	4.762	mm
Weight (g)	39.00	grams
Precision	A1	
Standard Clearance	C0	
Material	52100 Chrome steel (or equivalent)	

\* ABEC Grades 1, 3, 5, 7, and 9 are available.

\* Two metal shields = (ZZ), also available with a single metal shield = (Z).

**Figure 83 : 6003ZZ Single Row Deep Groove Bearing Technical Specs**



## 45-300 in/lbs Torque Gears

Model: 75-7MLD (LGU 75-M)

[Request Quote](#)

Quantity

[Add to Cart](#)

[Download CAD](#)

[Choose a CAD format](#)

[View 3D Model](#)



Line Drawing - Click to Enlarge

### Product Details

Nominal Reduction Ratio	7
Actual Reduction Ratio	7
Maximum Torque (Ncm)	1,765
Weight (g)	265.00
Input Shape	12x11x1
Output Shape	12x11x1
Output Shaft Penetration P (mm)	4.5
Fitting J	Hole 7- 4.5 Key 1- Width 5x depth 12
Dimension A (mm)	75.00
Dimension B (mm)	68.00
Dimension C (mm)	61.00
Dimension D (mm)	56.00
Dimension E	22
Dimension F (mm)	22.00
Dimension L1 Overall Length (mm)	22.60
Dimension L2 (mm)	8.40
Dimension L3 (mm)	12.60
Dimension M (mm)	4.20
Dimension N (mm)	2.20
Dimension O (mm)	2.20
Dimension Q2 (mm)	10.00
Dimension R (mm)	1.00

**Figure 84 : 75-7MLD (LGU 75-M) Technical Specs**

## Components Table List

ITEM NO.	PART NAMES	QTY.
1	Flywheel	1
2	75-7MLD Planetary Gear.stp	1
3	Flywheel Flange End Threaded	1
4	B18.3.1M - 10 x 1.5 x 30 Hex SHCS -- 30NHN	6
5	B18.3.1M - 5 x 0.8 x 55 Hex SHCS -- 22NHN	2
6	B18.2.2.4M - Hex flange nut, M10 x 1.5, with 15 WAF --N	7
7	B18.2.2.4M - Hex flange nut, M5 x 0.8 --N	1
8	B18.2.2.4M - Hex flange nut, M16 x 2 --N	1
9	Right Bicycle Frame	1
10	AST_Bearings_6000ZZ.prt	1
11	B18.22M - Plain washer, 10 mm, regular	1
12	B18.22M - Plain washer, 16 mm, regular	1
13	B18.22M - Plain washer, 5 mm, regular	2
14	Driving Shaft	1
15	Key	1
16	Cup	1
17	Friction Lining	1
18	Cone	1

19	AST_Bearings_6003ZZ.prt	2
20	Slider on the Cone	1
21	Driven Shaft	1
22	Extension Spring R2	1
23	Left Flange V2	1
24	Left Flange V2 B	1
25	2302K24	1
26	B18.3.3M - 6.5 x 20 SHSS --N	1
27	B18.3.3M - 6.5 x 30 SHSS --N	1
28	B18.3.3M - 6.5 x 40 SHSS --N	1
29	B18.3.3M - 6.5 x 16 SHSS --N	1
30	B18.3.3M - 6.5 x 10 SHSS --N	1
31	SpacerLeft	2
32	Compression spring assembly	1
33	Linkage Bar	1
34	2302K115	1
35	Chain2	1
36	B18.3.4M - 10 x 1.5 x 40 SBHCS --N	5
37	B18.2.4.5M - Hex jam nut, M10 x 1.5, with 16mm WAF --D-N	5
38	Spacer Middle Lower	1
39	Planetary Gear Fixed Frame	2
40	AST_Bearings_6001ZZ.prt	1
41	B27.8M - 3DM1-12	1
42	Middle Frame Support	1

43	B18.6.7M - M5 x 0.8 x 16 Indented HHMS -- 16N	2
44	AM-M5-N	2
45	B18.2.4.1M - Hex nut, Style 1, M5 x 0.8 --D-N	2
46	Brake Lever Sport	1
47	Handbrake	1
48	Ratchet Wheel	1
49	B18.3.5M - 4 x 0.7 x 60 Socket FCHS -- 20N	1
50	Compression spring Pawl Compression Spring	1
51	Pawl	1
52	Brake Wire Rope	1
53	Handbrake Spacer	1

Table 7: Components Table List

## MATLAB Code

```
clc
clear

mass_rider= 81; %kg, rider mass
mass_bicycle= 10.65 ;% kg, bike mass
mass_forward_wheel =0.8; % kg, average rim mass
mass_rear_wheel=0.915; % kg, tire weight
mass_payload = 8; % kg, mass payload.
mass_brake = 10; %kg, regenerative braking system mass.
diameter_rim=0.622 ;% m, rim diameter
diameter_wheel=0.6604; % m, tire diameter
v=40.00/3.6 %kph to m/s, bicycle speed

radius_wheel = diameter_wheel/2; %m, radius of both wheels.
total_mass = mass_rider + mass_bicycle + mass_payload + mass_brake % Total mass.
I_front_wheel=(mass_forward_wheel)*radius_wheel^2; %kg*m^2 moment of inertia of front wheel
I_rear_wheel=(mass_rear_wheel)*radius_wheel^2 ; %kg*m^2 moment of inertia of rear wheel
w=v/radius_wheel %rad/s, wheel angular speed

% Braking Capacity is equal to the total kinetic energy of the bicycle and cyclist.
braking_capacity = 1/2*total_mass*v^2 + 1/2*I_front_wheel*w^2 +
1/2*I_rear_wheel*w^2;

% Print Results.
fprintf('Braking Capacity, E_braking_capacity = %s J\n',braking_capacity);

syms eta1
syms If
syms Ie
syms n

%% Energy storage process
% syms n
eq1= eta1-If/(Ie/n^2+If)==0
%eta=0.25
If=0.1005 % kg*m^2
n_sprockets=29/18; % Sprocket ratio
n_g=7 ;% gear ratio of gearbox
n=n_g*n_sprockets % Overall velocity ratio

Ie=total_mass*radius_wheel^2+I_front_wheel+I_rear_wheel
vpasolve(eta1-If/(Ie/n^2+If)==0)

eta1=double(vpasolve(eta1-If/(Ie/n^2+If)==0,eta1)) % eta1
eta10=eta1
%% Energy regeneration process
syms eta2
eq2=[ eta2-Ie/(Ie+If*n^2)==0];
```

```

vpasolve(eq2,eta2)
eta2=double(vpasolve(eq2,eta2))    %eta2
eta=etal*eta2    %eta

% Regeneration efficiency plots
np=0:0.001:100;
etal=If./(Ie./np.^2+If);
eta2=Ie./(Ie+If.*np.^2);
eta=etal.*eta2*100;
plot(np,eta);
xlabel('Velocity ratio n');
ylabel('Overall Regeneration efficiency (%) ');
title('Influence of velocity ratio on overall regeneration efficiency when
I_e= 12.4444 kgm^2 and I_f=0.1005 kgm^2')

%% velocity after energy is added
% Flywheel speed after energy storage
fprintf('Flywheel angular speed after energy storage,rad/s :\n')
w_f=(etal0*braking_capacity/(0.5*If))^0.5  % Flywheel angular speed after
energy storage,rad/s
fprintf('Rear wheel angular speed after energy storage,rad/s :\n')
w_w=w_f/n  % Rear wheel angular speed
fprintf('Bike speed after energy storage,rad/s :\n')
v1= w_w*radius_wheel
disp(' m/s')
v1=v1*3.6
disp('km/h')  % Bike velocity after energy storage

fprintf('Stored energy on flywheel')
Es=0.5*If*w_f^2
disp('J')
%% Velocity after regeneration
% Velocity after regeneration
energy_in_flywheel=0.5*If*w_f^2

eta_2=Ie/(Ie+If*n^2)
E_released=Es*eta2
n_2=0.4383;
w_w_after_regen=sqrt(Es*eta_2^2/Ie) % set eta = 0.5, then use flywheel energy
= remaining flywheel energy + bicycle kinetic energy
w_f_after_regen=w_w_after_regen*n
v_afterregeneration=w_w_after_regen*0.5*diameter_wheel*3.6    %km/h, vehicle
velocity after regeneration

%% Cone Clutch calculations
Ie
n_sprockets
I1=Ie/(n_sprockets^2) % moment of inertia of the inertia system at the side
of the cone of the cone clutch
n_g
If
I2=n_g^2*(If) % moment of inertia of the inertia system at the side of the
cup of the cone clutch

```

```

w_rearwheel0=w; % initial rear wheel angular speed
w1= w_rearwheel0*n_sprockets % speed of the inertia system at the side of
the cone of the cone clutch,rad/s
% w2=0
w2=w_f_after_regen/n_g
% w_w_after_regen*n_sprockets % speed of the inertial system at the cap
side of the clutch
t1=4 % s, Time required finish the energy storage process

fprintf('Nominal clutch torque:')
T=I1*I2*(w1-w2)/t1/(I1+I2) %Nominal clutch torque

fprintf(' total dissipated energy during the clutch engagement of th eenergy
storage process:')
E=I1*I2*((w1-w2)^2)/2/(I1+I2) % total dissipated energy during the clutch
engagement of th eenergy storage process

```

## Selection of Bearing 1

```

clc
clear

n= 517 % rpm, shaft speed
F_a=0 % the axial load
F_r=273.0875 %the radial load
L_D=25*10^3 % initial design life of bearing
L_R=1*10^6 % revolutions,C10 life bearings

a=3 %
LF=1.2 % load factor
K_rel=1 % reliability of bearing
V=1;

X_1=1
Y_1=0
L_Rhr=L_R/n/60 % hr, bearing rating in hours

F_e=X_1*V*F_r+Y_1*F_a
C_10=LF*F_e*(L_D/(K_rel*L_Rhr))^(1/a) % catalog C10 rating with associated
life of 10^6 revolutions

```

## Selection of Bearing 2

```

clc
clear

n= 517 % rpm, shaft speed
F_a=0 % the axial load
F_r=189.1467 %the radial load
L_D=25*10^3 % initial design life of bearing
L_R=1*10^6 % revolutions,C10 life bearings

```

```

a=3      %
LF=1.2    % load factor
K_rel=1    % reliability of bearing
V=1;

X_1=1
Y_1=0
L_Rhr=L_R/n/60    % hr, bearing rating in hours

F_e=X_1*V*F_r+Y_1*F_a
C_10=LF*F_e*(L_D/(K_rel*L_Rhr))^(1/a)    % catalog C10 rating with associated
life of 10^6 revolutions

```

## Selection of Bearing 4

```

clc
clear

n= 2529.36    % rpm, shaft speed
F_a=0    % the axial load
F_r=111.23   %the radial load
L_D=25*10^3   % initial design life of bearing
L_R=1*10^6    % revolutions,C10 life bearings

a=3      %
LF=1.2    % load factor
K_rel=1    % reliability of bearing
V=1;

X_1=1
Y_1=0
L_Rhr=L_R/n/60    % hr, bearing rating in hours

F_e=X_1*V*F_r+Y_1*F_a
C_10=LF*F_e*(L_D/(K_rel*L_Rhr))^(1/a)    % catalog C10 rating with associated
life of 10^6 revolutions

```

## Cone Shaft Calculation

```

clc
clear

a_1= (7.3+0.5*12+7.2/2)*10^-3 % = distance between bearing 1 and sprocket 2
a_2=(14.8+7.2/2+12/2)*10^-3 % distance between bearing 2 and sprocket 2
r_2=(0.5*(79.65+34.16*2)*10^-3)*0.5 % Pitch radius of sprocket 2
T= 17.0992    %, maximum shaft torque ,Nm

F_2=T/r_2
F_a1=0
F_r1=a_2/(a_1+a_2)*F_2
F_a2=0
F_r2=a_1/(a_1+a_2)*F_2

```

## Spring Design Calculation

```
s=2*10^-2 % m, motion range of brake wire
b=4*10^-2 %m, length of the rigid bar
K1=1.121*10^3 % N/m, extension spring 1 rate

%%Verification of spring 2 fatigue strength
% spring parameters
L_0=19*10^-3 %m
ID=12.6*10^-3 %m,
OD=18.29*10^-3 %m,
k_2=82.134*10^3 %N/m,
L_s=11.7*10^-3 %m,
N_t=4.13,
d=2.84*10^-3 %m

alpha0=2*asin(s/4/b); % rad, initial bar position
alpha0deg=alpha0*180/pi

disp('cone clutch engagement position:')
alpha1=0.8*alpha0 %rad, cone clutch engagement position

disp('Distance between the fixed revolute joint of the rigid bar and the
fully engagement position of cone:')
a=2*b*cos(alpha1) % Distance between the fixed revolute joint of the rigid
bar and the fully engagement position of cone
y2=2*b-a % Deflection of spring 2 which actuates the cone

K=F/y2 %N/m, Spring rate of spring 2

alpha=0:0.000001:alpha1;
F2=2*K.* (b- (a^2+b^2-2*a*b.*cos(alpha)).^0.5).*sin(alpha); % F2= Fc-Fs1,
component of bar and spring 2 forces on the y axis
F2_max=max(F2)
plot(alpha,F2)
xlabel('Bar 1 position alpha (rad)');
ylabel('F_c-F_s1');

% Deflection of the spring 2 when the component of the actuation spring
% force reach the maximum value
y_1= 0.5*s+b*alpha1
K1min=F2_max/y_1

Fs1max=K1*2*s % maximum extensiioni spring 1 force
F_cmin=Fs1max+ F2_max %minimum cable force required

% %%Verification of spring 2 fatigue strength
% % spring parameters
% L_0=19*10^-3 %m
% ID=12.6*10^-3 %m,
```

```

% OD=18.29*10^-3 %m,
% k_2=82.134*10^3 %N/m,
% L_s=11.7*10^-3 %m,
% N_t=4.13,
% d=2.84*10^-3 %m
%
% F_max=128.5390 %N maximum spring 2 force
% F_min=0 %N , minimum spring 2 force

F=k_2*y2 %N spring 2 actuation force
F_max=F %N maximum spring 2 force
F_min=0 %N , minimum spring 2 force

%parameters for fatigue analysis
S_sa=241*10^6 % pa
S_sm=379*10^6 % Pa
S_se=309.9884*10^6 %pa

%From textbook
m=0.145
A=2211*10^6*(10^-3)^m

D=0.5*(ID+OD)
C=D/d
K_B=(4*C+2)/(4*C-3)
S_ut=A/d^m % Pa, Tensile strength
S_sy=0.56*S_ut % Pa, yield strength
S_su=0.67*S_ut % Pa, torsional modulus of rupture

%Fatigue calculations
F_a=0.5*(F_max-F_min) %N
F_m=0.5*(F_max+F_min) %N
tau_a=K_B*(8*F_a*D)/(pi*d^3) % pa
tau_m=K_B*(8*F_m*D)/(pi*d^3) % pa
n=(tau_a/S_se+tau_m/S_su)^-1 % Fatigue safety factor
fprintf('Fatigue safety factor n=%.5f',n)

% Stability
a=(L_0< 2.63*D/0.5)
2.63*D/0.5

```

## Ratcheting Mechanism Calculation

```

%%
clc
clear
[F_rx,F_p,F_ry,M_s,F_sx,F_sy]=Ratchet_force(32.8,0.81,5.71)
%%
clear
clc
[F_rx,F_p,F_ry,Fspring,M_s,F_sx1,F_push]=Ratchet_force_regen(32.8,2.8,5.71)
%%
clear

```

```

clc
[F_rx,F_p,F_ry,Fspring,M_s,F_sx1]=Ratchet_force_begin(32.8,0.81)
%%
clear
clc
[F_rx,F_p,F_ry,M_s,F_sx,F_sy]=Ratchet_force_stuck(32.8,0.3,5.71)

function
[F_rx,F_p,F_ry,Fspring,M_s,F_sx,F_sy]=Ratchet_force_begin(rate,delta_x)

%pawl force analysis
Fspring=rate*delta_x; %F=kx

F_sx=0;
F_p=Fspring;
M_s=-F_p^2; %moment about support

%Ratchet force analysis
F_ry=F_p;
F_rx=0;

%support
F_sy=Fspring
end

function [F_rx,F_p,F_ry,M_s,F_sx,F_sy]=Ratchet_force_stuck(rate,delta_x,M_hb)
%Ratchet force analysis
F_p=M_hb/(-cosd(45)*1-0.5*sind(45)) %moment about center of ratchet
F_rx=F_p*cosd(45);
F_ry=-F_p*sind(45);

%pawl force analysis

F_sx=F_p*sind(45);
M_s=-F_p*sind(45)*4.7-F_p*cosd(45)*2; %moment about support

%support
Fspring=rate*delta_x
F_sy=F_p*cosd(45)+Fspring

End

function
[F_rx,F_p,F_ry,Fspring,M_s,F_sx,F_push,F_sy]=Ratchet_force_regen(rate,delta_x
,M_hb)

%for ratchet
F_ry=0; % idle
F_rx=0;

%for pawl
Fspring=rate*delta_x;

```

```

F_push=Fspring; %asssume F_push equals to 5N
M_s=0;
F_p=0;
F_sx1=0;

%support
F_sy=Fspring

end

function
[F_rx,F_p,F_ry,Fspring,F_sy1,M_s,F_sx1]=Ratchet_force(rate,delta_x,M_hb)

%Ratchet force analysis
F_p=-M_hb/(cosd(45)*1.5) %moment about center of ratchet
F_rx=-(2^(1/2)*F_p)/2;
F_ry=-(2^(1/2)*F_p)/2;

%pawl force analysis
Fspring=rate*delta_x; %F=kx

F_sx1=-F_p*cosd(45);
F_sy1=Fspring+F_p*sind(45);
M_s=-F_p*sind(45)*2-F_p*cosd(45)*5; %moment about support

end

```

## 8. References

AST. (n.d.). 6000ZZ Single Row Deep Groove. Retrieved December 7, 2018, from

<https://www.astbearings.com/catalog.html?page=product&id=6000ZZ>

AST. (n.d.). 6003ZZ Single Row Deep Groove. Retrieved December 7, 2018, from

<https://www.astbearings.com/catalog.html?page=product&id=6003ZZ>

Budynas, R. G., & Nisbett, J. K. (2015). *Shigley's Mechanical Engineering Design*(10th ed.). New York City, NY: Mc Graw Hill.

Century Spring Corp. (n.d.). B3-43 - Compression Springs. Retrieved from

<https://www.centuryspring.com/catalog/compression-regular/B3-43CS>

Century Spring Corp. (n.d.). [Https://www.centuryspring.com/catalog/compression-regular/72123CS](https://www.centuryspring.com/catalog/compression-regular/72123CS). Retrieved December 7, 2018, from 72123 - Compression Springs

Century Spring Corp. (n.d.). B3-20 - Extension Springs. Retrieved December 7, 2018, from

<https://www.centuryspring.com/catalog/root/B3-20CS>

Kelly, I. (Director). (2012, April 12). *KERS bicycle technology university project at AIT*[Video file]. Retrieved December 7, 2018, from

<https://www.youtube.com/watch?v=5FJcEvijjks>

MATEX. (n.d.). STEEL PLANETARY GEARS. Retrieved December 7, 2018, from

<https://www.matexgears.com/steel-planetary-gears?page=product&cid=steel-planetary-gears&id=75-7mld>

McMaster-CARR. (n.d.). Roller Chain ISO Number 04B, 6 mm Pitch. Retrieved December 7, 2018, from <https://www.mcmaster.com/6027k71>

McMaster-CARR. (n.d.). Roller Chain Sprocket for ISO 08B Chain, 29 Teeth, for 16 mm Shaft Diameter. Retrieved December 7, 2018, from  
<https://www.mcmaster.com/2302k115>

McMaster-CARR. (n.d.). Roller Chain Sprocket for ISO 08B Chain, 18 Teeth, for 12 mm Shaft Diameter. Retrieved December 7, 2018, from  
<https://www.mcmaster.com/2302k24>

Passino, K. M. (n.d.). Technology for Mental Health. Retrieved December 7, 2018, from  
<http://www2.ece.ohio-state.edu/~passino/>

University of Pennsylvania. (2013, January 27). Bike Brake Cable Testing. Retrieved December 7, 2018, from <http://titanarm.com/post/48680663848/bike-brake-cable-testing>